

國立交通大學

材料科學與工程學系

博士論文

發光二極體功率與亮度的提升

Enhancement the power and the brightness of
light emitting diodes

研究生：彭韋智

指導教授：吳耀銓 教授

中華民國九十五年七月

發光二極體功率與亮度的提升
Enhancement the power and the brightness of
light emitting diodes

研究生：彭韋智

Student: Wei-Chih Peng

指導教授：吳耀銓 博士

Advisor: Dr. YewChung Sermon Wu

國立交通大學

材料科學與工程學系



Submitted to Department of Material Science and Engineering

College of Engineering

National Chiao Tung University

in partial Fulfillment of the Requirements

for the Degree of

Doctor of Philosophy

in Materials Science and Engineering in

July 2006

Hsinchu, Taiwan, Republic of China

中華民國九十五年七月

發光二極體功率與亮度的提升

學生:彭韋智

指導教授:吳耀銓 博士

國立交通大學材料科學與工程研究所

摘要

本論文主要研究目的是提供一些方法來提升磷化鋁鎵銦與氮化鎵發光二極體之元件特性。其中，主要是藉由晶圓接合技術製作高功率與高亮度發光二極體並探討使用不同晶圓接合機制對其之發光二極體元件特性之影響。

發光頻率介於黃光至紅光之間的 LED，一般都是在砷化鎵基板上，以磷化鋁鎵銦 (AlGaInP) 製作而成，然而由於此型機板的低熱傳導性質，使得該類 LED 只能做低功率元件的應用。為克服此一缺點，透過晶圓接合(wafer bonding)的技術，可在銅或碳化矽基板上製作高功率的 AlGaInP LED。銅基板 LED 這種作法需要在 AlGaInP LED 結構與銅基板間加入一層氧化銦錫(ITO)膜，並與以加熱，發現在 500°C 下加熱 30 分鐘，銅尚不會穿透 ITO 層，而樣品又可以順利黏合。銅為基板的高功率 LED 可以在八倍於砷化鎵基板紅光 LED 的注入電流(injection current)下操作，對於 LED 而言，銅由於具有較高的熱導率及較低的熱阻抗，因此產生的熱量比砷化鎵少，這使得銅基板 LED 的操作電流可以達到 800 mA，而其發光峰值強度可達 1230 mcd。於室溫下連續以 20 mA 的電流操作 500 個小時後，其發光強度衰減的幅度不到 5%。此外，以碳化矽為基板且具有金屬鏡面的紅光發光二極體，在 20 mA 的注入電流下操作其發光強度可達傳統砷化鎵基板紅光 LED 的 3.2 倍；其操作電流也優於砷化鎵基板 LED 可以達到 650 mA。

於氮化鎵系列發光二極體方面，也成功的利用膠接合法與雷射分離技術將氮化鎵磊晶層轉移至 2 吋之矽基板上，藉由反射鏡面與表面粗化的配合在 20 mA 的注入電流下操

作其垂直型以矽為基板的藍光 LED 的光輸出功率可高於傳統藍寶石基板 LED 的 20%；其操作電流 280 mA 也優於傳統基板 LED (180 mA)。其垂直型矽基板藍光 LED 之發光圖形較藍寶石基板對稱，且經過 1000 小時的元件壽命測試仍保有高的穩定性。此外，運用表面粗化、晶圓接合與雷射分離技術製作一具有雙面粗化(於 p-GaN 和 undoped-GaN)的新結構氮化鎵發光二極體，發現在 20 mA 的注入電流下操作其正向與背向的發光強度分別為傳統 LED(p-GaN 與 undoped-GaN 均無粗化)的 2.77 和 2.37 倍。另外，也可藉由改變基板與發光層間之 undoped-GaN 的表面粗糙度進而調整 LED 的發光角度與光輸出功率。最後，氮化鎵發光二極體利用雙面粗化並運用銀鏡面於藍寶石基板上之特性將被提出。



Enhancement the power and the brightness of light emitting diodes

Student: Wei-Chih Peng

Advisor: Dr. YewChung Sermon Wu

Department of Material Science and Engineering

National Chiao Tung University

Abstract

The primary objective of this dissertation is provided some approaches to enhance the performance of AlGaInP and InGaN-GaN LED. It could use wafer-bonding technology to transfer AlGaInP or GaN thin film on the high conductivity substrate. Furthermore, InGaN-GaN LED with roughening both the p-GaN surface and the undoped-GaN surface by double transfer methods and applying a mirror coating to the sapphire substrate have also demonstrated.

LED emitting in the yellow to red region of the spectrum are typically made from AlGaInP and based on a GaAs substrate. But due to the low thermal conductivity of the substrate, these LED are limited to low-power applications. To overcome this drawback, high-power AlGaInP LED with Cu and SiC substrates using wafer bonding is fabricated. For Cu-substrate LED, this involves placing an indium-tin-oxide (ITO) film between the AlGaInP LED structure and the Cu substrate and then applying heat. It is found that Cu did not penetrate the ITO layer when samples were bonded at 500°C for 30 mins. Copper-substrate LED can operate at an injection current which is eight times higher than that of traditional GaAs-substrate LED. Copper's higher thermal conductivity and lower thermal resistance compared with GaAs means that less heat is generated in the LED. This allows the

Cu-substrate LED to operate a current of up to 800 mA and reach a peak luminous intensity of 1230 mcd. The degradation of the intensity was less than 5% after 500 hours running at 20 mA at room temperature. Furthermore, the luminous intensity of SiC-substrate LED with mirror system is 3.2 times higher than that of conventional LED at the injection current of 20 mA. The saturation current could reach at 650 mA, which is better than that of GaAs-substrate LED.

For the GaN-based LED, vertical InGaN-GaN LED epitaxial films are successfully fabricated on a 50mm Si substrate using glue bonding and laser lift-off technology. It is found that the light output of the vertical InGaN LED chip exceeded that of the conventional sapphire-substrate LED by about 20% at an injection current of 20 mA. The vertical InGaN LED operate at a much higher injection forward current (280 mA) than were sapphire substrate LED (180 mA). The radiation pattern of the vertical InGaN LED is more symmetrical than that of the sapphire substrate LED and the vertical InGaN LED remain highly reliable after 1000 h of testing. Furthermore, a new structure of InGaN LED with double roughened (p-GaN and undoped-GaN) surfaces is fabricated by surface-roughening, wafer-bonding and laser lift-off technologies. It is found that the frontside luminance intensity of double roughened LED was 2.77 times higher than that of the conventional LED at an injection current of 20 mA. The backside luminance intensity is 2.37 times higher than that of the conventional LED. Moreover, the effect of the roughness of the undoped-GaN layer on the performance of double roughened LED is also investigated. It is found as the root mean square (rms) roughness of undoped-GaN layer increase from 18.6 to 146.7 nm, the output power increase from 7.2 to 10.2 mW, and the view angle decrease from 133.6° to 116°, respectively. Finally, the performance of an InGaN LED with a roughened undoped-GaN surface and a silver mirror on the sapphire substrate is also investigated.

誌 謝

感謝指導教授吳耀銓博士在實驗及論文上的耐心指導以及晶元光電謝明勳博士在我求學期間的協助與提攜，其次對半導體中心、交大材料所、以及晶元光電等設備支持，促使本研究能夠順利完成。

研究期間感謝實驗室諸位的幫忙與鼓勵，包括趙志偉、許晉源學長，同學劉柏均、胡國仁與學弟妹侯智元、廖崢、黃秉緯、胡晟民、張志榜、林博文、徐志偉、林其慶、吳琪廷、林沛彥、詹俊彬、陳一凡、彭顯智、林廷政、汪砥華等以及晶元光電的世欽、小慧、威佑、壽志、美君、青山、志強等人，你們的相伴豐富了我的學習生涯，讓我生活充滿豐富的色彩。

僅以此論文獻給我的家人，感謝他們在我求學期間於精神上的全力支持，讓我能專心於學業上，也在一次的感謝曾經幫助與關心過我的人。

彭韋智

2006年7月于新竹交大

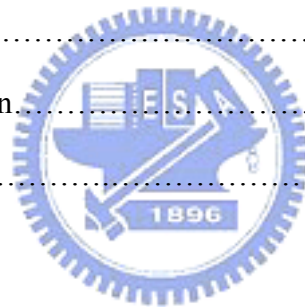
Table of Contents

Abstract (Chinese)	III
Abstract (English)	V
Acknowledgements (Chinese)VII
Table of Contents	VIII
Table Lists	XI
Figure Captions	XII
Chapter 1 Introduction	1
1-1 Background theory for light emitting diode.....	1
1-1-1 History of LED.....	1
1-1-2 Physical functions.....	2
1-1-3 Device configuration and efficiency.....	3
1-2 Wafer bonding.....	5
1-2-1 The introduce of wafer bonding.....	5
1-2-2 The mechanism of wafer bonding.....	6
1-2-3 The classify of wafer bonding.....	7
1-3 Applications of III-V compound semiconductor by wafer bonding technology.....	9
1-4 Organization of this dissertation.....	10
Chapter 2 High power AlGaInP light emitting diode with Cu and SiC substrate fabricated by wafer bonding	24
2-1 Introduction.....	24
2-2 Cu-substrate LED.....	25

2-2-1 Experiments.....	25
2-2-2 Results and Discussion.....	26
2-3 SiC-substrate LED.....	29
2-3-1 Experiments.....	29
2-3-2 Results and Discussion.....	30
2-4 Summary.....	31

Chapter 3 Performance of InGaN-GaN light emitting diode fabricated using glue bonding on 50mm Si substrate..... 45

3-1 Introduction.....	45
3-2 Device Fabrication.....	46
3-3 Results and Discussion.....	47
3-4 Summary.....	49



Chapter 4 Enhanced performance of InGaN-GaN light emitting diode by roughening both the p-GaN surface and the undoped-GaN surface..... 58

4-1 Introduction.....	58
4-2 Improved luminance intensity of InGaN-GaN LED by roughening both the p-GaN surface and the undoped-GaN surface.....	60
4-2-1 Device Fabrication.....	60
4-2-2 Results and Discussion.....	61
4-3 Enhanced light output in double roughened GaN light-emitting diodes via various texturing of undoped-GaN layer.....	64

4-3-1 Device Fabrication.....	64
4-3-2 Results and Discussion.....	65
4-4 Summary.....	68
Chapter 5 Enhanced performance of an InGaN-GaN light -emitting diode by roughening the undoped -GaN surface and applying a mirror coating to the sapphire substrate.....	84
5-1 Introduction.....	84
5-2 Device Fabrication.....	85
5-3 Results and Discussion.....	86
5-4 Summary.....	88
Chapter 6 Conclusion and Future work.....	96
Reference	98
Vita	105
Publication List	106



Table List

Chapter 1

Table I Commonly used wafer-bonding techniques.

Chapter 4

Table I The definition of CV-LED, PR-LED and DR-LED.

Table II The performances of DR-LED with various treatments on u-GaN layer.



Figure Captions

Chapter 1

Fig. 1-1 The evolution of light emitting diodes.

Fig. 1-2 Band diagram illustrating non-radiative recombination (a) via a deep level (b) via an Auger process and (c) radiative recombination.

Fig. 1-3 Band structure near a semiconductor p-n junction: (a) homojunction under zero bias, (b) homojunction and (c) heterojunction under forward bias.

Fig. 1-4 The bandgap energy and corresponding wavelength versus lattice constant of AlGaInP and InGaN system at room temperature.

Fig. 1-5 The schematic of a typical surface-emitting LED.

Fig. 1-6 Schematic of surface waviness.

Fig. 1-7 Saturation values of surface or bonding energy measured by the crack opening method as a function of temperature after long-time heat treatments (up to 100 h).

Fig. 1-8 An infrared transmission image of a wafer with four devices showing bonding failure during fabrication of the device. The fringes and dark regions indicate un-bonded areas.

Fig. 1-9 The bonding flowchart of AlGaInP LED with a GaP transparent substrate (TS).

Fig. 1-10 The LED chip of (a) GaAs substrate LED and (b) GaP transparent substrate LED.

Chapter 2

Fig. 2-1 A successful Cu-substrate-bonded LED sample.

Fig. 2-2 A scanning electron micrograph of the cross section of the LED structure.

Fig. 2-3 Auger depth profiles of AlGaInP LED/ ITO-Cu sample bonded at 500°C for 30 minutes.

Fig. 2-4 Current-voltage characteristic of the Cu-substrate-bonded LED devices fabricated

by wafer bonding technology.

Fig. 2-5 Peak spectral wavelength against DC injection current for the LED with a GaAs substrate and a Cu substrate.

Fig. 2-6 *L-I* curves for conventional GaAs-substrate LED and Cu-substrate LED.

Fig. 2-7 Luminescence-output intensity variation as functions of time. During this life test measurement, a 20 mA current was injected into the Cu-substrate LED at room temperature.

Fig. 2-8 Schematic diagram of the LED/ metal/ SiC wafer fusion process: (a) SiC substrate and LED wafer with In and BeAu metal; (b) wafer bonding process; (c) removal of GaAs substrate and etch stop layer; and (d) mesa-etched and electrodes deposition.

Fig. 2-9 The reflectivity of the BeAu/Au mirror.

Fig. 2-10 The I-V characteristics of SiC-substrate LED.

Fig. 2-11 The L-I curves of conventional GaAs-substrate LED and SiC-substrate LED.

Fig. 2-12 Peak spectral wavelength against DC injection current for the LED with a GaAs substrate and a SiC substrate.

Chapter 3

Fig. 3-1 (a) Schematic illustration of the vertical InGaN LED structure. (b) The SEM image of roughened surface.

Fig. 3-2 (a) The image of an InGaN LED wafer bonded on a 50mm diameter Si substrate. Wafer was successfully cut into isolated devices with an area of $300 \times 300 \mu\text{m}^2$. (b) The SEM image of the cross section of the LED structure after dicing process.

Fig. 3-3 Current-voltage (*I-V*) characteristics of the vertical and conventional InGaN LED.

Fig. 3-4 The effects of injection the current on the luminous intensity of the vertical and conventional InGaN LED.

Fig. 3-5 The effects of injection the current on the light output and the peak spectral wavelength of vertical and conventional InGaN LED.

Fig. 3-6 The radiation patterns of (a) sapphire-based LED and (b) vertical InGaN LED.

Fig. 3-7 Reliability test of vertical InGaN LED under stress-condition of 55°C and 50 mA.

Chapter 4

Fig. 4-1 Schematic diagrams of (a) CV-LED (without any surface-roughening treatment), (b) PR-LED (with roughened p-GaN surface) and (c) DR-LED (with double roughened surfaces).

Fig. 4-2 Scanning electron micrographs and AFM image of (a) p-GaN surface without any surface- roughening treatment, (b) roughened p-GaN surface and (c) roughened undoped-GaN surface.

Fig. 4-3 The mapping data of the PR-LED.

Fig. 4-4 The mapping data of the DR-LED (2 inch wafer).

Fig. 4-5 Luminance intensity of three LED chips vs the forward injection current. (a) Intensity measured from the frontside (topside through the transparent metal layer) of the LED chip. (b) Intensity measured from backside substrate side (through the sapphire/ transparent glue/ glass) of the LED chip.

Fig. 4-6 Possible photon paths inside the structures of the (a) CV-LED, (b) PR-LED and (c) DR-LED.

Fig. 4-7 The external quantum efficiency and the output power of the CV-LED, PR-LED and DR-LED.

Fig. 4-8 Schematic diagram of the DR-LED transfer process: (a) PR-LED bonding to a host substrate; (b) laser lift-off and roughened u-GaN processes; (c) bonding to a sapphire substrate; and (d) removal of host substrate and glue layer.

Fig. 4-9 Schematic illustration of the InGaN LED structure and surface morphologies of ITO layer on p-GaN surface: (a) CV-LED and (b) PR-LED.

Fig. 4-10 The side-view SEM micrographs of the u-GaN layers: (a) without KOH treatment, (b) with 60 °C, (c) with 80 °C and (d) with 100 °C KOH treatment.

Fig. 4-11 The reverse current-voltage ($I-V$) characteristics of the PR-LED and DR-LED with various temperature treatments.

Fig. 4-12 The TEM image of the LED generated the dislocations in the structure after the laser lift-off process.

Fig. 4-13 The light output of DR-LED with various treatments on u-GaN layer.

Fig. 4-14 The radiation patterns of DR-LED with various temperature treatments on u-GaN layer.

Chapter 5

Fig. 5-1 Schematic diagrams of the (a) C-LED, (b) M-LED, (c) R-LED and (d) RM-LED.

Fig. 5-2 Scanning electron micrograph of roughened undoped-GaN surface treated with 45% KOH solution for 1 minute at 100°C.

Fig. 5-3 The reflectivity of Ag mirror.

Fig. 5-4 The $I-V$ characteristic of the LED.

Fig. 5-5 The effects of injection current on the luminous intensity and the light output of the LED.

Fig. 5-6 Possible photon paths of the (a) M-LED and (b) RM-LED.

Chapter 1 Introduction

1-1 Background theory for light emitting diode

1-1-1 History of LED

Light-emitting diode (LED) is a semiconductor device that emits incoherent narrow-spectrum light when electrically biased in the forward direction. The color of the emitted light depends on the chemical composition of the semiconducting material used, and can be near-ultraviolet, visible or infrared. LED development began with infrared and red devices made with gallium arsenide. Rubin Braunstein of the Radio Corporation of America first reported on infrared emission from GaAs and other semiconductor alloys in 1955. Experimenters at Texas Instruments, Bob Biard and Gary Pittman, found in 1961 that gallium arsenide gave off infrared light when electric current was applied. Biard and Pittman were able to establish the priority of their work and received the patent for the infrared light-emitting diode. Nick Holonyak Jr. of the General Electric Company developed the first practical visible-spectrum LED in 1962. In 1972, J. I. Pankove et al. fabricated the first blue LED using III-nitrides materials with a Metal-i-n structure [1]. Since then, related researches went on continually. However, the device performance was limited by the poorly conducting p-type GaN. Until in the late 1980s, I. Aksaski and H. Amano et al. [2, 3] developed the low-temperature buffer layer and Low-Energy Electron Beam Interaction (LEEBI) techniques to obtain conductive p-type GaN, the first GaN blue LED constructed of a real p-n junction, which greatly improved the device performance. In 1992, S. Nakamura et al. [4] achieved conductive p-type GaN with high temperature

thermal annealing in nitrogen ambient. **Figure 1-1** shows the evolution of LED. The full-color semiconductor lighting has become a reality with these great progresses of techniques.

1-1-2 Physical functions

An LED is a diode, which is semiconductor material with impurities to create a structure called a p-n junction. As in other diodes, current flows easily from the p-side (anode) to the n-side (cathode), but not in the reverse direction. The charge-carriers of electrons and electron holes flow into the junction from electrodes with different voltages. When an electron meets a hole, it falls into a lower energy level, and releases energy in the form of a photon as shown **Fig. 1-2**.

Figure 1-3a shows the band structure a p-n junction with no voltage applied to the diode. The n-type material contains electrons which behave as the current carriers in its conduction band, whereas the p-type material has holes for carriers in its valence band. When a forward voltage is applied to the diode, the energy levels are caused to shift as illustrated in **Figure 1-3(b) and 1-3(c)**. Under these conditions there is a significant increase in the concentration of electrons in the conduction band near the junction on the n-side and the concentration of holes in the valence band near the junction on the p-side. The electrons and holes recombine and energy is given off in the form of photons. The energy of the photon resulting from this recombination is equal to that associated with the energy gap. All of the light is created by spontaneous emission due to electron and hole recombination for the LED. It was Planck who postulated that the energy of a photon was related to its frequency by a constant. If the frequency of oscillation is given by ν , then the energy of the photon is just $h\nu$, where h is Planck's constant, which has a value of 4.14×10^{-15} eVseconds.

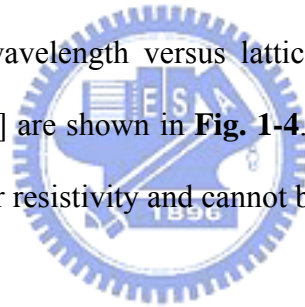
$$E = h \nu \quad (1.1)$$

The wavelength (or color) of the light emitted, depends on the band gap energy of the materials forming the p-n junction.

$$\lambda \text{ (nm)} = hc / E(\text{eV}) = 1240 / E(\text{eV}) \quad (1.2)$$

where c is the speed of light ($c=3 \times 10^8$)

Thus, a semiconductor with a 2 eV band-gap should give off light at about 620 nm (in the red). A 3 eV band-gap material would emit at 414 nm (in the violet). The energy bandgap and corresponding wavelength versus lattice constant of AlGaInP and InGaN system at room temperature [5] are shown in **Fig. 1-4**. The higher bandgap materials have higher melting point and higher resistivity and cannot be easily doped to high levels.



1-1-3 Device configuration and efficiency

The schematic of a typical surface-emitting LED is shown in **Fig. 1-5**. The LED are usually built on an n-type substrate and the structure is grown by epitaxial techniques with electrode attached to the p-type layer. Many commercial LED, such as AlGaInP and GaN-InGaN, also use GaAs and sapphire substrate, respectively. The processes occurring in a junction LED can be divided into three stages. The first is the excitation or injection process, in which the energy of carriers is raised by forward bias injection. Next is the recombination process, which most of these carriers give up their excess energy as photons. Finally, the extraction process generated photons must leave the semiconductor. The

overall device efficiency, η_o , may then be expressed as

$$\eta_o = \eta_{in} \eta_r \eta_{extraction} \quad (1.3)$$

where η_{in} , η_r and $\eta_{extraction}$ are the injection, radiative recombination and extraction efficiency, respectively. The internal quantum efficiency is defined as

$$\eta_{int} = \frac{\text{Number of photons emitted from active region per second}}{\text{Number of electrons injected into LED per second}} = \frac{P_{int} / (h \nu)}{I / e} \quad (1.4)$$

where P_{int} is the optical power emitted from the active region and I is the injection current.

Photons emitted by the active region should escape from the LED die. However, not all the power emitted from the active region is emitted into free space. This is due to several possible loss mechanisms. For example, light emitted by the active region can be reabsorbed in the substrate of the LED or the metallic contact surface. The light extraction efficiency is defined as

$$\begin{aligned} \eta_{extraction} &= \frac{\text{Number of photons emitted into free space per second}}{\text{Number of photons emitted from active region per second}} \\ &= \frac{P / (h \nu)}{P_{int} / (h \nu)} \end{aligned} \quad (1.5)$$

where P is the optical power emitted into free space.

The extraction efficiency [6] can be a severe limitation for high-performance LED. The external quantum efficiency gives the ratio of the number of useful light particles to the number of injected charge particles, which define as

$$\begin{aligned} \eta_{ext} &= \frac{\text{Number of photons emitted into free space per second}}{\text{Number of electrons injected into LED per second}} \\ &= \frac{P / (h \nu)}{I / e} = \eta_{int} \eta_{extraction} \end{aligned} \quad (1.6)$$

1-2 Wafer bonding

1-2-1 The introduce of wafer bonding

The question on why broken pieces of any solid material usually cannot be reversibly rejoined even the matting surfaces are perfectly complementary. The main factors that prevent reversible rejoining appear to be the changes of the surfaces immediately after separation including surface reconstruction, roughening, adsorption, oxidation and contamination that significantly reduce the surface energy or prevent the surfaces from coming in close proximity. Based on this understanding, wafer bonding is introduced that two wafers with mirror-polished, flat and clean wafers of almost any material, when brought into contact at room temperature, are locally attracted to each other by van der Waals forces and adhere or bond to each other. It was found that the standard direct wafer bonding was attributed to relatively weak van der Waals forces and subsequent annealing at high temperature is required to achieve a strong bond. This phenomenon has been known for a long time for optically polished pieces of materials and was first investigated for polished pieces of quartz glass by Lord Rayleigh in 1936 [7]. In the early 1980s almost simultaneously an attempt was made by researchers at Toshiba [8] and IBM [9] to use this room temperature adhesion phenomenon coupled with an appropriate heating step for silicon wafers in order to replace epitaxial growth of thick silicon wafers or to fabricate Silicon-On-Insulator (SOI) structures, respectively. Thus, wafer bonding and layer transfer technology has emerged as one of the fundamental technologies for the fabrication of integrated materials. In order to bond dissimilar materials having different thermal expansion coefficients at wafer level, low temperature bonding is essential. Low

temperature bonding is also crucial for materials having low decomposition temperatures or being temperature sensitive even they are thermally matched. Thus, the necessity of understanding and controlling wafer bonding of dissimilar materials is very important.

1-2-2 The mechanism of wafer bonding

The mechanism of wafer bonding technology includes two-step process, joining and bonding. In the joining operation, the process will pull the two atomically flat surfaces into intimate contact allowing the surrounding areas to achieve Van Der Waals bond. If there are large particles on the surface, the voids will produce between the bonding interfaces. In other words, a 1 μm particle creates a void, which is about 1 mm in diameter [10]. Therefore, the smoothness, flatness and cleanliness of the bonding surface are very important.

It is possible to calculate at least approximately whether wafers with a certain waviness and roughness will bond or not [11]. For these calculations, let us assume gaps between wafers caused by flatness nonuniformity with a lateral extension R (or spatial period $2R$) much larger than their depth (or gap height) h as schematically shown in **Fig. 1-6** [12]. The condition for gap closing depends on the ratio of R to the wafer thickness t_w . For $R > 2t_w$ (Fig. 5a), the condition for gap closing w depends on wafer thickness t_w and is given by

$$h < \frac{R^2}{\sqrt{\frac{2}{3} \frac{E' t_w^3}{\gamma}}} \quad (1.7)$$

where E' is given by $E/(1-\nu)$ with ν being Poisson's ratio. For $R < 2t_w$ (Fig. 5b), the condition for gap closing is independent of wafer thickness t_w and given by

$$h < 3.6 (R\gamma/E^2)^{1/2} \quad (1.8)$$

For the bonding process, the two surface materials are heated to allow covalent bonding after the two surfaces are joined. There are basically three types of bonding within the silicon system. These are oxide bonding, in which one or both surfaces have a grown oxide, hydrophilic, in which both wafers have bare hydrophilic surfaces and hydrophobic in which both wafers have hydrophobic surfaces. Bonding even under reduced pressure low vacuum is helpful in bonding wafers with high surface roughness. Bonding in different atmospheres such as oxygen or nitrogen is also possible. The different behavior of the bonding or surface energy for hydrophobic and hydrophilic silicon wafers as a function of heat treatment temperature for extended times of many days after room temperature bonding in air is shown in **Fig. 1-7**. It can be seen that for hydrophilic surfaces about half of the full bonding energy can be reached already at temperatures around 150°C. An example of a multi-wafer microelectromechanical systems (MEMS) device is fabricated by direct wafer bonding. While devices have been fabricated, bonding failure such as that shown in **Fig. 1-8** [13] is a common problem. As researchers seek to develop more complex multi-wafer MEMS that require bonding thicker wafers with etched features, there is a greater need to understand the mechanics of the direct wafer bonding process and the factors that lead to bonding failure.

1-2-3 The classify of wafer bonding

Wafer bonding techniques can be classified into two categories, direct wafer bonding [10, 14] and intermediate layer bonding. Direct wafer bonding refers to the process of bonding clean, highly polished wafers without an intermediate adhesive layer. The process relies on short-range surface forces to bond the wafers at room temperature and a subsequent thermal treatment to strengthen the bond. The technique is currently employed in the commercial

manufacture of silicon-on-insulator substrates and has been identified as an enabling technology for the fabrication of MEMS [15]. Furthermore, other direct wafer bonding techniques are silicon–silicon fusion bonding [16] and silicon–glass anodic bonding [17]. While these bonding techniques provide high bonding strength and hermetic sealing, they require high temperature processing and even high voltage for anodic bonding.

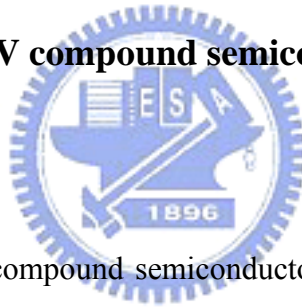
The indirect, intermediate layer bonding includes eutectic bonding [18], solder bonding [19] and adhesive bonding [20]. **Table 1-I** lists these wafer bonding techniques and their main characteristics [21]. Intermediate layer wafer bonding offers several advantages: (1) the bonding temperature is relatively low (below 400°C); (2) the intermediate layer tolerates particles and structures on the wafer surface, hence the surface flatness requirement is considerably lower than that for direct wafer bonding; (3) high bond strength is achievable; (4) wafers of different materials can be joined together.

The eutectic bonding does not require high temperature processing but it requires specific material composition such as silicon (Si) and gold (Au) with eutectic temperature of 363°C to achieve a low eutectic point. In solder bonding, layers of metal or metal-alloy-based solders are used to bond two wafers. Usually metal layers are deposited on both wafers. The metal solders can be applied by sputtering, evaporation, chemical-vapor deposition, electroplating. The wafers are brought into close contact and are heated to the melting temperature of the solder. The solder reflows and wets both wafer surfaces, which causes intimate contact and bonding of the surfaces. A popular solder material is lead-tin (Pb–Sn) solder, which melts at a temperature of 360 °C. The gold-tin (Au–Sn) and tin-copper (Sn–Cu) solders are also suitable solder materials. Any oxides present at the metal surfaces can prevent the wetting of the surfaces with the liquid solder, which causes poor bonding. The advantages of solder bonding are the low bonding temperatures and the ability to join various wafer materials with a hermetic bond. The solder reflow process can also tolerate, to some extent,

particles and structures at the wafer surfaces.

In adhesive bonding, an intermediate adhesive layer is used to create a bond between two surfaces to hold them together. Although successfully used in many industries including airplane, aerospace, and car manufacturing industries to join various similar and dissimilar materials, adhesive bonding did not have a significant role during initial semiconductor wafer bonding research. In contrast to these applications, recent research and development of adhesive wafer bonding involves bonding of large substrates using the well-defined and defect-free intermediate adhesive layers. Recent developments of reliable and high yield adhesive bonding processes have made adhesive wafer bonding a generic and in some cases enabling wafer bonding technique for a variety of applications.

1-3 Applications of III-V compound semiconductor by wafer bonding technology



Wafer bonding of III–V compound semiconductors has become increasingly important as a key technique for fabricating optoelectronic devices. It enables interface formation between different materials, which due to large lattice mismatch, cannot be epitaxially grown on one another without the formation of a high density of threading dislocations. The applied fields involve manufacturing of high brightness LED [22] vertical cavity surface emitting lasers (VCSELs) [23–25]. Bonding of dissimilar III-V compounds is now commercially used for high brightness LED applications and starts to replace the epitaxial growth technology of LED structure grow on GaAs or sapphire substrate. However, wafer bonding of dissimilar materials is complicated by the different thermal expansion coefficients, which can cause severe problems during heating of the bonded wafers to strengthen the bonds at the interface. Wafer bonding of dissimilar materials usually requires annealing temperature and

uniform pressure on each of the wafers [26, 27].

Few examples of wafer bonding of AlGaInP LED is proposed, for instance, Hewlett Packard prepared the AlGaInP LED using a wafer-bonding technique at $\sim 600^{\circ}\text{C}$ that replaced the GaAs substrate with a GaP transparent substrate (TS) [28]. The bonding flowchart is shown in **Fig. 1-9**. They demonstrate the feasibility of wafer bonding 75-mm diameter GaP-AlGaInP epitaxial films to GaP substrates and the product had in high volume manufacturing. Another wafer-bonding approach was to bond an AlGaInP LED structure onto an Au/AuBe/SiO₂/Si mirror substrate (MS) with bonding temperature of 300°C [29-31]. These studies have demonstrated high efficiency and reliability in LED performance. **Figure 1-10** show the GaAs substrate (AS) and TS LED [32].

Moreover, the heat dissipation of the sapphire substrate is also poor, so the GaN-based LED are generally operated at low injection current. These problems can be solved by transferring GaN LED onto Si [33-34] or Cu substrates [35]. Much of this investigation is focused on the intermetallic bonding.

In this work, some approaches to enhance the performance of AlGaInP and InGaN-GaN LED will be proposed.

1-4 Organization of this dissertation

The primary objective of this dissertation is provided some approaches to enhance the performance of AlGaInP and InGaN-GaN LED. It could using wafer-bonding technology to transfer AlGaInP or GaN thin film on the high conductivity substrate. Furthermore, InGaN-GaN LED with roughening both the p-GaN surface and the undoped-GaN surface by double transfer methods and applying a mirror coating to the sapphire substrate have also demonstrated.

There are six chapters in this dissertation. In chapter 1, the background theory for light emitting diode and the mechanism of wafer bonding and the applications of III-V compound semiconductor by wafer bonding technology will be introduced.

In chapter 2, high-power LED fabricated on Cu and SiC substrates were investigated. The AlGaInP LED structure was bonded to a Cu substrate by using indium-tin-oxide (ITO) as the diffusion barrier layer. It was found that Cu-substrate-bonded LED devices could be operated in a much higher injection forward current than that used in traditional GaAs-substrate LED and the degradation of the luminescence-output intensity was less than 5 % after 500 hours of life test as shown in section 2-2. In section 2-3, the AlGaInP LED with SiC substrate by wafer bonding was proposed. It was found that the luminous intensity and saturation current of SiC-substrate LED was much higher than that of GaAs-substrate LED which due to the reason of the high reflectivity mirror and high conductivity substrate.

In chapter 3, vertical InGaN-GaN LED epitaxial films were successfully fabricated on a 50mm Si substrate using glue bonding and laser lift-off technology. A high-temperature stable organic film, rather than a solder metal, was used as the bonding agent. It was found that the light output of the vertical InGaN LED chip exceeded that of the conventional sapphire-substrate LED by about 20% at an injection current of 20 mA. The vertical InGaN LED operated at a much higher injection forward current than were sapphire substrate LED. Furthermore, the vertical InGaN LED remain highly reliable after 1000 h of testing.

In chapter 4, an InGaN-GaN light emitting diode (LED) with double roughened (p-GaN and undoped-GaN) surfaces was fabricated by surface-roughening, wafer-bonding and laser lift-off technologies. It was found that the frontside and backside luminance intensity were higher than that of the conventional LED. This is because the double roughened surfaces can provide photons multiple chances to escape from the LED surface, and redirect photons, which were originally emitted out of the escape cone, back into the escape cone as shown in

section 4-2. Furthermore, the effect of the roughness of the undoped-GaN layer on the performance of double roughened LED was also investigated in section 4-3. It was found as the root mean square (rms) roughness of undoped-GaN layer increased, the output power and the view angle would be increased and decreased, respectively.

In chapter 5, an InGaN-GaN LED with a roughened undoped-GaN surface and a silver mirror on the sapphire substrate was successfully fabricated through a double transfer method. It was found that, at an injection current of 20 mA, its luminance intensity and the output power was larger than conventional LED's.

Finally, the summary of the overall results and the future work was shown in chapter 6.



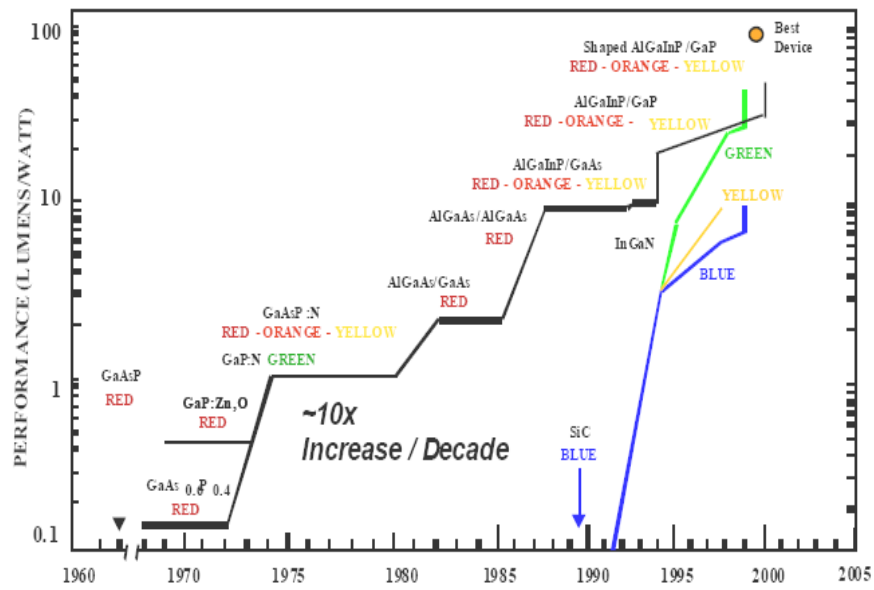


Fig. 1-1. The evolution of light emitting diodes.
 [Quoted from Stringfellow et al.]

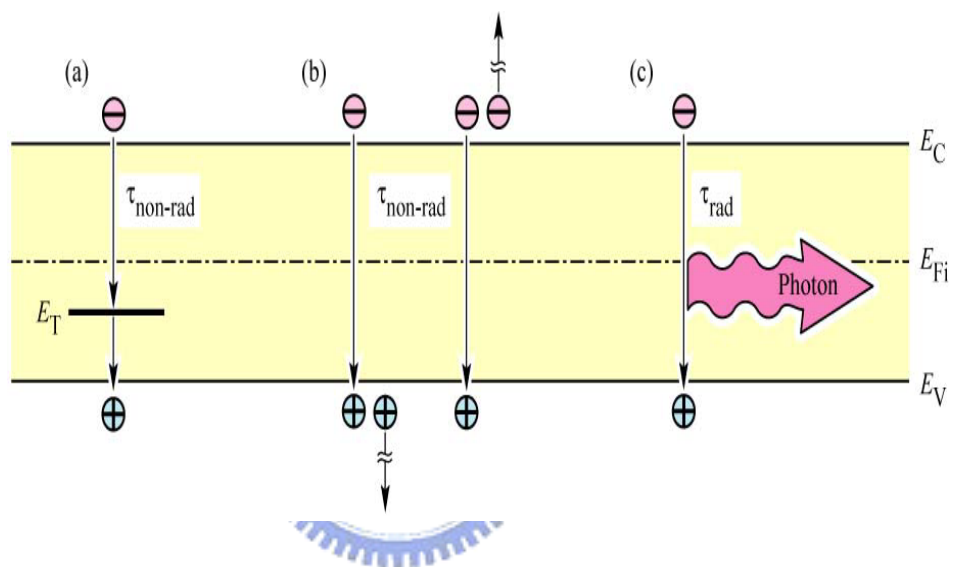
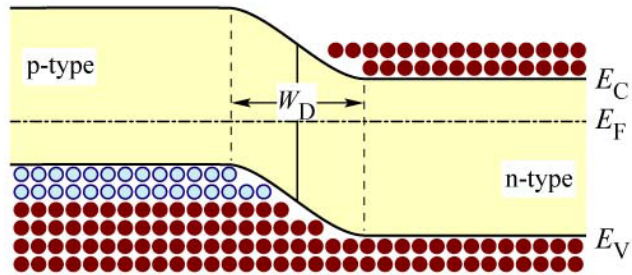
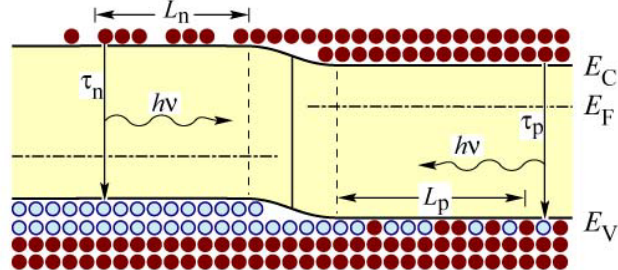


Fig. 1-2. Band diagram illustrating non-radiative recombination (a) via a deep level (b) via an Auger process and (c) radiative recombination. [5]

(a) Homojunction under zero bias



(b) Homojunction under forward bias



(c) Heterojunction under forward bias

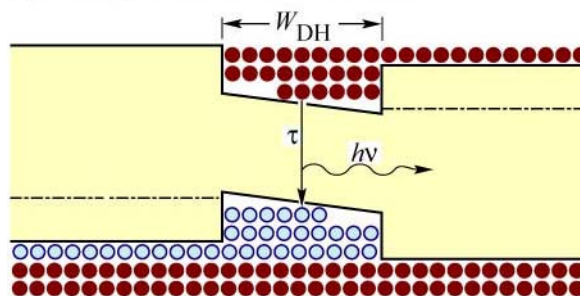


Fig. 1-3. Band structure near a semiconductor p-n junction: (a) homojunction under zero bias, (b) homojunction and (c) heterojunction under forward bias. [5]

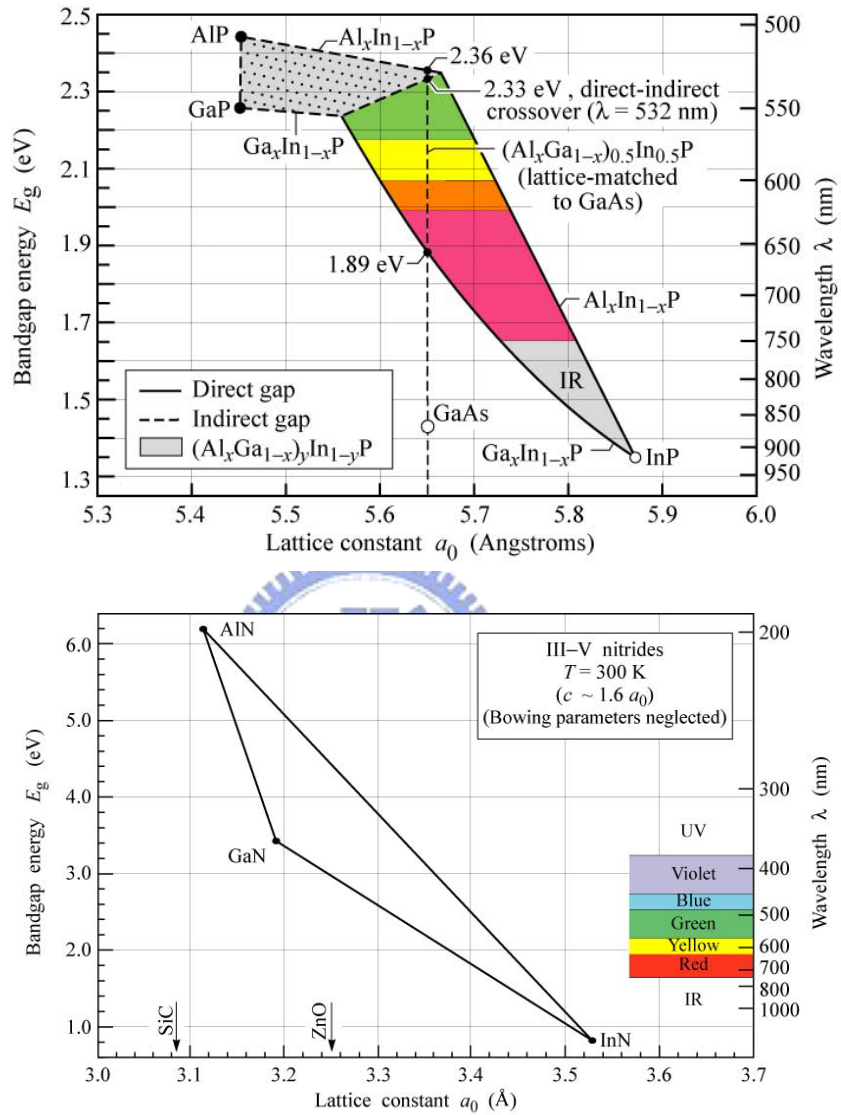


Fig. 1-4. The bandgap energy and corresponding wavelength versus lattice constant of AlGaInP and InGaIn system at room temperature. [5]

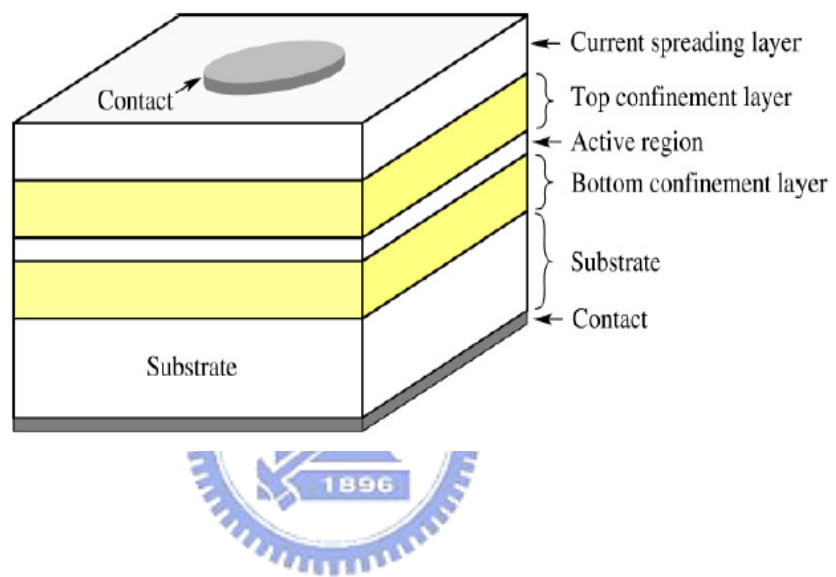


Fig. 1-5. The schematic of a typical surface-emitting LED.

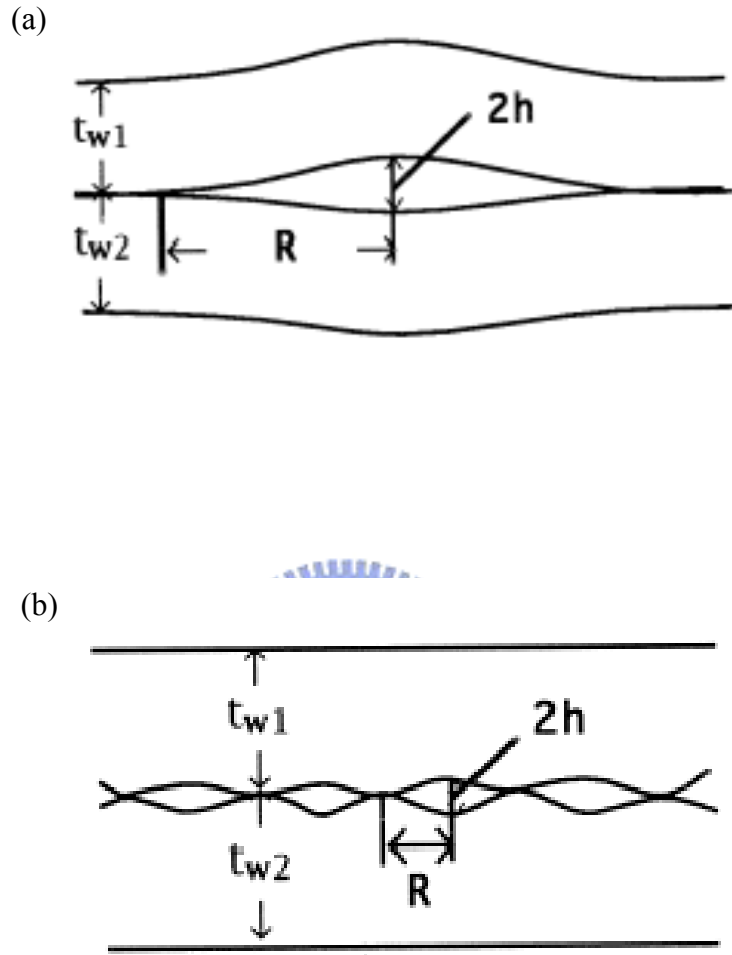


Fig. 1-6. Schematic of surface waviness. (*U. Gosele et al.*)

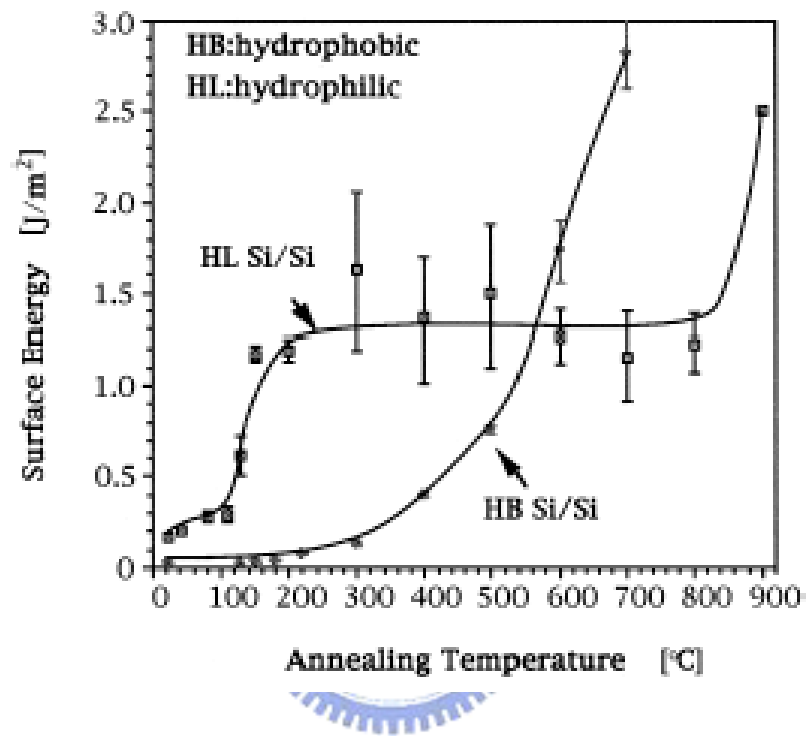


Fig. 1-7. Saturation values of surface or bonding energy measured by the crack opening method as a function of temperature after long-time heat treatments (up to 100 h) [10].

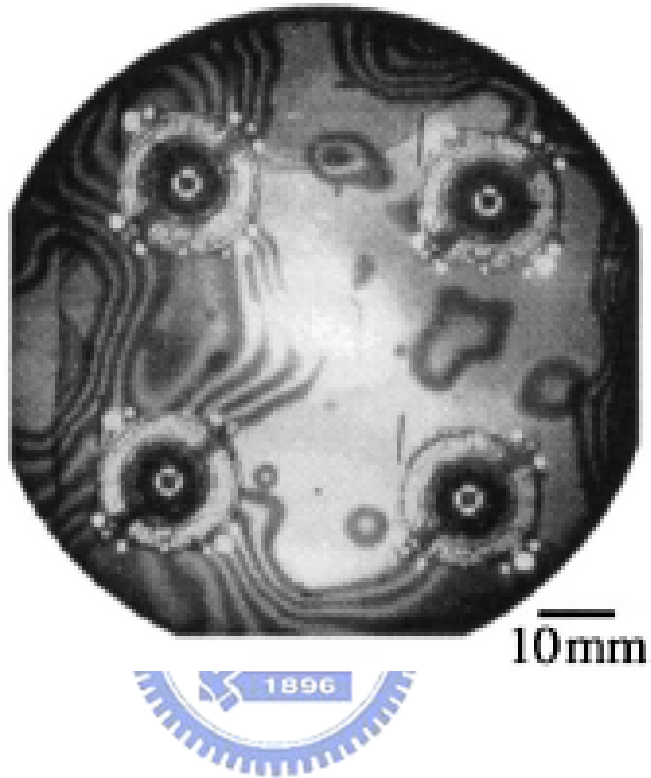


Fig. 1-8. An infrared transmission image of a wafer with four devices showing bonding failure during fabrication of the device. The fringes and dark regions indicate un-bonded areas. [8]

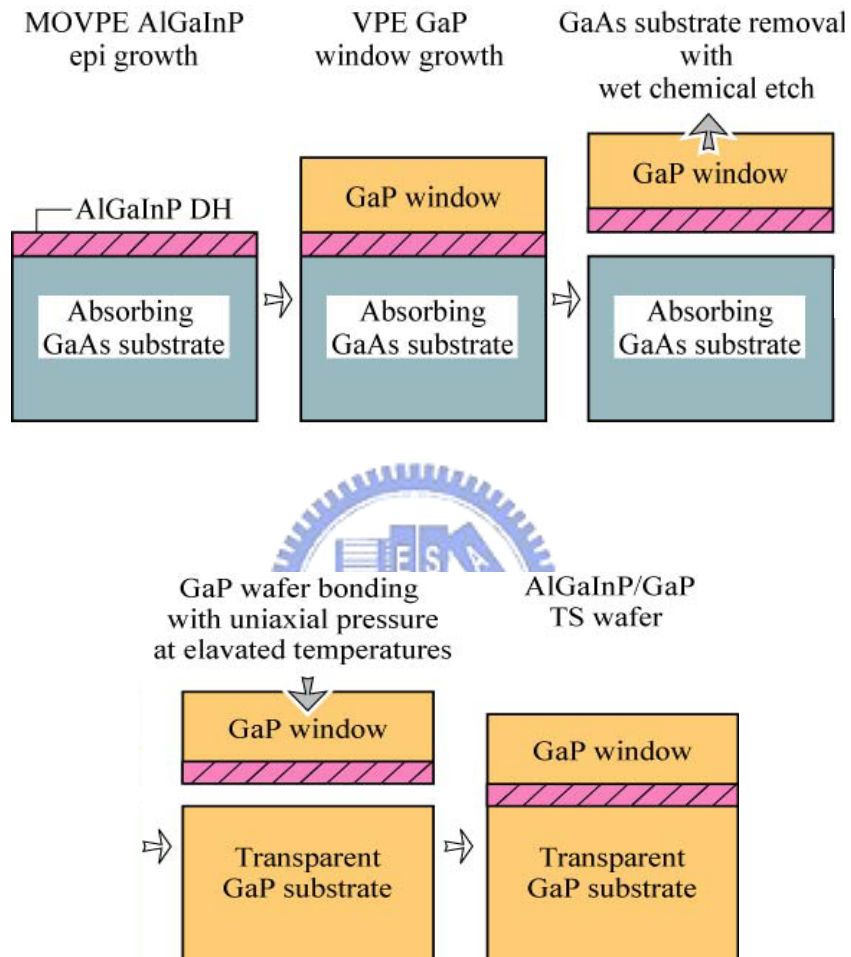


Fig. 1-9. The bonding flowchart of AlGaInP LED with a GaP transparent substrate (TS). [18]

(a) AS LED



(b) TS LED

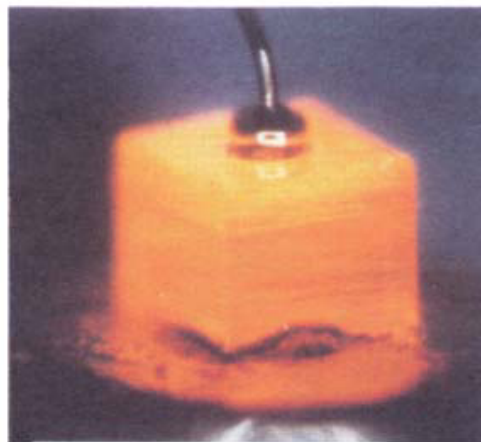


Fig. 1-10. The LED chip of (a) GaAs substrate LED and (b) GaP transparent substrate LED. [32]

Wafer bonding technique	Typical bonding conditions	Advantages and disadvantages	Application areas
Direct bonding	600–1200 °C Room-temperature schemes have been reported Small or no bond pressure	+ high bond strength + hermetic + resistant to high temperatures – high surface flatness required – high bond temperatures not always compatible with electronic wafers	SOI wafer fabrication
Anodic bonding	150–500 °C 200–1500 V No bond pressure	+ high bond strength + hermetic + resistant to high temperature – bond temperatures in combination with voltage not always compatible with electronic wafers	Sensor packaging
Solder bonding	150–450 °C Low bond pressure	+ high bond strength + hermetic + compatible with electronic wafers – solder flux	Bump and flip-chip bonding
Eutectic bonding	200–400 °C Low to moderate bond pressure	+ high bond strength + hermetic + compatible with electronic wafers – sensitive to native oxides at surfaces	Hermetic packaging Bump and flip-chip bonding
Adhesive bonding	Room temperature up to 400 °C Low to moderate bond pressure	+ high bond strength + low bond temperature + works practically with any substrate material including electronic wafers – no hermetic bonds – limited temperatures stability	MEMS, Sensor packaging, 3D-ICs, temporary bonds

TABLE I. Commonly used wafer-bonding techniques. [21]

Chapter 2 High power AlGaInP light emitting diode with Cu and SiC substrate fabricated by wafer bonding

2-1 Introduction

The epitaxial growth techniques have significantly improved the brightness and efficiency of light-emitting diodes (LED). These improvements, along with higher reliability, lower costs, and the inherent properties of solid-state devices for low-voltage operation have enabled LED to be applied widely in solid-state lighting and displays. LED operating in the wavelength region ranging from red to green light have been employed by the AlGaInP alloy system grown on GaAs substrates [1]. However, its use in high-efficiency applications has been limited because of the substrate absorption and the internal reflection. Fortunately, the wafer bonding process can solve these problems. For instance, Hewlett Packard prepared the AlGaInP LED using a wafer-bonding technique that replaced the GaAs substrate with a GaP transparent substrate (TS) [2-4]. Another wafer-bonding approach was to bond an AlGaInP LED structure onto an Au/AuBe/SiO₂/Si mirror substrate (MS) [5-7]. These studies have demonstrated high efficiency and reliability in LED performance. Nevertheless, despite improving luminous efficiency, LED sources are limited to use in low power applications due to the low thermal conductivity of the substrate. To achieve higher light output performance, it is necessary to drive the LED at a higher current. In this study, AlGaInP LED with wafer-bonded on Cu substrates and SiC substrate were proposed. The performances of the bonded LED were also been investigated.

2-2 Cu-substrate LED

2-2-1 Experiments

The AlGaInP MQW LED structures were grown on GaAs substrates through low-pressure metalorganic chemical vapor deposition (MOCVD). The LED structure consisted of an n-GaAs buffer layer, an n-InGaP etching stop layer, an n-GaAs ohmic contact layer, an AlInP n-cladding layer, an undoped $(\text{Al}_{0.15}\text{Ga}_{0.85})_{0.5}\text{In}_{0.5}\text{P}$ MQW active region, an AlInP p-cladding layer, and a p-GaP window layer. An ITO layer was deposited on the AlGaInP LED to act as a current-spreading layer. On the other hand, the host Cu substrate played the role of a heat sink substrate. These two wafers were cleaned in acetone and isopropyl alcohol with ultrasonic agitation, followed by rinsing in de-ionized (DI) water. Next, the copper substrate was etched in a solution of 1HCl: 10H₂O to remove the oxide layer from the surface; the substrate was then rinsed in DI water. Following the surface treatment, the samples were dried by nitrogen gas and placed in contact with each other immediately using a designed fixture [8] that ensured uniform pressure on each of the wafers. Then, the fixture was loaded into a furnace and annealed at temperatures varying from 400°C to 600°C for 30 min in argon ambient. After the wafers were removed and were allowed to cool to room temperature, the absorbing GaAs substrate and the InGaP etching stop layer were removed by chemical etching in solutions of 1NH₄OH: 10H₂O₂ and 1HCl: 10H₂O, respectively. The fused epilayer was mesa-etched into isolated devices with $250 \times 250 \mu\text{m}^2$ area. The Au/AuGe dots with a diameter of 100 μm were deposited onto the n-side (n⁺-GaAs contact layer) and then alloyed for ohmic contact metalizations. It should be noted that the Cu substrate is a conductor, which can act as p-side contact; thus it is not necessary to deposit

any metal for p-side contact. In comparison, the LED samples with the GaAs and Cu substrates were prepared from the same AlGaInP LED epitaxial material, and the samples described here were only cut into chips without encapsulation before electrical and optical measurements. Room-temperature current–voltage (I – V) measurements were taken with a KEITHLEY 4200 semiconductor characterization system. The electroluminescence (EL) characteristics of these fabricated LED were recorded by injecting DC currents into the LED.

2-2-2 Results and Discussion

Figure 2-1 shows a successful sample of an AlGaInP LED wafer bonded on a Cu substrate at 500°C for 30 min. After removing the GaAs substrate, no peeling or cracks were observed on the mirror-like surface despite the large difference between the thermal expansion coefficients of GaAs ($6.86 \times 10^{-6}/^{\circ}\text{C}$) and Cu ($16.8 \times 10^{-6}/^{\circ}\text{C}$). The fused epilayer then was mesa-etched into isolated devices, deposited with contact dots, and then alloyed for ohmic contact metalizations.

Figure 2-2 shows the cross section image of this bonded LED structure. Neither cavity nor unbonded area was found on the bonded interface. The Auger depth profiles of AlGaInP LED/ ITO/ Cu substrate are shown in **Fig. 2-3**. It revealed no Cu element diffused into the AlGaInP active layer of LED structure. For the purpose of comparison, an ITO-free AlGaInP LED substrate was also bonded to Cu substrate at same condition. The Cu element was found to diffuse into the AlGaInP LED structure and destroy the LED structure. The results indicated that ITO layer employed here not only acted as a current spreading layer but also a barrier layer.

When ITO film was used as the bonding intermediate layer, it was also found that the bonding temperature would affect the bonding yield of the Cu-substrate LED. The sample did

not bond at temperatures below 400°C. At temperatures greater than 400°C, the bonded area increased when temperature increased as a result of both the reaction and diffusion rates increasing with temperature. However, when bonding temperature reached 600°C, the Cu element could penetrate through the ITO layer and destroy the LED structure.

Figure 2-4 presents the current versus voltage (I - V) of the Cu-substrate LED bonded at 500°C for 30 min. The device exhibited normal p - n diode behavior with a forward voltage of 1.96 V at 20 mA, which was similar to that of GaAs-substrate LED. This indicated that the wafer-bonding process did not degrade the performance of LED. It is worthy to note that the series resistance of Cu-substrate LED (1~2 Ω) is lower than that of GaAs-substrate LED (5-7 Ω) [9]. A small series resistance is the most important factor for decreasing the Joule heating effect, thus it indicates an increase in the quantum efficiency of the LED.

The effects of heat sink observed in high power LED are very important with regard to the removal of heat from LED devices. The performance of the LED would otherwise degrade when the operation temperature increased. **Figure 2-5** shows the peak spectral wavelength as a function of the DC drive current. During the test conditions, these two LED samples, which had been cut into chips without encapsulating, were put on a metal chunk. The data shows that the emission peak wavelengths shift toward longer wavelengths with increasing DC drive current, which is caused by the joule heating. Unlike the 4nm red shift exhibited at 170 mA in GaAs-substrate LED, the Cu-substrate LED devices exhibits a more favorable 2 nm red shift at 170 mA. The red shift of the emission wavelength occurred as the temperature increased. From the shift in emission wavelength and a wavelength shift with temperature of 0.096 nm/°C for 620 nm AlGaInP LED [10], it could be estimated that the thermal resistance of the Cu-substrate LED was approximately 60 °C/W smaller than that of GaAs-substrate LED. Thus the temperature of GaAs-substrate LED was about 20°C higher than that of the Cu-substrate LED at the forward current of 170 mA.

Figure 2-6 shows the effects of injection current on the luminous intensity of the conventional GaAs-substrate LED and the Cu-substrate-bonded LED. When the injection current was less than 100 mA, the luminous intensities of two samples were the same, meaning that the wafer-bonding process did not degrade the performance of Cu-substrate LED. When the injection current reached 100 mA, the GaAs-substrate LED were saturated at the luminous intensity of 400 mcd. However, the intensity of the Cu-substrate LED did not saturate at 100 mA. The maximum luminous intensity of Cu-substrate LED could reach as high as about 1230 mcd at 800 mA, which was three times higher than the saturation intensity of the GaAs-substrate LED at 100 mA. It was obvious that the luminous intensity of Cu-substrate LED was much higher than that of GaAs-substrate LED.

These results were due to a much smaller series resistance of the Cu-substrate LED as compared with GaAs-substrate LED, thereby reducing the total amount of joule heating. Since the reduction of the joule heating would increase the quantum efficiency of the LED. Therefore, Cu-substrate LED had a smaller red shift, and could be driven at a higher current and therefore obtain a higher luminous intensity. This difference might also be a result of the disparity between their respective thermal conductivities; the thermal conductivity of Cu ($401 \text{ Wm}^{-1}\text{K}^{-1}$) is nine times higher than that of GaAs ($46 \text{ Wm}^{-1}\text{K}^{-1}$). Therefore, by using these wafer bonding techniques to bond LED to Cu substrates, the joule-heating problem in conventional LED can be significantly reduced.

The other important issue of the Cu-substrate LED is the reliability. Copper is an impurity long known to cause strong degradation in LED [11]. The efficiency of Cu-contaminated LED would significantly decrease after life test. In this study, the life test of Cu-substrate LED was performed at forward current of 20 mA in room temperature, corresponding to 32 A/cm^2 . As shown in **Fig. 2-7**, the degradation of the luminescence-output intensity was less than 5 % after 500 hours of life test.

2-3 SiC-substrate LED

2-3-1 Experiments

The AlGaInP MQW LED structures were grown on GaAs substrates through low-pressure metalorganic chemical vapor deposition (MOCVD). An Au/AuBe/Au layer was deposited on the AlGaInP LED to act as an ohmic contact and mirror layer. On the other hand, the bonding metals of Ti/Au/In were deposited on the host SiC substrate that played the role of a heat sink substrate. The thermal conductivity of single crystal SiC substrate was $370 \text{ Wm}^{-1}\text{K}^{-1}$. The purpose of choosing the indium as the bonding metal between the LED structure and SiC was to achieve good bonding yield of bonded-sample during low temperature ($< 300^\circ\text{C}$). These two wafers were cleaned in acetone and isopropyl alcohol with ultrasonic agitation, followed by rinsing in de-ionized (DI) water. Following the surface treatment, the samples were dried by nitrogen gas and placed in contact with each other immediately using a fixture that ensured uniform pressure on each of the wafers. Then, the fixture was annealed at temperatures of 250°C for 60 min. After the wafers were removed and were allowed to cool to room temperature, the absorbing GaAs substrate and the InGaP etching stop layer were removed by chemical etching in solutions of $1\text{NH}_4\text{OH}: 10\text{H}_2\text{O}_2$ and $1\text{HCl}: 10\text{H}_2\text{O}$, respectively. The fused epilayer was mesa-etched into isolated devices with $300 \times 300 \mu\text{m}^2$ area before the ITO layer was deposited on the n-GaAs ohmic contact layer. The Cr/Au with a diameter of $100 \mu\text{m}$ and Ti/Au were deposited onto the ITO layer and the backside of SiC substrate, respectively. Following the wafer was alloyed for ohmic contact metalizations. **Figure 2-8** shows the schematic diagram of the flowchart bonded LED. In comparison, the LED samples with the GaAs and SiC substrates were prepared from the

same AlGaInP LED epitaxial material, and the samples described here were only cut into chips without encapsulation before electrical and optical measurements.

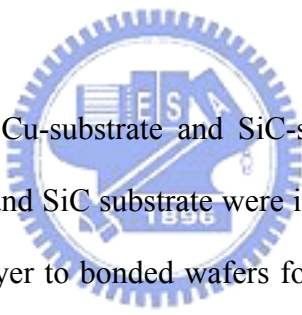
2-3-2 Results and discussion

Figure 2-10 presents the current versus voltage (I - V) of the SiC-substrate LED bonded at 250°C for 60 min. The device exhibited normal p - n diode behavior with a forward voltage of 2.1V at 20 mA with the chip size of $300 \times 300 \mu\text{m}^2$. This indicated that the wafer-bonding process did not degrade the performance of LED. **Figure 2-11** shows the effects of injection current on the luminous intensity of the conventional GaAs-substrate LED and the SiC-substrate-bonded LED. When the injection current was 20 mA, the luminous intensities of SiC-substrate LED (248 mcd) was higher than that of conventional LED (77 mcd), indicating that the wafer-bonding process did not degrade the performance of SiC-substrate LED and the Au/BeAu/Au mirror provide a high reflectivity to enhance the light intensity as shown in **Fig. 2-9**. When the injection current reached 90 mA, the GaAs-substrate LED were saturated at the luminous intensity of 190 mcd. However, the intensity of the SiC-substrate LED did not saturated at 100 mA. The maximum luminous intensity of SiC-substrate LED could reach as high as about 4300 mcd at 650 mA, which was about twenty times higher than the saturation intensity of the GaAs-substrate LED at 100 mA. It was obvious that the luminous intensity of SiC-substrate LED was much higher than that of GaAs-substrate LED.

Figure 2-12 shows the peak spectral wavelength as a function of the DC drive current. The data shows that the emission peak wavelengths shift toward longer wavelengths with increasing DC drive current, which is caused by the joule heating. Unlike the 13nm red shift exhibited at 90 mA in GaAs-substrate LED, the Cu-substrate LED devices exhibits a more

favorable 1 nm red shift at 90 mA. The red shift of the emission wavelength occurred as the temperature increased. From the shift in emission wavelength and a wavelength shift with temperature of 0.096 nm/°C for 620 nm AlGaInP LED [10], it could be estimated the temperature of GaAs-substrate LED was about 125°C higher than that of the SiC-substrate LED at the forward current of 90 mA. This difference might also be a result of the thermal conductivities; the thermal conductivity of 4H-SiC ($370 \text{ Wm}^{-1}\text{K}^{-1}$) is eight times higher than that of GaAs ($46 \text{ Wm}^{-1}\text{K}^{-1}$). Therefore, by using these wafer bonding techniques to bond LED to SiC substrates, the joule-heating problem in conventional LED can be also significantly reduced.

2-4 Summary



In summary, high-power Cu-substrate and SiC-substrate LED fabricated by bonding AlGaInP LED structure to Cu and SiC substrate were investigated in this study. An ITO film was used as an intermediate layer to bonded wafers for the Cu-substrate LED. It was found that the sample did not bond at temperatures below 400°C. When bonding temperature reached 600°C, the Cu element diffused through the ITO layer and destroyed the LED structure. Fortunately, Cu did not penetrate the ITO layer when samples were bonded at 500°C for 30 minutes, and the high-power Cu-substrate LED were successfully fabricated. In Cu-substrate LED, the joule heating exhibited in conventional GaAs-substrate LED was significantly reduced because the Cu substrate has larger thermal conductivity and lower thermal resistance as compared with GaAs substrate. It was found that Cu-substrate LED could be operated in a much higher injection forward current, 800 mA, which was eight times higher than that used in GaAs-substrate LED. The luminous intensity of the Cu-substrate LED could reach as high as 1230 mcd, which was three times higher than that of the

GaAs-substrate LED. For the SiC-substrate-bonded LED, the luminous intensity of SiC-substrate LED was 3.2 times higher than that of conventional LED at the injection current of 20 mA. The improvement of the emission of light could be reflected downward using a mirror with reflectivity of 87 % at 620 nm. The saturation current could reach at 650 mA, which was better than GaAs-substrate LED.



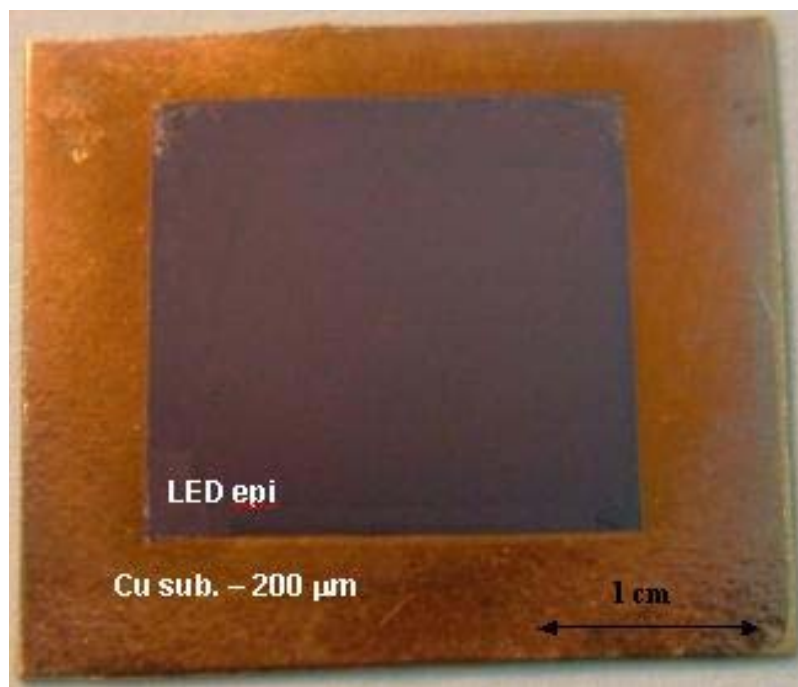


Fig. 2-1. A successful Cu-substrate-bonded LED sample.

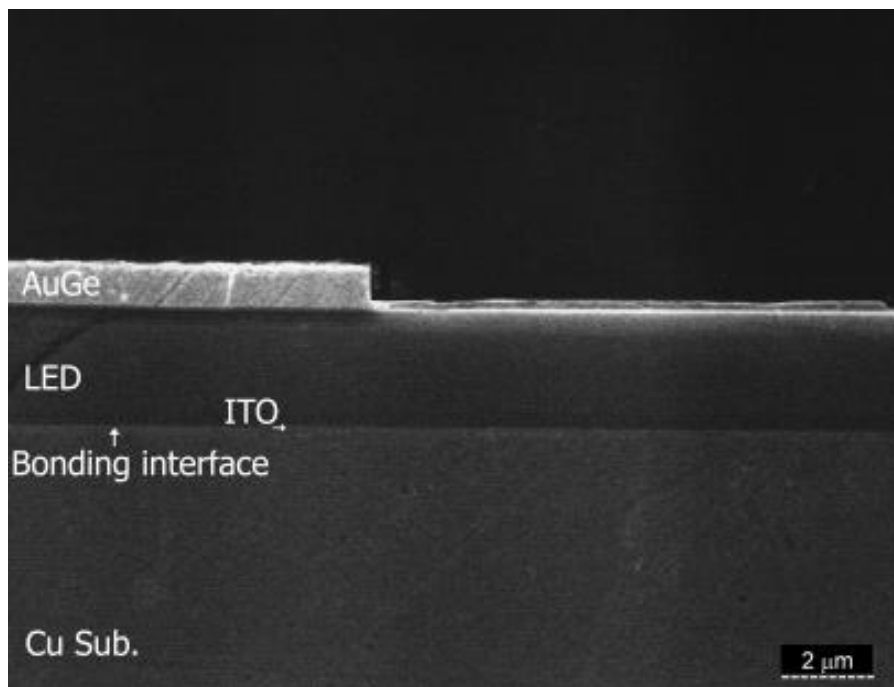


Fig. 2-2. A scanning electron micrograph of the cross section of the LED structure.

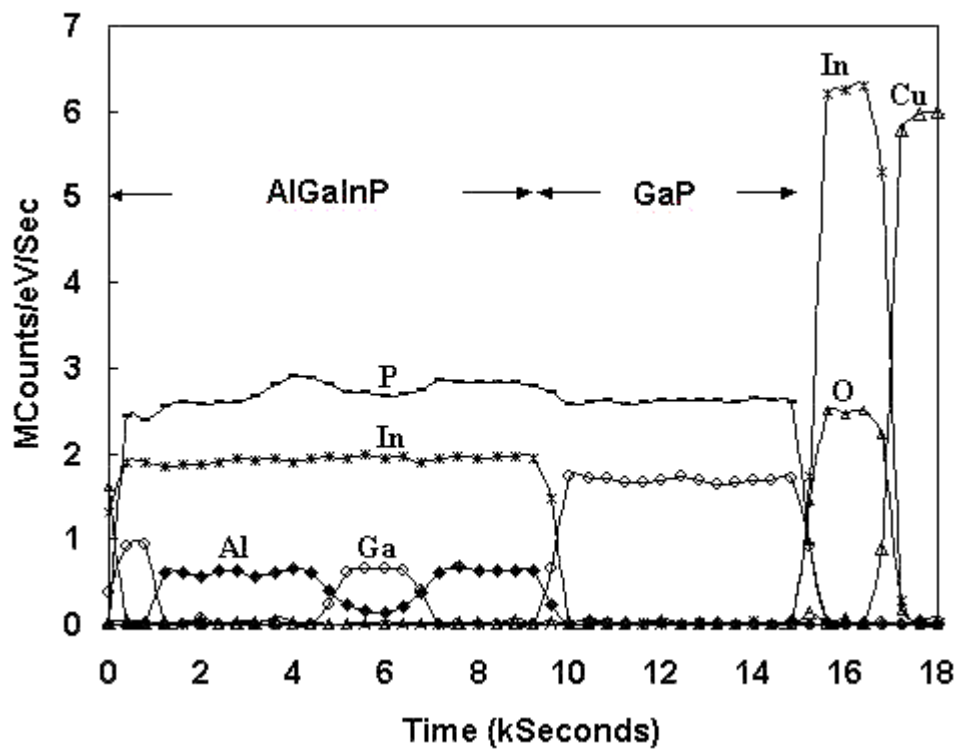


Fig. 2-3. Auger depth profiles of AlGaInP LED/ ITO-Cu sample bonded at 500°C for 30 minutes.

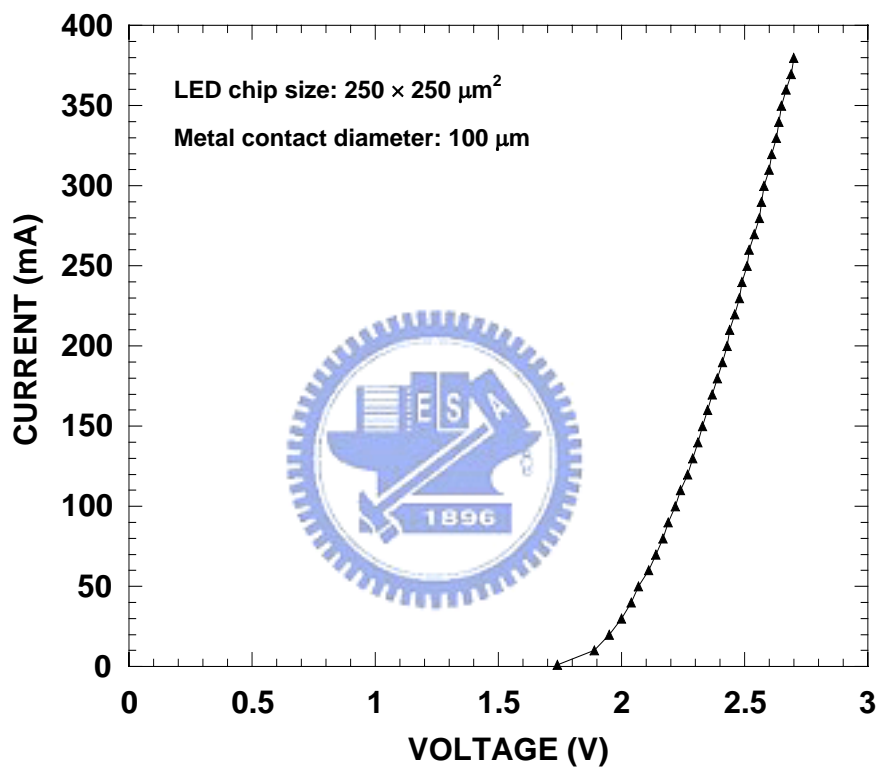


Fig. 2-4. Current-voltage characteristic of the Cu-substrate-bonded LED devices fabricated by wafer bonding technology.

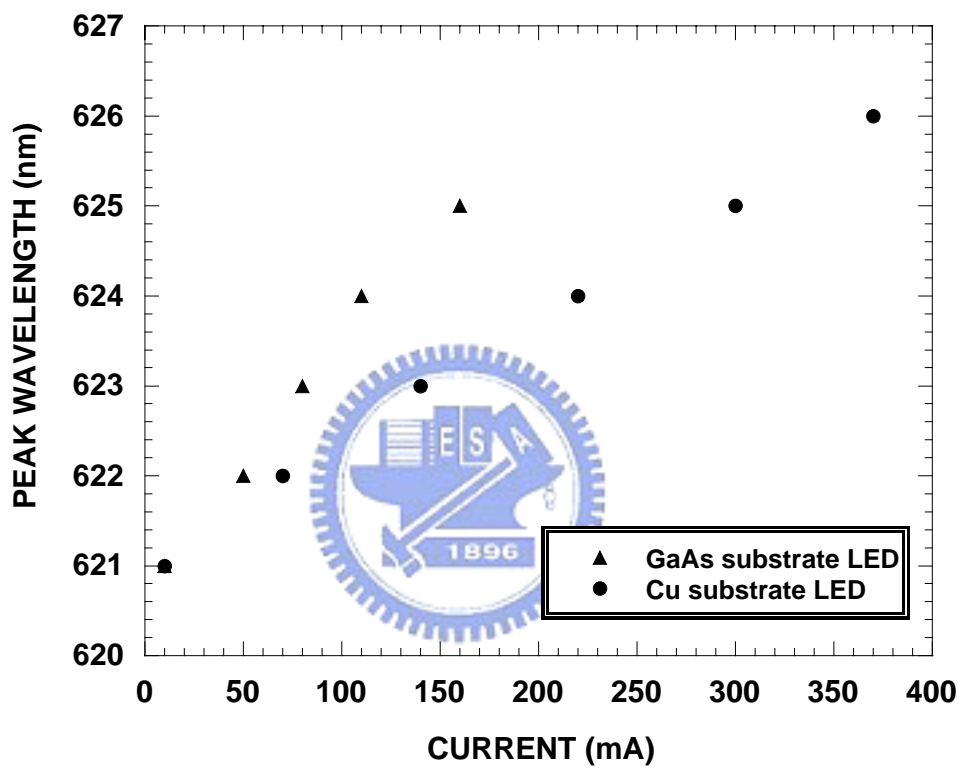


Fig. 2-5. Peak spectral wavelength against DC injection current for the LED with a GaAs substrate and a Cu substrate.

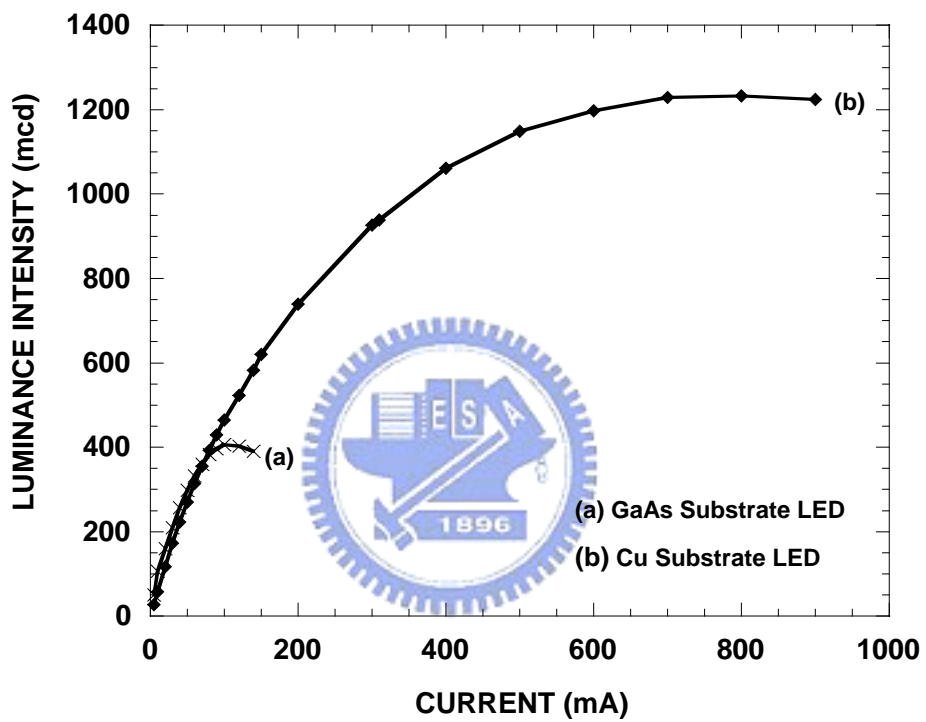


Fig.2-6. $L-I$ curves for conventional GaAs-substrate LED and Cu-substrate LED.

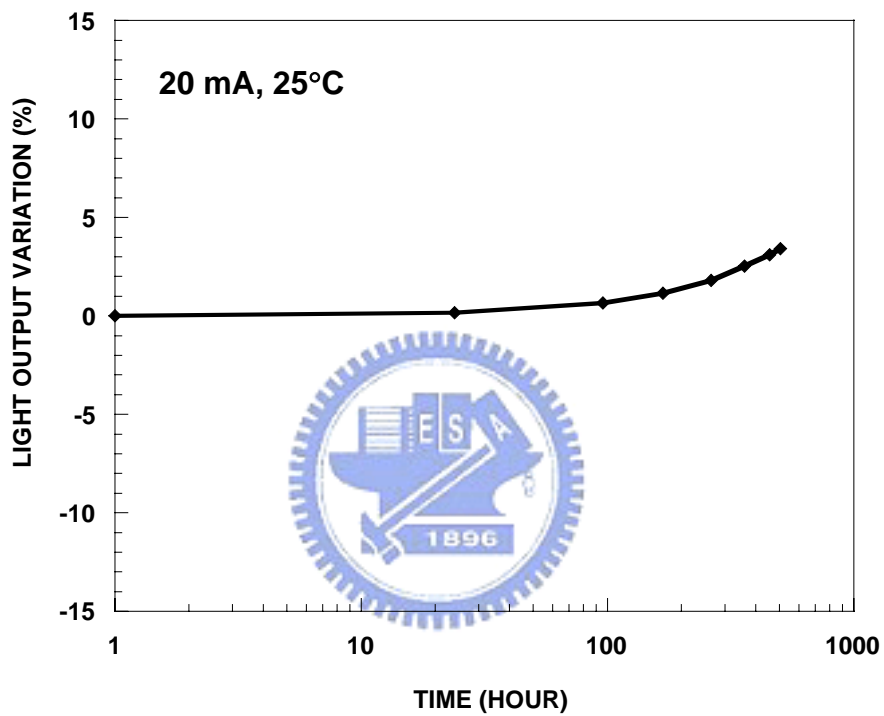


Fig. 2-7. Luminescence-output intensity variation as functions of time. During this life test measurement, a 20 mA current was injected into the Cu-substrate LED at room temperature.

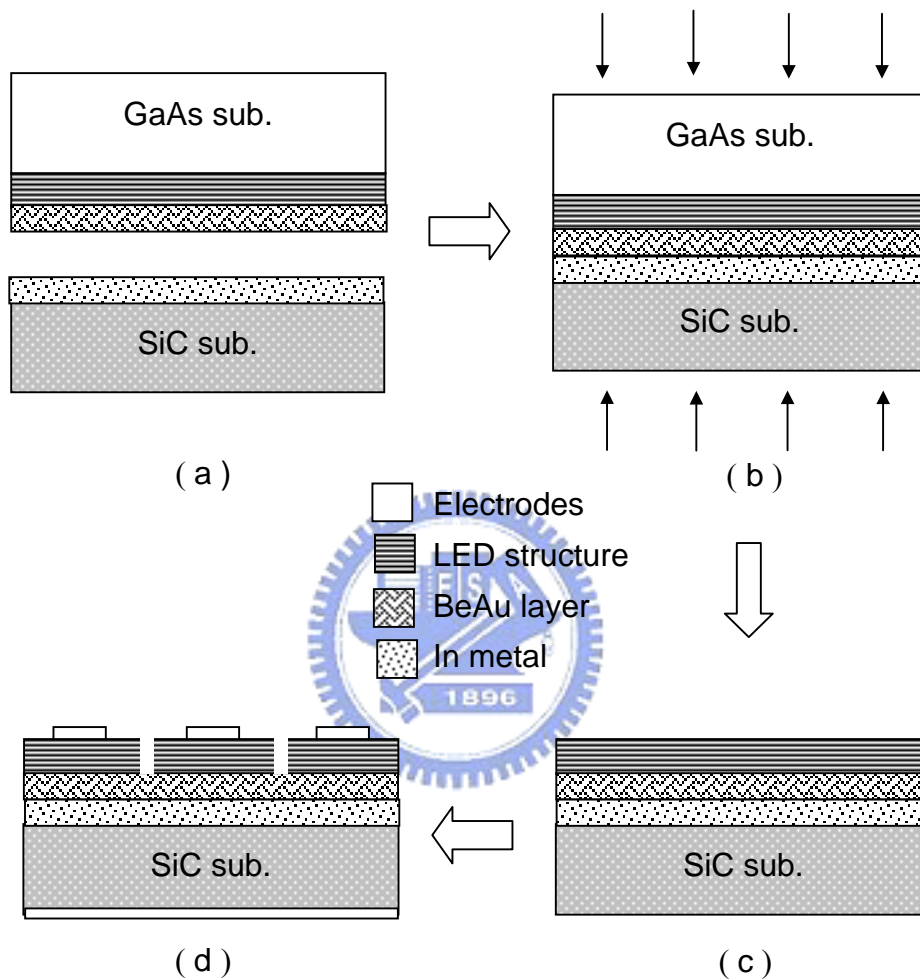


Fig. 2-8. Schematic diagram of the LED/ metal/ SiC wafer fusion process: (a) SiC substrate and LED wafer with In and BeAu metal; (b) wafer bonding process; (c) removal of GaAs substrate and etch stop layer; and (d) mesa-etched and electrodes deposition.

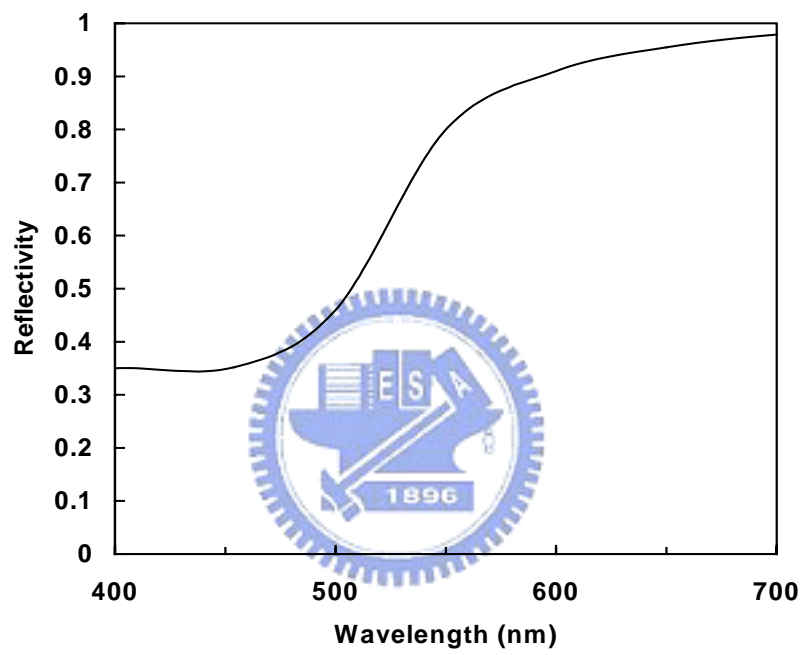


Fig. 2-9. The reflectivity of the BeAu/Au mirror.

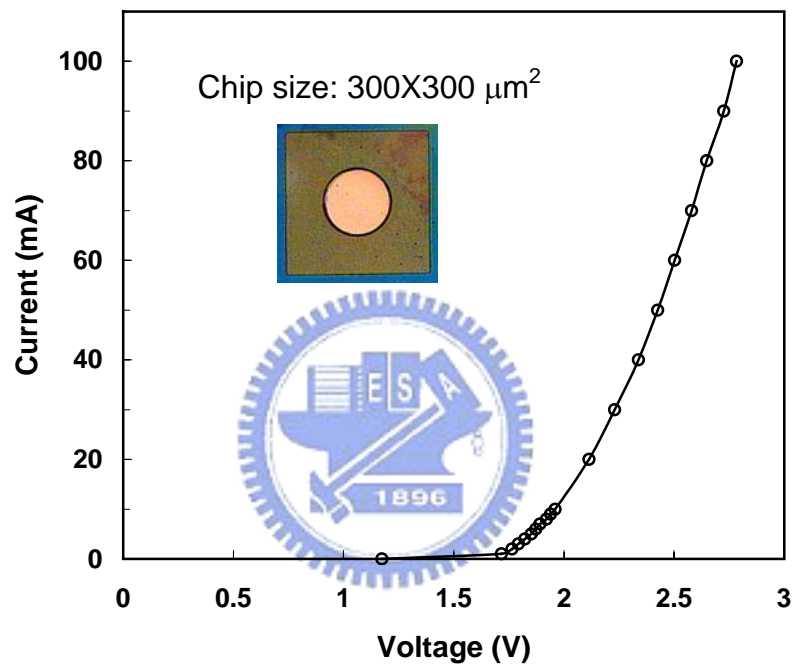


Fig. 2-10. The I-V characteristics of SiC-substrate LED.

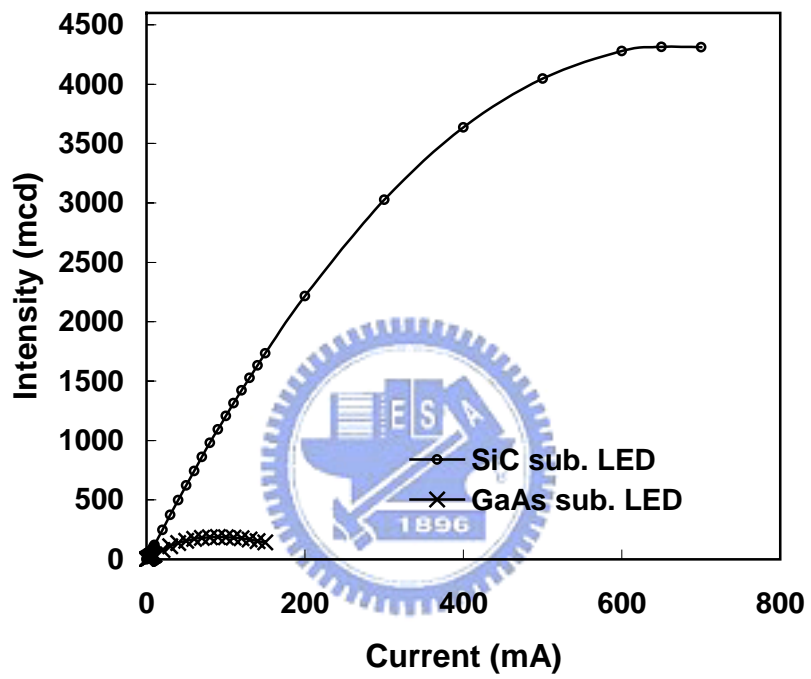


Fig. 2-11. The L-I curves of conventional GaAs-substrate LED and SiC-substrate LED.

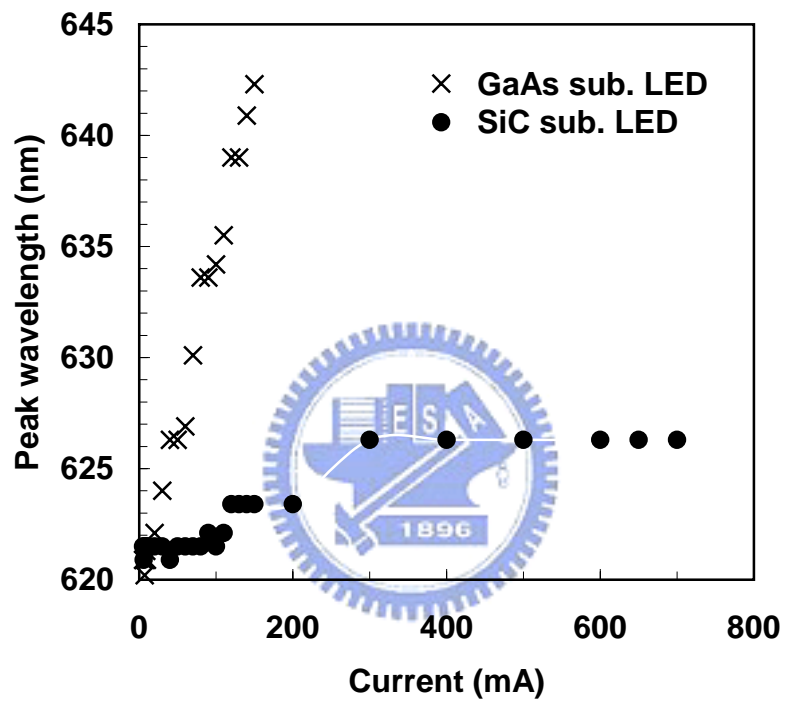


Fig. 2-12. Peak spectral wavelength against DC injection current for the LED with a GaAs substrate and a SiC substrate.

Chapter 3 Performance of InGaN-GaN light emitting diode fabricated using glue bonding on 50mm Si substrate

3-1 Introduction

High-brightness GaN-based light-emitting diode (LED) has attracted considerable attention for their versatile applications in mobile phones, full-color displays and lighting [1]. Although the development of these GaN-based LED is very successful, the poor conductivity of p-GaN limits the performance of LED because of current crowding [2]. This problem can be solved using a thin Ni/Au layer or a highly transparent (> 80%) indium tin oxide (ITO) layer as a current spreading layer [3]-[4]. However, the poor electrical characteristics (electrical resistivity = $10^{11} - 10^{16}$ ohm-cm) of the nonconducting sapphire substrate necessitate the need for p- and n- metal electrodes on the top surface of the devices. Hence, some of the active layer in the n-contact region is sacrificed. Moreover, the heat dissipation of the sapphire substrate is also poor, so the GaN-based LED are generally operated at low injection current. These problems can be solved by transferring GaN LED onto Si [5]-[6] or Cu substrates [7]. Much of this investigation is focused on the intermetallic bonding. In this work, an n-side-up InGaN LED with vertical electrodes was fabricated by glue bonding. A high-temperature stable organic film is utilized as the bonding agent to prevent any possible reaction with the metal reflector.

3-2 Device Fabrication

A 50mm sapphire-substrate LED and Si substrates were used. The InGaN-GaN films were grown on a sapphire substrate by low-pressure metal organic chemical vapor deposition (MOCVD). The LED structures comprise a 0.3 μm -thick Mg-doped GaN, an InGaN-GaN multiple quantum well (MQW), a 2 μm -thick Si-doped GaN, a 2 μm -thick undoped GaN layer film and a GaN buffer layer on sapphire substrate. The mirror system composed of an ITO p-side contact layer, an Al_2O_3 low index layer and an Al metal layer deposited on the surface of the Mg-doped GaN. Using a comprehensive load of 10 kg/cm^2 , this LED wafer was bonded to a metal dot-array silicon substrate which was covered with a high-temperature stable organic film by spin dry process. The organic film is a polycyclic aromatic hydrocarbon (C_8H_6), composed of a benzene ring fused to a cyclobutene ring. It was then cured at 200°C for 60 min.

The InGaN LED wafer was subsequently bonded to a Si substrate. By exposing the sapphire substrate to a frequency-tripled Nd: YAG 1 mm^2 spot, 355nm laser [8] with 170 mJ energy, the GaN was locally decomposed at the GaN and sapphire boundary. After scanning the GaN surface through sapphire substrate, the sapphire substrate was successfully separated. No peeling or cracking was observed on the bonded sample, indicating that the bond strength was sufficiently strong to endure the sapphire substrate removing process. The n-GaN roughening surface was obtained by subjecting the undoped GaN to boiling KOH solution and using inductively coupled plasma (ICP) to remove undoped GaN until the Si-doped GaN was exposed. The Ti/Al/Pt/Au dots with a diameter of 100 μm and Ti/Au were deposited onto the n-side (n^+ -GaN contact layer) and the underside of the Si substrate. **Figure 3-1** presents the structure and the roughened surface of the vertical InGaN LED. Finally, as shown in **Fig. 3-2**, the vertical InGaN LED was

successfully cut into isolated devices, each with an area of $300 \times 300 \mu\text{m}^2$. The ability of the interface to remain stable and uninterrupted through the dicing process, again indicates that the interfaces was sufficiently high.

For comparison, a standard sapphire-substrate LED with an ITO current spreading layer was prepared from the same InGaN-GaN LED epitaxial material. The samples described herein were only cut into chips without encapsulation.

3-3 Results and Discussion

The vertical InGaN LED devices are easier to process and have advantages over conventional sapphire-based LED. The dicing process for vertical InGaN LED devices can replace the complicated process of dry etching to mesa, laser scribing and breaking of the sapphire-based LED. The light emitting area is increased by 15% because only a single electrode is present on the topside of vertical InGaN LED devices as shown in **Fig. 3-4**.

Figure 3-3 plots the current against voltage (I - V) of LED with an area of $300 \times 300 \mu\text{m}^2$. The vertical InGaN LED exhibited normal p - n diode behavior with a forward voltage of 3.2 V at 20 mA, which were similar to conventional LED, indicating that neither wafer bonding nor the device process degrades the performance of LED. Furthermore, the organic film does not affect the electrical conductivity between the device contact (p-side) and metal dot-array Si substrate.

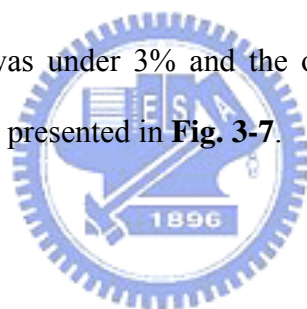
Figure 3-4 depicts the effects of injection current on the luminous intensity of the vertical and conventional InGaN LED. During optical testing, the LED was put onto a copper plate with the collection angle at about 27° . The light intensity of the vertical InGaN LED chip is 2.8 times that of the conventional LED at an injection current of 20 mA. As presented in **Fig. 3-1**, this difference is caused by the improvement of the emission of light

from the vertical InGaN LED by using only one electrode, reflecting the downward-traveling light by the mirror, and roughening the n-GaN surface. Furthermore, the current can spread uniformly without an n-metal layer (Ni/Au) or a transparent layer (ITO), because the vertical LED structure was p-side-down and n-side-up, with an n-metal electrode. Accordingly, the vertical InGaN LED does not exhibit the current crowding problem on the top emission area. Therefore, the emission of light is better than that of the conventional sapphire-based LED. The light output of the vertical InGaN LED (6.8 mW @ 465 nm) was exceeds the sapphire-based LED (5.7 mW @ 464 nm) by about 20% at 20 mA as shown in **Fig. 3-5**.

Figure 3-5 also reveals that vertical InGaN LED can be operated with an injection forward current of 280 mA, which is 100 mA greater than sapphire-substrate LED, because the thermal conductivity of Si ($168 \text{ Wm}^{-1}\text{K}^{-1}$) is 4.8 times higher than that of sapphire ($35 \text{ Wm}^{-1}\text{K}^{-1}$). However, this improvement in heat dissipation is not as large as expected because the thermal conductivity of the organic film ($0.29 \text{ Wm}^{-1}\text{K}^{-1}$) was poor. The thermal impedance of the sapphire-based LED is about 2.9 times than that of vertical InGaN LED. The effects of heat dissipation on the performance of LED are plotted as a peak shift as a function of DC drive current. When the DC drive current increased from 100 mA to 200 mA, the emission peak wavelengths of the sapphire-based LED shifted toward longer wavelengths - from 462.3nm to 465.1 nm, whereas that of vertical InGaN LED on the Si substrate shifted from 462.6nm to 463.5 nm. From the shift in emission wavelength and assuming a wavelength shift with temperature of $0.03 \text{ (nm/}^\circ\text{C)}$ [9], we estimate the rising junction temperature of the sapphire-based LED and vertical InGaN LED is 93°C and 30°C from 100 mA to 200 mA, respectively. These peak shifts were caused by Joule heating [10]. Evidently, this Si wafer bonding technique reduced the Joule-heating problem of conventional sapphire-based LED.

Figure 3-6 displays the radiation pattern of the conventional LED and vertical InGaN LED chips. It shows that the radiation pattern of the vertical InGaN LED chip is more symmetrical than that of sapphire-based LED, which could be attributed to the distribution of the electrodes. The view angle (half-center brightness or 50% of the full luminosity) of the vertical InGaN LED chip is smaller than that of sapphire-based LED, since the vertical InGaN LED were designed to have greater extraction efficiency using only one electrode, reflecting downward light, and have a rougher n-GaN surface. Accordingly, most light is easily reflected upward. Additionally, the vertical InGaN LED was fabricated by replacing the transparent sapphire substrate with a Si substrate. Thus, only a few photons could be emitted from the side, i.e. improved efficiency.

A life test was performed on the vertical InGaN LED at a forward current of 50 mA at 55°C. The voltage variation was under 3% and the output luminescent intensity did not degrade after 1000 h testing, as presented in **Fig. 3-7**.



3-4 Summary

In summary, vertical InGaN-GaN light emitting diode were successfully fabricated on 50mm diameter Si wafers using wafer bonding and laser lift-off technology. This bonding method enabled the emission of light from the vertical InGaN LED device to be improved such that a single electrode could be used and the light could be reflected downward using a mirror and rougher n-GaN surface. Hence, the light output of the vertical LED chip is 20 % greater than that of conventional sapphire-substrate LED at 20 mA. The radiation pattern of the vertical InGaN LED chip is more symmetrical than that of sapphire-based LED, and the power angle of the vertical InGaN LED chip is smaller than that of sapphire-based LED. The vertical LED could be operated at a much higher injection forward current (280 mA)

than sapphire substrate LED (180 mA) because the sapphire substrate was replaced with a Si substrate. Additionally, the performance of the vertical InGaN LED did not degraded during 1000 h of testing.



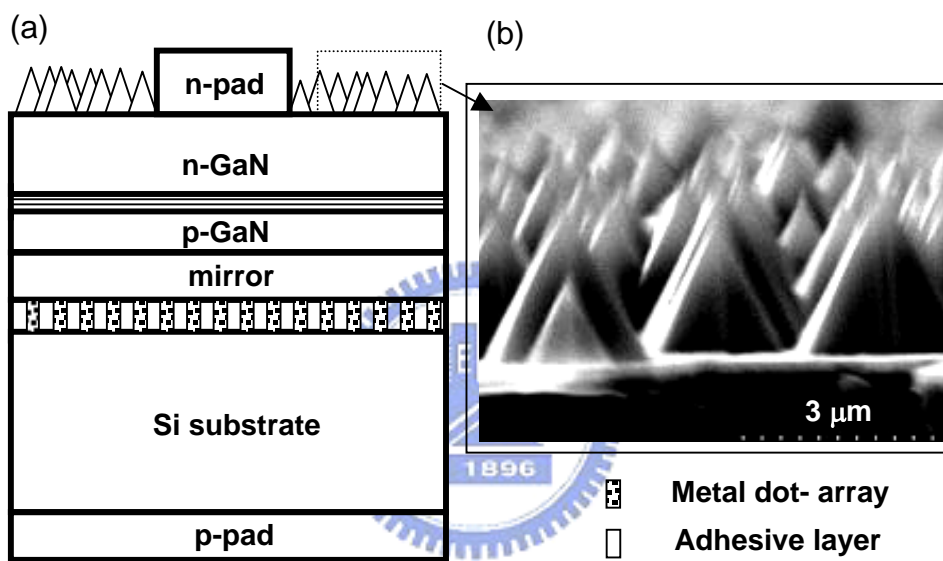


Fig. 3-1. (a) Schematic illustration of the vertical InGaN LED structure. (b) The SEM image of roughened surface.

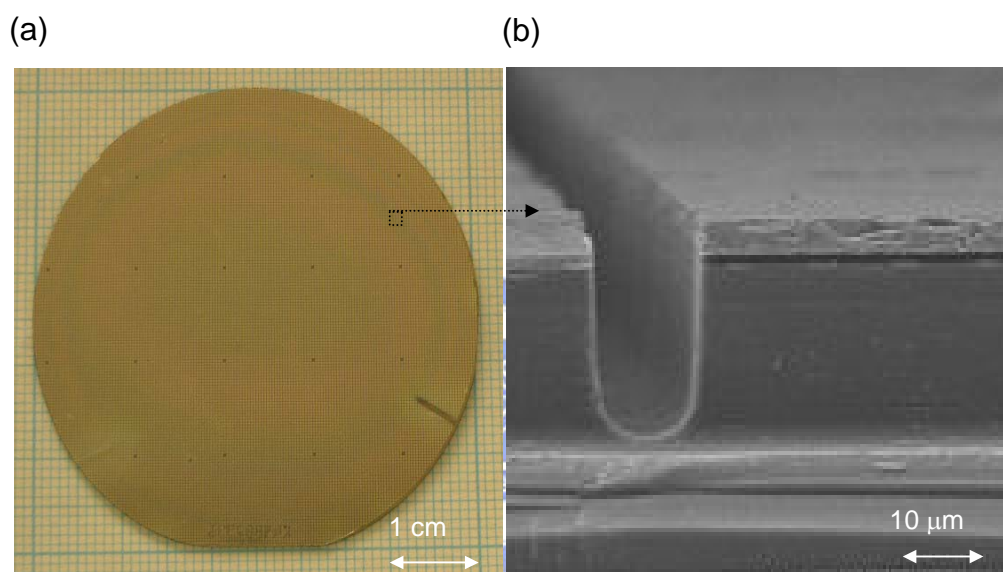


Fig. 3-2. (a) The image of an InGaN LED wafer bonded on a 50mm diameter Si substrate. Wafer was successfully cut into isolated devices with an area of $300 \times 300 \mu\text{m}^2$. (b) The SEM image of the cross section of the LED structure after dicing process.

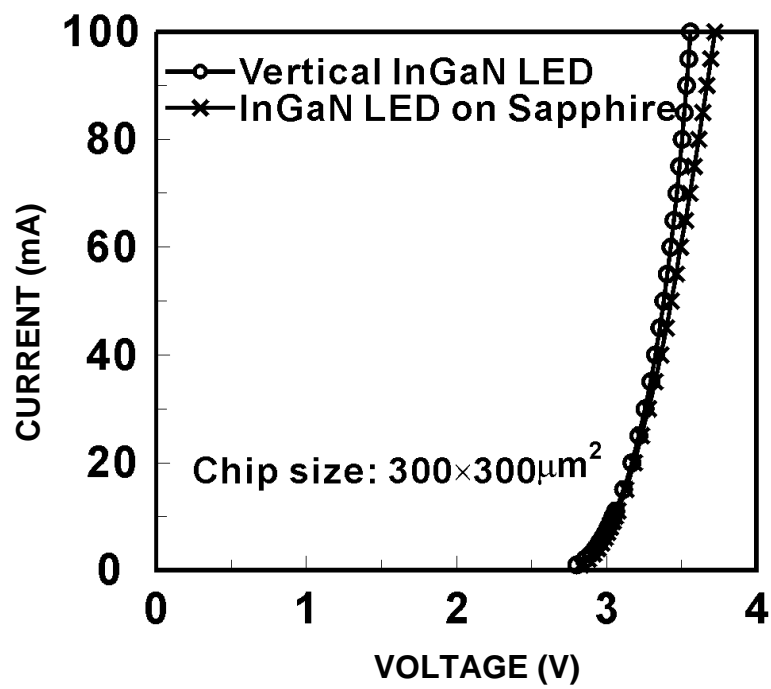


Fig. 3-3. Current-voltage ($I-V$) characteristics of the vertical and conventional InGaN LED.

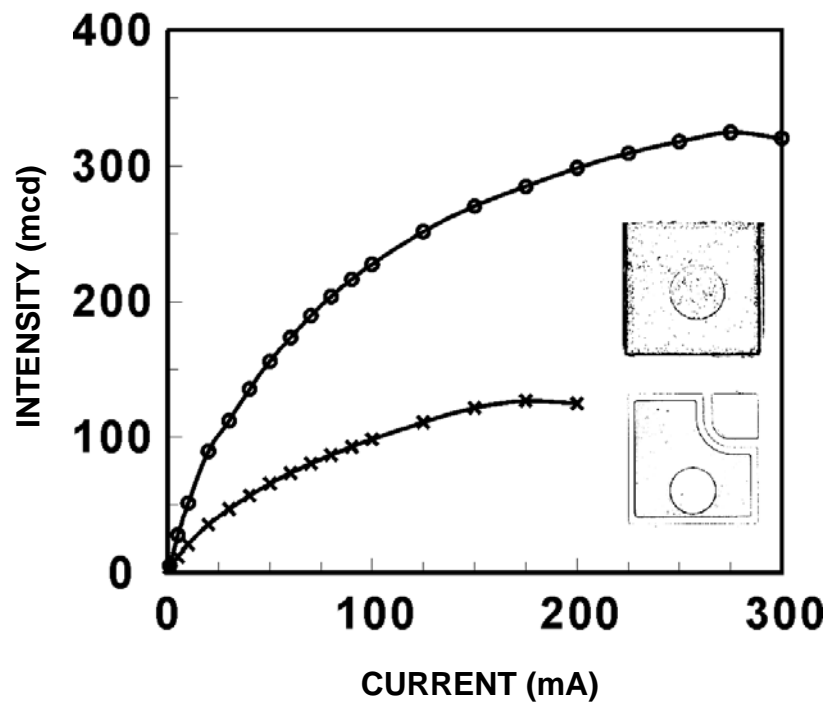


Fig. 3-4. The effects of injection the current on the luminous intensity of the vertical and conventional InGaN LED.

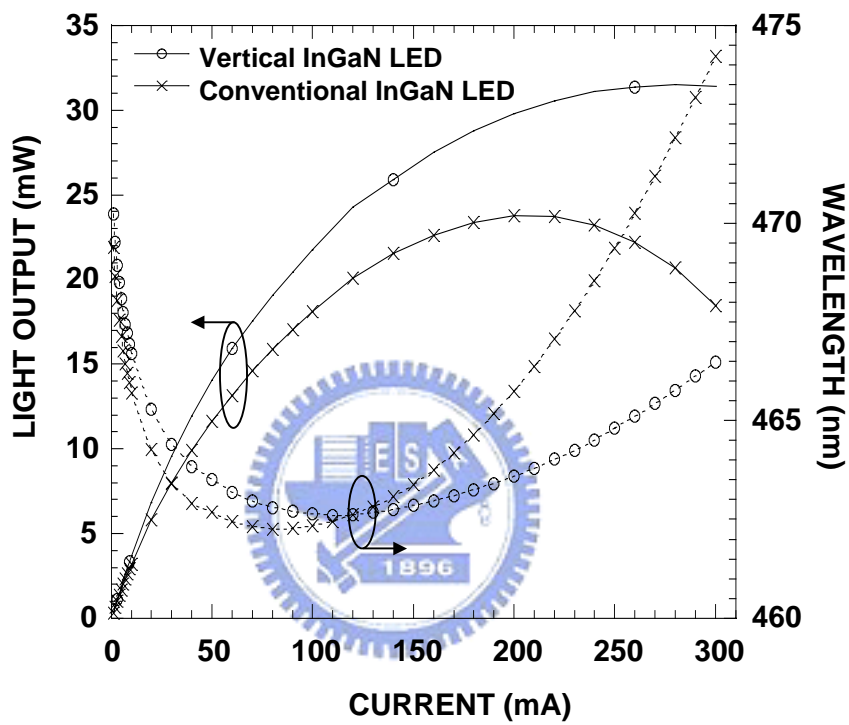


Fig. 3-5. The effects of injection the current on the light output and the peak spectral wavelength of vertical and conventional InGaN LED.

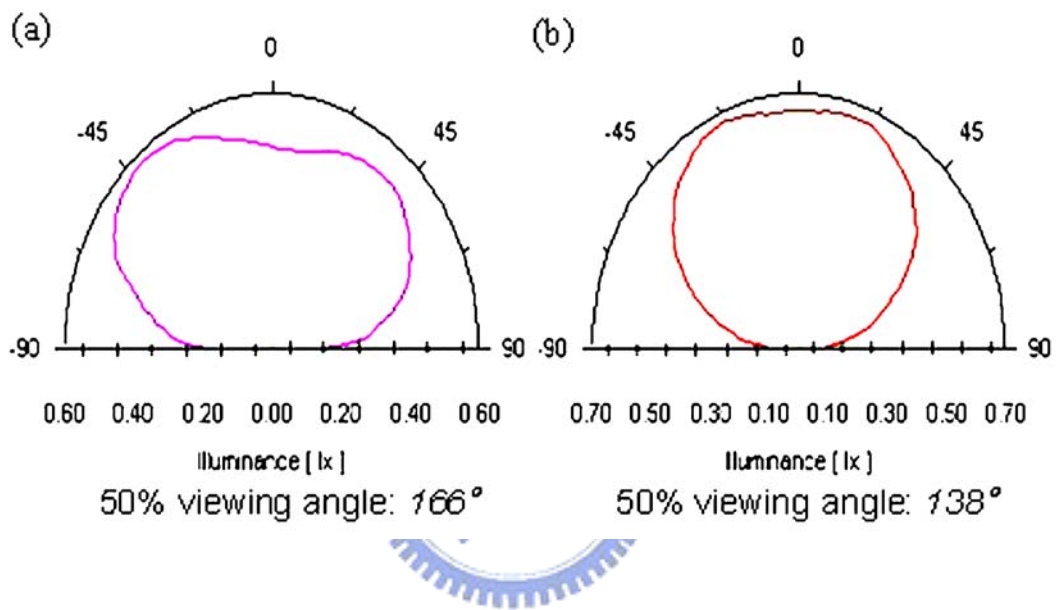


Fig. 3-6. The radiation patterns of (a) sapphire-based LED and (b) vertical InGaN LED.

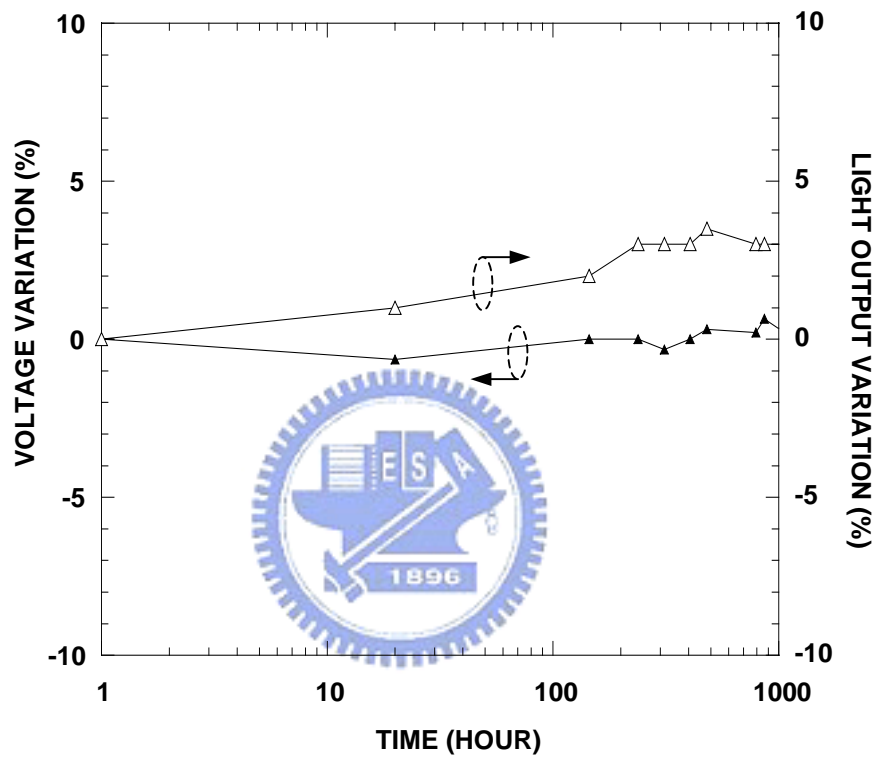


Fig. 3-7. Reliability test of vertical InGaN LED under stress-condition of 55°C and 50 mA.

Chapter 4 Enhanced performance of InGaN-GaN light emitting diode by roughening both the p-GaN surface and the undoped-GaN surface

4-1 Introduction

The epitaxial growth techniques have significantly improved the brightness and efficiency of light-emitting diode (LED) [1]. Some techniques have been employed to reduce the dislocation density by the methods of epitaxial lateral overgrowth (ELO) [2,3], lateral epitaxial patterned sapphire (LEPS) [4,5], and SiN_x interlayer [6] using a metalorganic vapor phase epitaxy. These improvements, along with higher reliability, lower costs, and the inherent properties of solid-state devices for low-voltage operation have enabled LED to be applied widely in mobile phones, full-color displays, lighting and mini projector [7]. High-efficiency white LED has considerable potential to replace fluorescent lamps in the near future [8,9]. The LED operating in the wavelength region ranging from blue to green light has been employed by the InGaN-GaN alloy system grown on sapphire substrates. Internal quantum efficiency and light extraction efficiency are two principal approaches for improving the efficiency of LED; both of which can be achieved through the improvement of the crystal quality and modification of the structure of the epitaxial layer. However, the efficiency of conventional LED is limited by their inability to emit all of the light that is generated from the active layer. When the LED derived with an injection current, light emitting from its active layer (in all directions) reaches the emitting surfaces at many different angles. According to

Snell's law, light traveling from a GaN having a high index of refraction ($n=2.5$) to an air with a low index of refraction ($n=1.0$) that is only within a critical angle of 23° will cross to the air. There is approximately only 4% of the internal light can escape from a surface. The light reaches the surface beyond the critical angle will not cross but will experience total internal reflection that continue to be reflected within the LED until it is absorbed. Thus, much of the light generated by conventional LED does not emit and would degrade its efficiency. One method of reducing the percentage of total internal reflection light is to create light scattering centers in the form of random texturing on the LED's surface [10]. However, the thickness of the top layer p-GaN cladding is very thin in conventional LED structures. Consequently, it is not easy to control the dry etching depth and plasma damage to the p-GaN during the dry etching process. Some methods have been used to improve the light extraction efficiency by roughening the top surface [11-15] or the mesa sidewall [16] of LED. It could also utilize wafer-bonding technology to transfer n-side-up GaN-based LED on Si substrates with a hexagonal “conelike” surface on n-GaN [17]. All these studies described above were focused on a single roughened top surface of nitride-based LED. In this work, LED with double roughened (p-GaN and undoped-GaN) surfaces was proposed. It was fabricated using surface-roughening, wafer-bonding and laser lift-off technologies. The performances of the conventional LED with and without roughened p-GaN surface and double roughened LED were investigated in chapter 4-2. The LED with different roughness of undoped-GaN (u-GaN) layers between an InGaN-GaN multiple quantum well (MQW) and sapphire substrate will be discussed in chapter 4-3.

4-2 Improved luminance intensity of InGaN-GaN LED by roughening both the p-GaN surface and the undoped-GaN surface

4-2-1 Device Fabrications

Three kinds of LED were investigated in this study. Their specifications and structures are schematically illustrated in **Fig.4-1**. Samples designated as "CV-LED" were conventional LED without any surface-roughening treatment. Samples designated as "PR-LED" were LED with a p-GaN roughened surface, while "DR-LED" were LED with double roughened (p-GaN and undoped-GaN) surfaces. The basic processes of these LED were almost the same. The InGaN-GaN films were grown by low-pressure metalorganic chemical vapor deposition (MOCVD) on a sapphire substrate. The LED structures and growth temperature were consist of a p-type Mg-doped GaN at 950°C, an InGaN-GaN MQW with six pair of InGaN (3nm)/GaN (9nm) at 800°C, a 2 μ m-thick n-type Si-doped GaN at 1050°C, a 2 μ m-thick undoped GaN layer film at 1050°C and buffer layer at 550°C on sapphire substrate. The major difference was that the thickness of p-type GaN of CV-LED was 0.2 μ m, which was thinner than that of PR-LED and DR-LED samples, 0.5 μ m. This extra length of p-type GaN layer was used to create the roughened p-type GaN surface by lowering the epitaxy growth temperature [15].

For the CV-LED and PR-LED, the device mesa with 300 μ m \times 300 μ m dimension was defined by inductively coupled plasma (ICP) to remove Mg-doped GaN and MQW until Si-doped GaN was exposed. Then, the indium tin oxide (ITO) layer with the resistivity of 2 \times 10⁻⁴ Ω .cm was then deposited on the p-GaN layer ($\rho \sim 4 \Omega$.cm) to form a p-side contact layer and a current spreading layer. Finally, the Cr/Au was deposited onto the ITO layer and n-GaN layer as the electrodes. The structures of CV-LED and PR-LED were shown in **Fig.**

4-1 (a) and 4-1 (b), respectively.

As for the fabrication of DR-LED devices, PR-LED wafer was bonded to a host substrate covered with adhesive layer. It was then annealed at 200°C for 60 min. After bonding, the sapphire substrate was removed by laser lift-off with a frequency-tripled Nd YAG laser at 355nm [18]. The roughened undoped-GaN surface was obtained by treatment with 60°C KOH solution for 1 minute. The wafer was then bonding to sapphire substrate with an adhesive layer. Finally, the host substrate was removed. The structure of DR-LED was shown in **Fig. 4-1(c)**.

4-2-2 Results and Discussion

Figure 4-2 shows the surface morphologies and AFM images of LED surfaces. Clearly, the surface of CV-LED is much smoother than that of PR-LED. Their surfaces were measured using atomic force microscopy (AFM) to identify the degree of texturing. The root mean square (rms) roughness of p-GaN surface without any treatment is only 11.8 nm, while that of roughened p-type GaN surface is 71.6nm. As for the surface of the roughened undoped-GaN layers, as shown in **Fig. 4-2(c)**, the surface was full with three-dimensional islands after the KOH solution treatment. The height and size of the GaN islands were 300~ 700 nm and 0.1~ 0.4 μm , respectively. The rms roughness of this undoped-GaN surface was 91.9 nm.

The I - V characteristics of the PR-LED and DR-LED exhibited normal p - n diode behaviors with forward voltages about 3.3 V at 20 mA as shown in **Fig. 4-3** and **Fig. 4-4**, which was similar to that of CV-LED (3.2 V at 20 mA). The V_{f1} and V_{f2} represent the forward voltage at 10 μA and 20 mA, I_r and I_v symbolize reverse current (μA) at -5V and luminance intensity (mcd) at 20 mA, WLP and WLD show the peak and dominant wavelength at 20 mA. This similarity indicated that the surface-roughening process,

wafer-bonding process and laser lift-off process did not degrade the performance of DR-LED. Furthermore, **Fig. 4-4** display the double roughened InGaN-GaN LED devices were successfully fabricated on a 50mm sapphire substrate using double transfer method with high yield and better luminance intensity than that of PR-LED.

To further investigate the influence of roughened GaN surfaces on light-output performance of a LED chips. The luminance intensities of unpackaged LED were measured from both the frontside (top side through the transparent ITO layer) and backside (substrate side through the sapphire/transparent glue/glass) of the device. The light intensity as a function of injected forward current are shown in **Fig. 4-5(a)** and **Fig. 4-5(b)**, respectively. It is obvious that roughened surfaces of LED did enhance the luminance intensities. Comparing with the CV-LED chip, the light intensity for the PR-LED chip with a roughened p-GaN surface was increased by 60 % for the frontside and by 56% for the backside at an injection current of 20 mA. These results are similar to the conclusions drawn by Hu, Lee, Kang and Park [4] during their microroughening of the p-GaN surface studies. They produced a microroughened *p*-GaN top surface using the metal clusters as a wet etching mask and measured the light-output powers of unpackaged LED chips from both frontside and the backside of the device. They also found the light-output powers were increased on both sides. Comparing with the conventional LED chip, the light-output power for the LED chip with a microroughened top surface was increased by 52.4 % for the frontside and by 30 % for the backside, respectively. They believed the microroughened surface structure improve the escape probability of photons due to the angular randomization of photons inside the LED structure, resulting in an increase in the light extraction efficiency of LED.

As for the luminance intensity of our DR-LED, the light intensities from both sides were greatly enhanced. The frontside luminance intensity was 133 mcd, which was 2.77 times higher than that of the CV-LED, and 1.73 times higher than that of the PR-LED. As for the

backside luminance intensity, it was 178 mcd, which was 2.37 times higher than that of the CV-LED, and 1.52 times higher than that of the PR-LED. Clearly, this tremendous enhancement was caused by the roughened p-GaN surface and the roughened undoped-GaN surface.

The light-extraction efficiency in the GaN-based LED is limited mainly due to the difficulty for light to escape from high refractive index semiconductors. The key to enhance the escape probability is to give the photons multiple opportunities to find the escape cone [3]. As shown in **Fig. 4-6**, roughened surfaces not only can provide photons multiple chances to escape from the LED surface, but also redirect photons, which were originally emitted out of the escape cone, back into the escape cone. **Figure 4-6(a)** shows the possible photon paths for CV-LED without any roughened surface. For a PR-LED, the angular randomization of photons can be achieved by surface scattering from the roughened p-GaN surface, as shown in **Fig. 4-6(b)**. Thus, the roughened surface structure can provide photons multiple chances to escape from the LED, and redirect photons back into the escape cone. A DR-LED device has two roughened surfaces, as shown in **Fig. 4-6(c)**. Compared to the PR-LED, the extra-roughened undoped-GaN layer can greatly increase the escape probability of photons, resulting in an increase in the luminance intensity of LED, as shown in **Fig. 4-5**.

Fig. 4-7 illustrates the external quantum efficiency and the output power of the CV-LED, PR-LED and DR-LED. The external quantum efficiency of the CV-LED, PR-LED and DR-LED was 13.9 %, 18.4 % and 21.4 % at 20mA. On the other hand, the output power observed from of the DR-LED was 16 % larger than that observed from of PR-LED, and 55% higher than that of the PR-LED. With a DC 20mA current injection, it was found that the output powers were 11.38, 9.78 and 7.34 mW for the CV-LED, PR-LED and DR-LED, respectively.

4-3 Enhanced light output in double roughened GaN light-emitting diodes via various texturing of undoped-GaN layer

4-3-1 Device Fabrications

As listed in Table I, three kinds of LED were used in this study. Samples designated as "CV-LED" were conventional LED without any surface-roughening treatment. Samples designated as "PR-LED" were LED with p-GaN roughened surface, while "DR-LED" were LED with double roughened (p-GaN and undoped-GaN) surfaces. The devices processes of PR-LED and DR-LED were similar to CV-LED. The InGaN-GaN films were grown by low-pressure metal organic chemical vapor deposition (MOCVD) on a sapphire substrate. The LED structures consist of a 5 nm-thick Si-doped n^+ -InGaN tunnel contact structure, a 0.4 μm -thick Mg-doped GaN, an InGaN-GaN multiple quantum well (MQW), a 2 μm -thick Si-doped GaN, a 2 μm -thick undoped-GaN layer film and a buffer layer on a sapphire substrate. The purpose of the Si-doped n^+ - InGaN layer was used to form the ohmic contact between ITO and p-GaN [19]. The device mesa with the chip size of $250 \times 450 \mu\text{m}^2$ was then defined by an inductively coupled plasma (ICP) to remove the Mg-doped GaN and MQW until the Si-doped GaN was exposed. Then, the indium tin oxide (ITO) layer deposited by E-beam coater on the n^+ - InGaN layer to form a p-side contact layer and a current spreading layer. The Cr/Au was deposited onto the ITO layer to form a p-side and n-side electrode. The roughened p-type GaN surfaces of the PR-LED and DR-LED samples were created by lowering the epitaxy growth temperature of the p-type GaN [15].

The fabrication process of the DR-LED is shown in **Fig. 4-8**. The PR-LED was utilized to fabricate the DR-LED. The PR-LED wafer was bonded to a host substrate covered with an adhesive layer. After bonding, the sapphire substrate was then removed by

shining a frequency-tripled Nd YAG laser [18] at 355nm with 1mm² spot and 170 mJ energy, through the transparent sapphire substrate, which locally decomposed the GaN at the boundary between GaN and sapphire. After scanning the entire sample, the sapphire substrate was successfully separated. The Ga residues were then removed by a wet chemical etch using diluted HCl: H₂O (1:1) solution for 60 sec. Subsequently, the u-GaN epitaxial layer was treatment with a 45 % aqueous potassium hydroxide (KOH) solution for 1 minute at 60, 80 and 100°C to obtain different degrees of roughened u-GaN surfaces. The wafer was then bonded to a sapphire substrate, which had an organic adhesive layer. The organic film was a polycyclic aromatic hydrocarbon (C₈H₆), composed of a benzene ring fused to a cyclobutene ring. A 0.5-0.6 μm thickness was obtained through a spin dry process where the organic film was dispensed onto the LED and Si wafer at 500 rpm for 5 sec (spread) and 5000 rpm for 20 sec to control the thickness. It was then annealed at 200°C for 60 minutes with a comprehensive load of 10 kg/cm². Finally, the host substrate was removed. For baseline comparison the performance of the CV-LED, PR-LED and DR-LED were prepared from the same InGaN-GaN LED epitaxial structure, and sapphire was chosen as the DR-LED's substrate. The samples described herein were only cut into chips without encapsulation.

4-3-2 Results and Discussion

Figure 4-9 shows the structures and surface morphologies of the ITO layer on the p-GaN surface. Clearly, the surface of CV-LED was much smoother than that of the PR-LED. Their surfaces were measured using an atomic force microscopy (AFM) to identify the degree of texturing. The root mean square (rms) roughness of the ITO surface without any treatment was only 7 nm, while that of the roughened ITO surface was 59 nm.

This roughening treatment resulted in an increase of output power by a factor of 1.3 from the top surface. These results are similar to the conclusions drawn by Horng et al. [20] during their texturing ITO surface studies. They produced a micro-roughened ITO surface using natural lithography with polystyrene spheres as the etching mask. Under optimum etching conditions, an output power exceeded that of the planar-surface LED by about 28% at 20 mA.

Fig. 4-10 (a)~(d) shows the side-view SEM micrographs of the u-GaN layers. The SEM images were taken at an angle of 70 degrees from the perpendicular direction of the etched surface. Clearly, the roughness of u-GaN layer increased with the temperature of the 45 % KOH etching solution. Unfortunately, the etching temperature was limited to 100°C. When the etching temperature was greater than 100°C, the KOH solution began to destroy the adhesive layer between the LED and the host substrate. AFM was used to study the roughness of u-GaN surfaces. As shown in Table II, the rms roughness of the u-GaN layer without treatment is only 18.6 nm. As the temperature of 45 % KOH solution increased from 60 to 80 and 100°C, the rms roughness of u-GaN surfaces increase from 91.9 to 107.7 and 146.7 nm, respectively.

Figure 4-11 shows the reverse I - V curves of the DR-LED. Their leakage currents were in the range of 0.15–0.20 μ A (@ -5 V), which were much higher than that of PR-LED (0.04 μ A @ -5 V). These degradations have been caused by the laser lift-off process, which generated the dislocations in the LED structure as shown in **Fig. 4-12**.

The light output versus injection current curves for the DR-LED with various roughness of u-GaN layers are shown in **Fig. 4-13**. The light outputs of LED at 20 mA are shown in Table II. The optical measurements were performed in an integrating sphere. It was found that the light output increased with increasing temperature of the 45 % KOH solution. The 100°C-etched DR-LED provided the best performance, and presented a

maximum output power of 10.2 mW, which was 41 % larger than that of the DR-LED without KOH treatment. The output power of PR-LED was the same as compared with the DR-LED without KOH treatment. The improvement of the light output could be related to the light scattering from the roughening surface between the n-GaN and sapphire substrate. The key to the enhanced escape probability was to give the photons multiple opportunities to find escape cone. The roughened u-GaN surface not only provided the photons multiple chances to escape from the LED surface, but also redirected the photons which were originally emitted out of the escape cone, back into the escape cone.

Figure 4-14 displays the radiation patterns of the DR-LED with various roughness of the u-GaN layers. Their view angles (half-center brightness, which is the angle for 50% of the full luminosity) were shown in Table II. It was found that the view angle decreased with increasing 45 % KOH etching temperature. In other words, the view angle decreased with increasing roughness of u-GaN layers. The view angle of DR-LED without KOH treatment is 133.6°. As the 45 % KOH etching temperature increased from 60 to 80 and 100°C, the view angle decreased from 120° to 117° and 116°, respectively. The roughened u-GaN surface not only provided the photons multiple chances to escape from the LED backside surface, but also redirected the photons which were originally emitted out of the backside escape cone, back into the frontside escape cone [22]. Therefore, the view angles decreased with increasing roughness of u-GaN layers. It is obvious that double roughened (p-GaN and undoped-GaN) InGaN LED could increase escape probability of the light since the emitting angle is larger than the critical angle. The results of smaller view angle indicate that the double roughened InGaN LED has considerable potential for mini projector applications.

4-4 Summary

In summary, DR-LED with double roughened (p-GaN and undoped-GaN) surfaces was investigated in this study. It was fabricated by surface-roughening, wafer-bonding and laser lift-off technologies. The roughened surface of p-GaN was created by lowering the epitaxy growth temperature, while that of n-GaN was obtained by dipping into the 60°C KOH solution. It was found that surface-roughening, wafer-bonding and laser lift-off processes did not degrade the performance of DR-LED. At an injection current of 20 mA, the frontside luminance intensity of double roughened LED was 133 mcd, which was 2.77 times higher than that of the conventional LED, and the backside luminance intensity was 178 mcd, which was 2.37 times higher than that of the conventional LED. This is because the double roughened surfaces not only can provide photons multiple chances to escape from the LED surface, but also redirect photons, which were originally emitted out of the escape cone, back into the escape cone. Furthermore, the effect of the roughness of u-GaN layer on the performance of DR-LED was also investigated. The roughness of u-GaN surfaces could be controlled by increasing the temperatures of KOH etching solution. As the temperature of 45 % KOH solution increased from 60 to 80 and 100°C, the rms roughness of u-GaN surfaces increase from 91.9 to 107.7 and 146.7 nm, respectively. Unfortunately, the etching temperature was limited to 100°C because the KOH solution would destroy the adhesive layer between the LED and the host substrate. Comparing the DR-LED without the KOH treatment, the output power of 100°C-etched DR-LED was increased by 41 %, and the view angle was decreased by 17.6 degrees. Therefore, the DR-LED achieved higher light output than that of PR-LED and CV-LED.

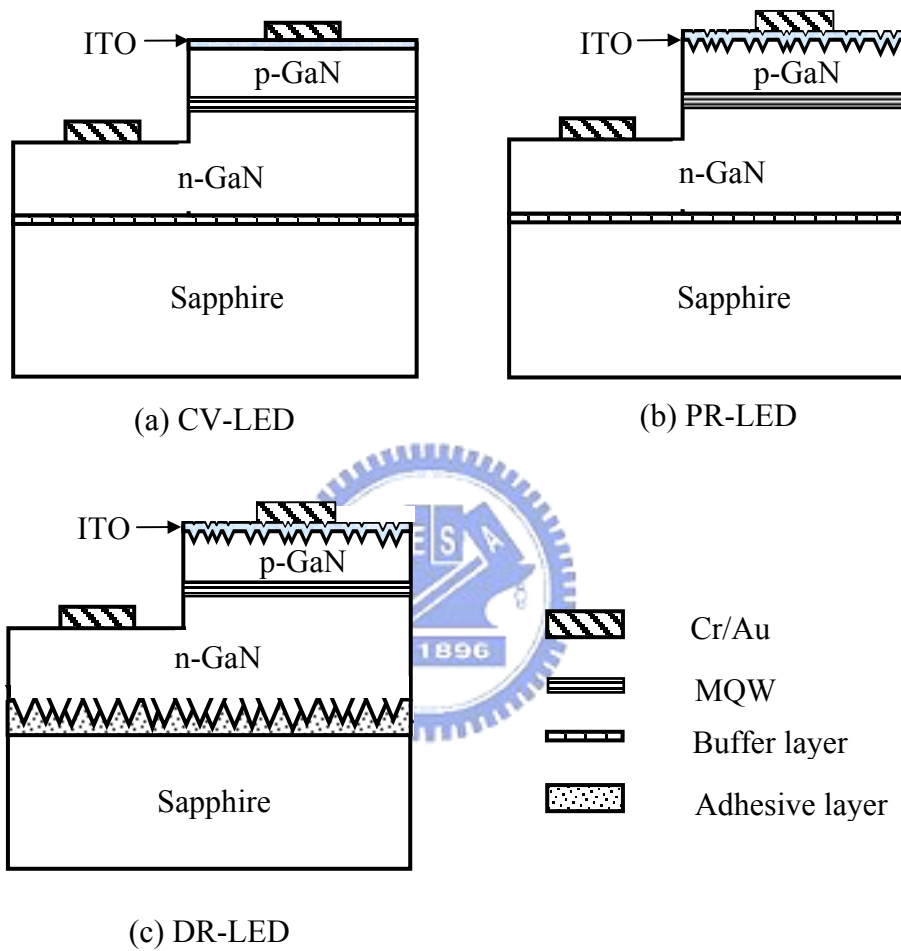


Fig. 4-1. Schematic diagrams of (a) CV-LED (without any surface-roughening treatment), (b) PR-LED (with roughened p-GaN surface) and (c) DR-LED (with double roughened surfaces).

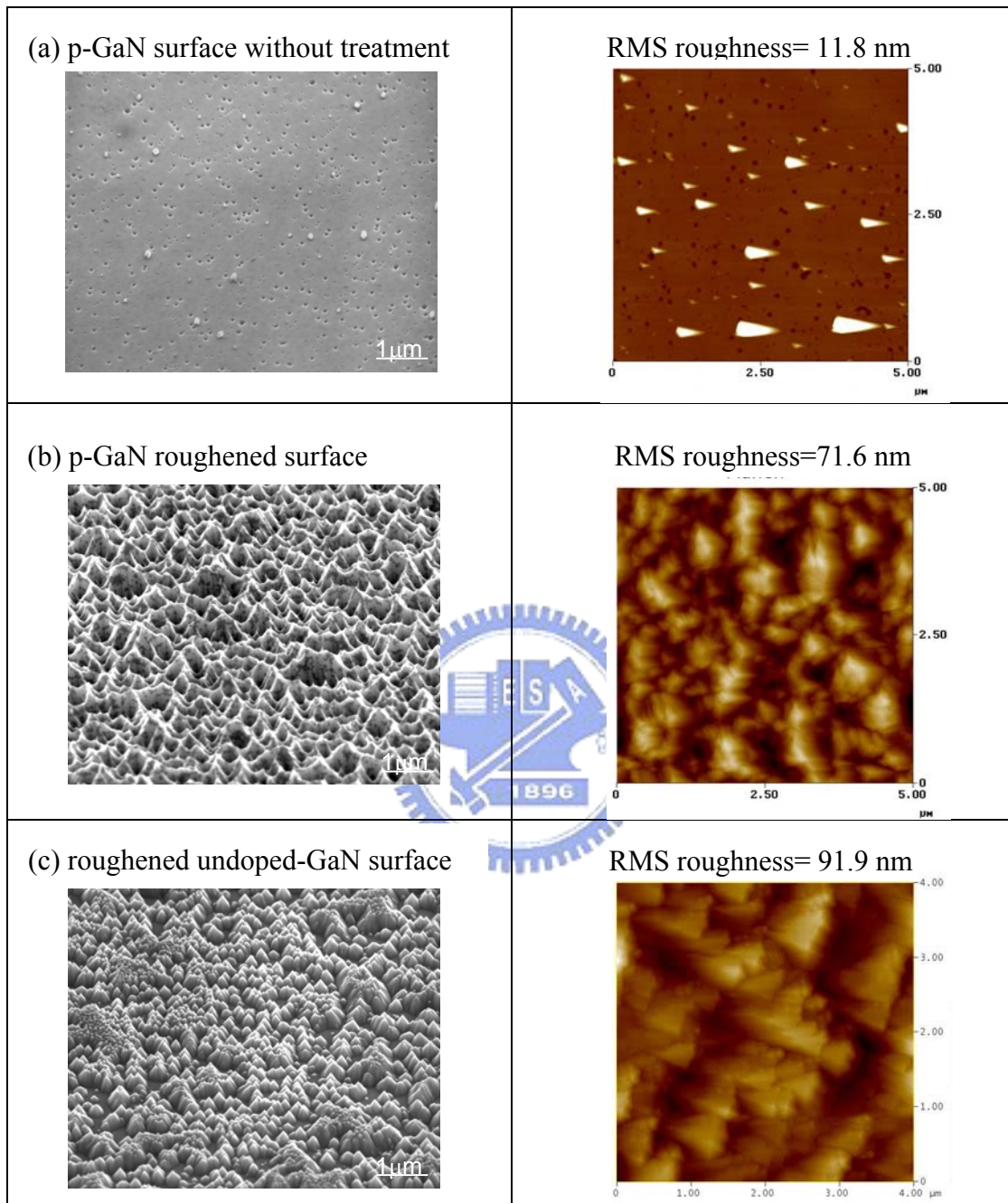


Fig. 4-2. Scanning electron micrographs and AFM image of (a) p-GaN surface without any surface- roughening treatment, (b) roughened p-GaN surface and (c) roughened undoped-GaN surface.

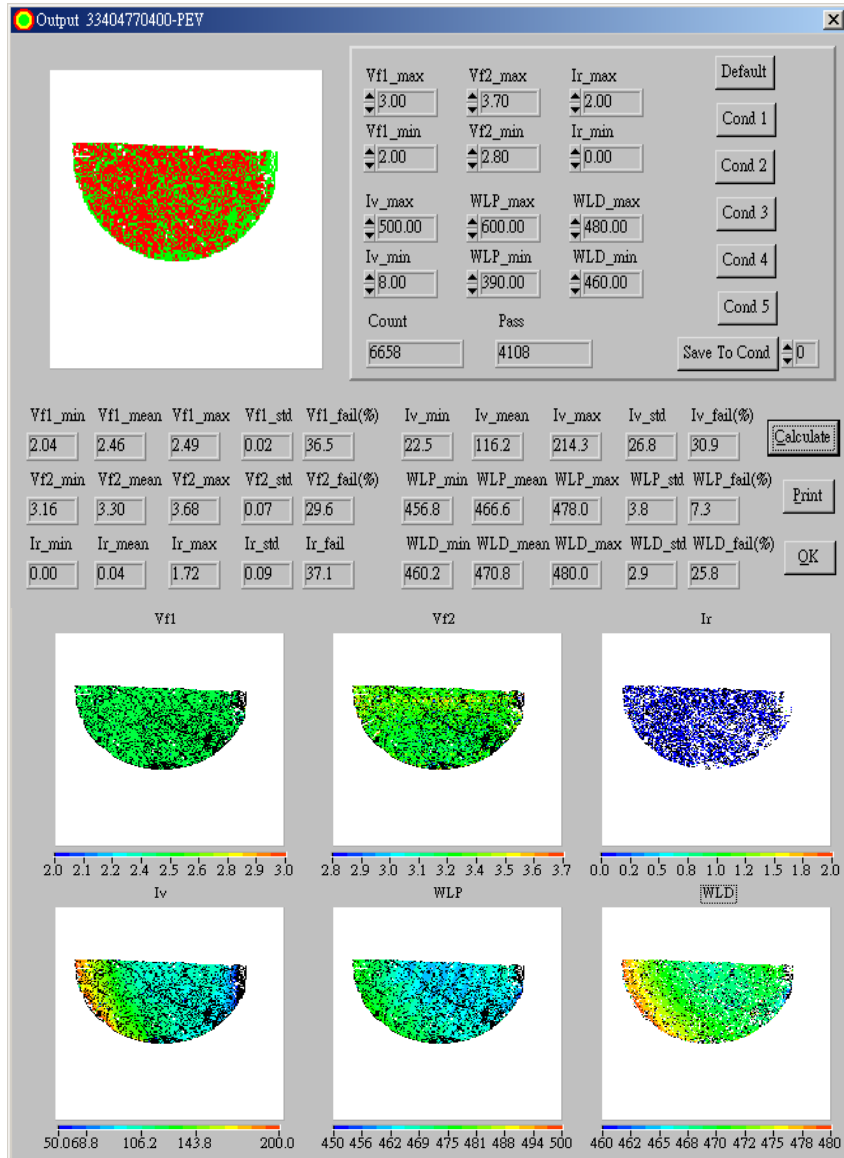


Fig. 4-3. The mapping data of the PR-LED.

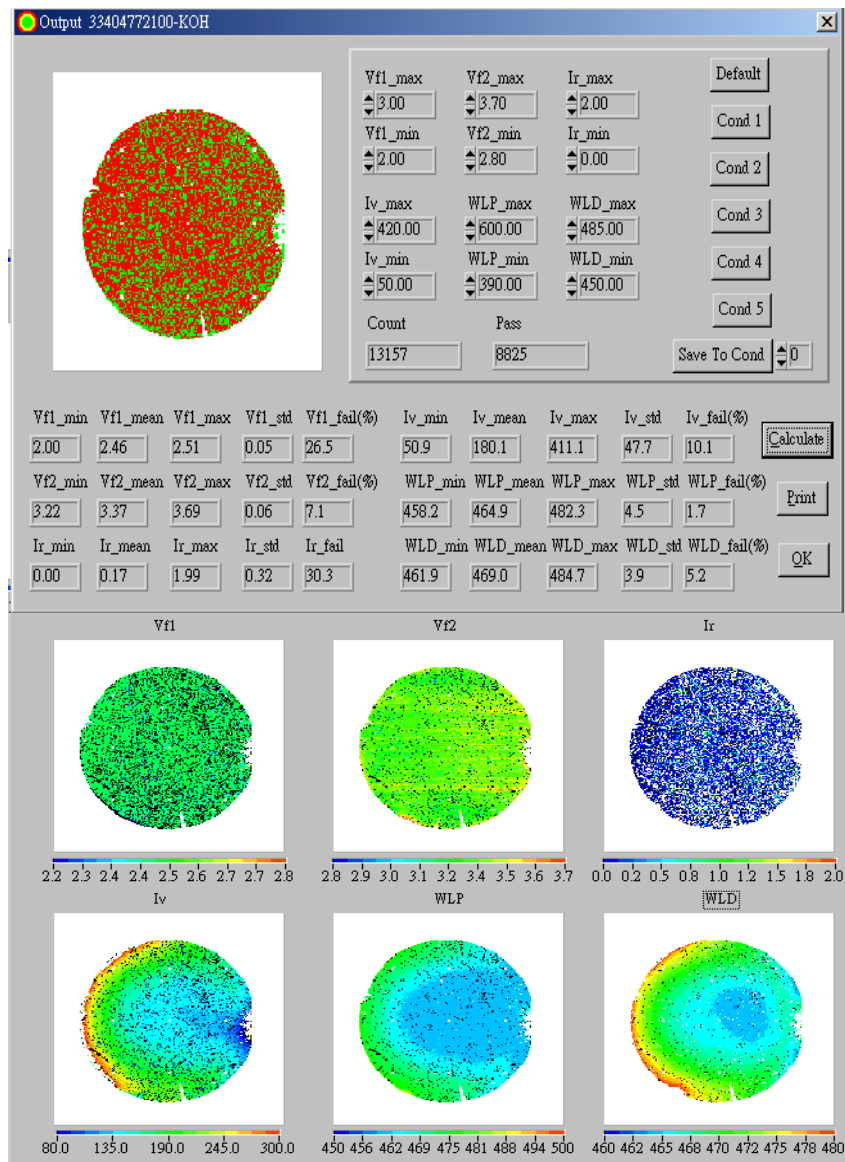


Fig. 4-4. The mapping data of the DR-LED (2 inch wafer).

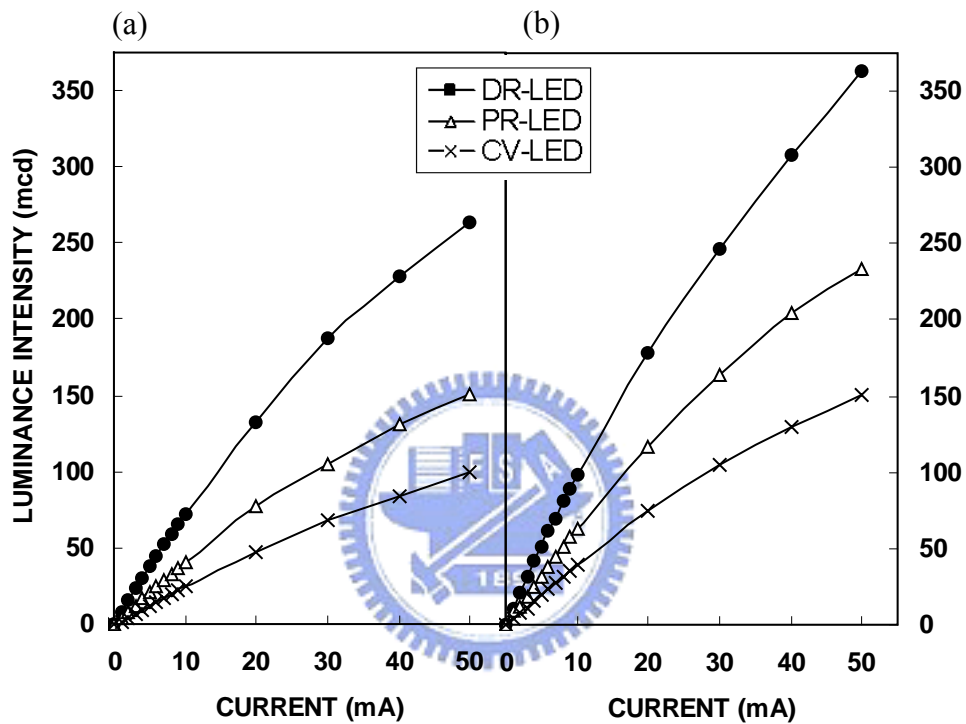


Fig. 4-5. Luminance intensity of three LED chips vs the forward injection current. (a) Intensity measured from the frontside (topside through the transparent metal layer) of the LED chip. (b) Intensity measured from backside substrate side (through the sapphire/ transparent glue/ glass) of the LED chip.

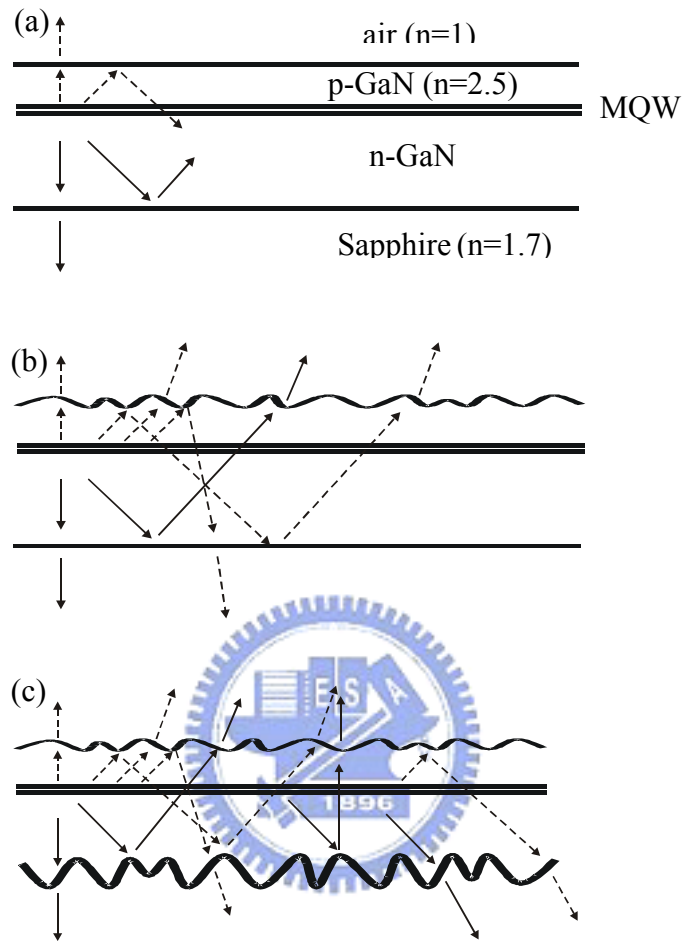


Fig. 4-6. Possible photon paths inside the structures of the (a) CV-LED, (b) PR-LED and (c) DR-LED.

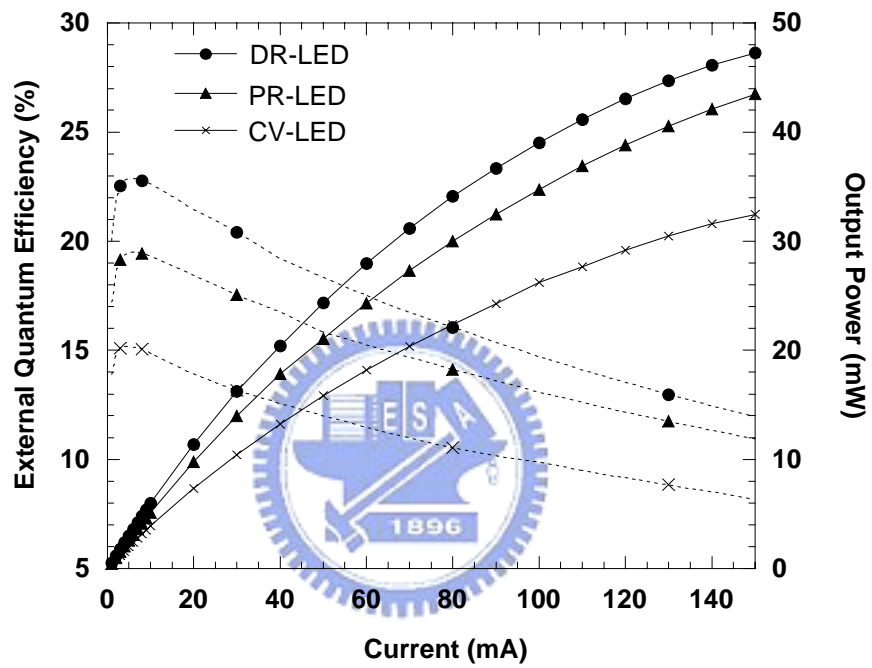


Fig. 4-7. The external quantum efficiency and the output power of the CV-LED, PR-LED and DR-LED.

Table I

CV-LED	conventional LED with smooth p-GaN surface
PR-LED	LED with roughened p-GaN surface
DR-LED	LED with roughened (p- and u- GaN) surfaces

Table II

KOH treatment	No	60 °C	80 °C	100 °C
RMS of u-GaN	18.6 nm	91.9 nm	107.7 nm	146.7 nm
$V_f@20mA$	3.4 V	3.4 V	3.4 V	3.5 V
Light output	7.2 mW	8.2 mW	9.3 mW	10.2 mW
View angle	133.6°	120°	117°	116°

Table 4-I. The definition of CV-LED, PR-LED and DR-LED.

Table 4-II. The performances of DR-LED with various treatments on u-GaN layer.

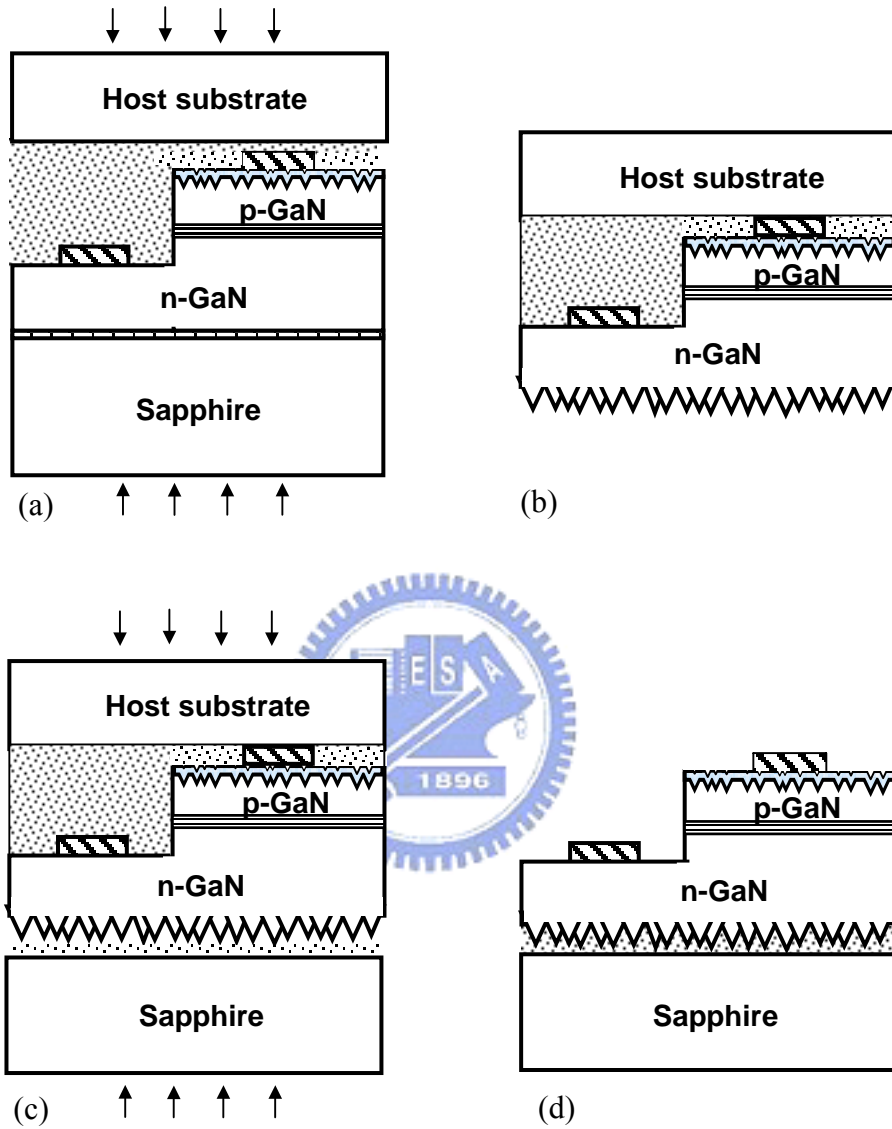
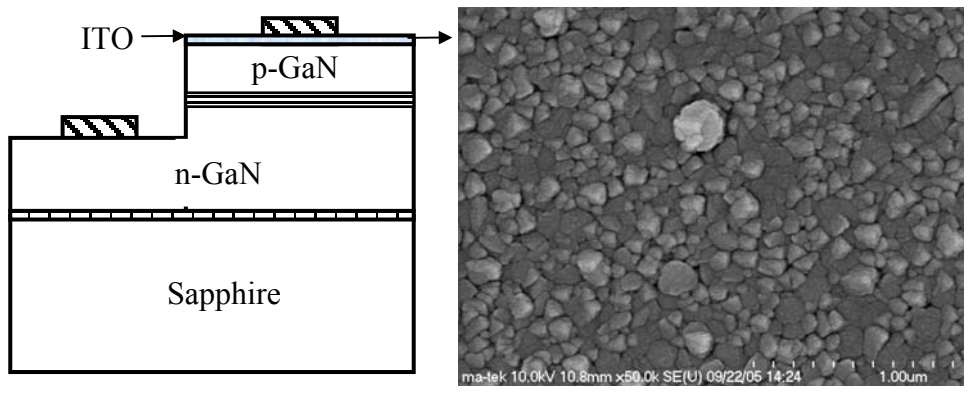
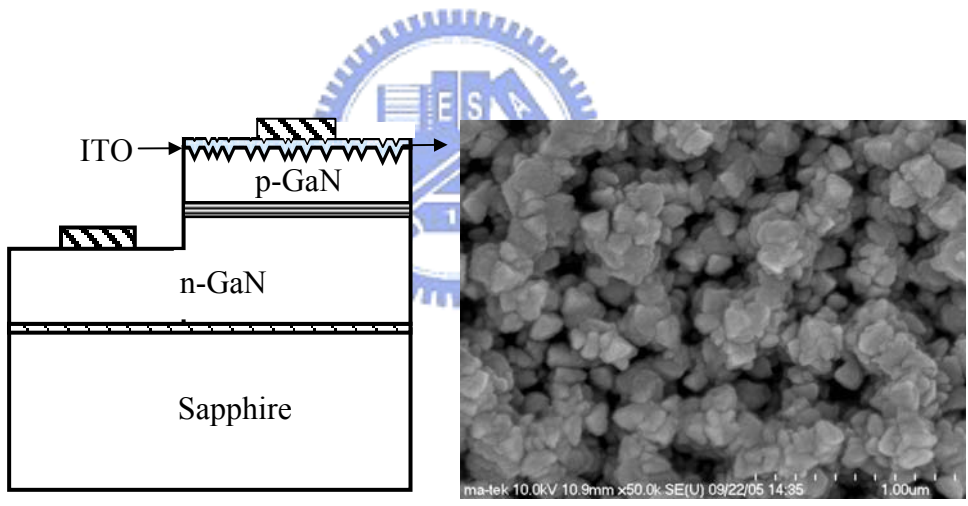


Fig. 4-8. Schematic diagram of the DR-LED transfer process: (a) PR-LED bonding to a host substrate; (b) laser lift-off and roughened u-GaN processes; (c) bonding to a sapphire substrate; and (d) removal of host substrate and glue layer.



(a) CV-LED



(b) PR-LED

Fig. 4-9. Schematic illustration of the InGaN LED structure and surface morphologies of ITO layer on p-GaN surface: (a) CV-LED and (b) PR-LED

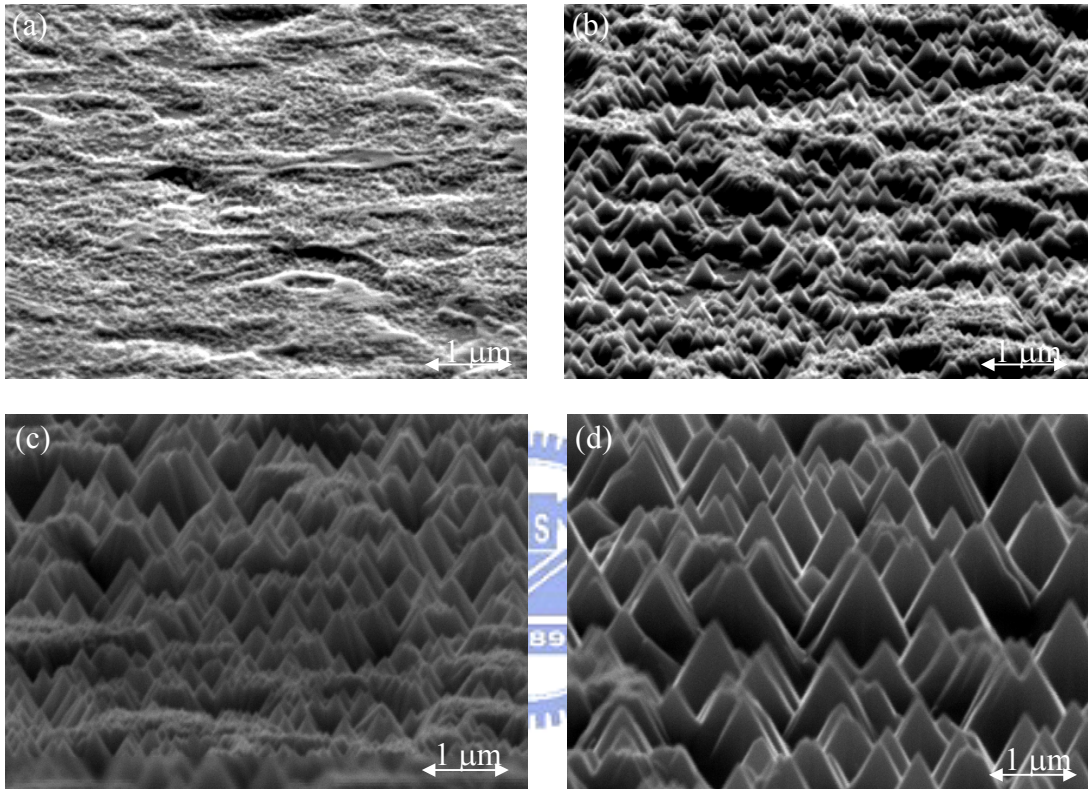


Fig. 4-10. The side-view SEM micrographs of the u-GaN layers: (a) without KOH treatment, (b) with 60 °C, (c) with 80 °C and (d) with 100 °C KOH treatment.

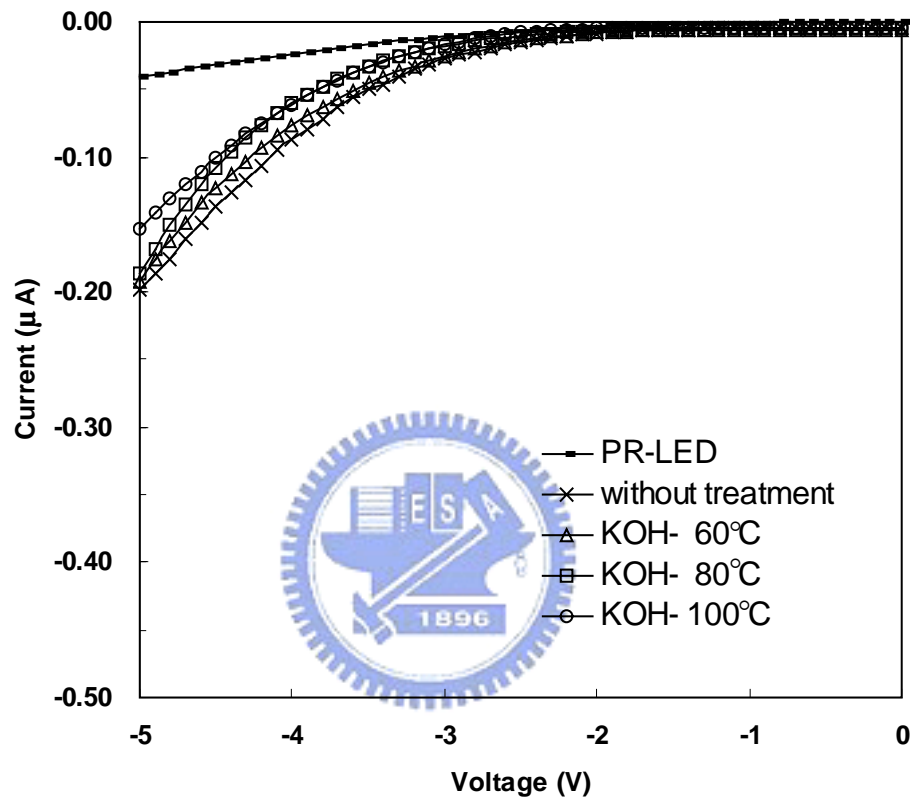


Fig. 4-11. The reverse current-voltage ($I-V$) characteristics of the PR-LED and DR-LED with various temperature treatments.

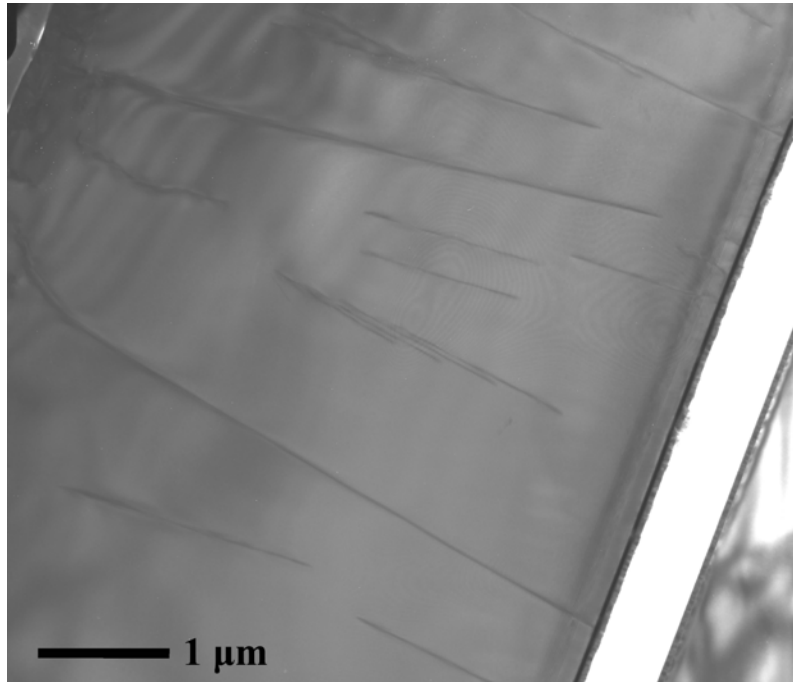


Fig. 4-12. The TEM image of the LED generated the dislocations in the structure after the laser lift-off process.

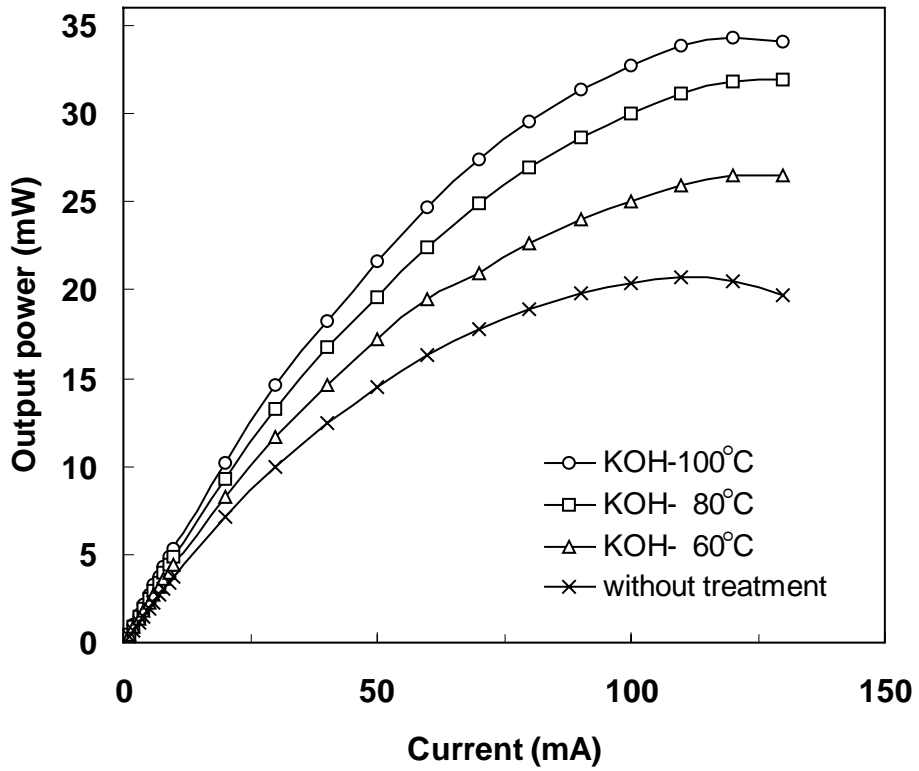


Fig. 4-13. The light output of DR-LED with various treatments on u-GaN layer.

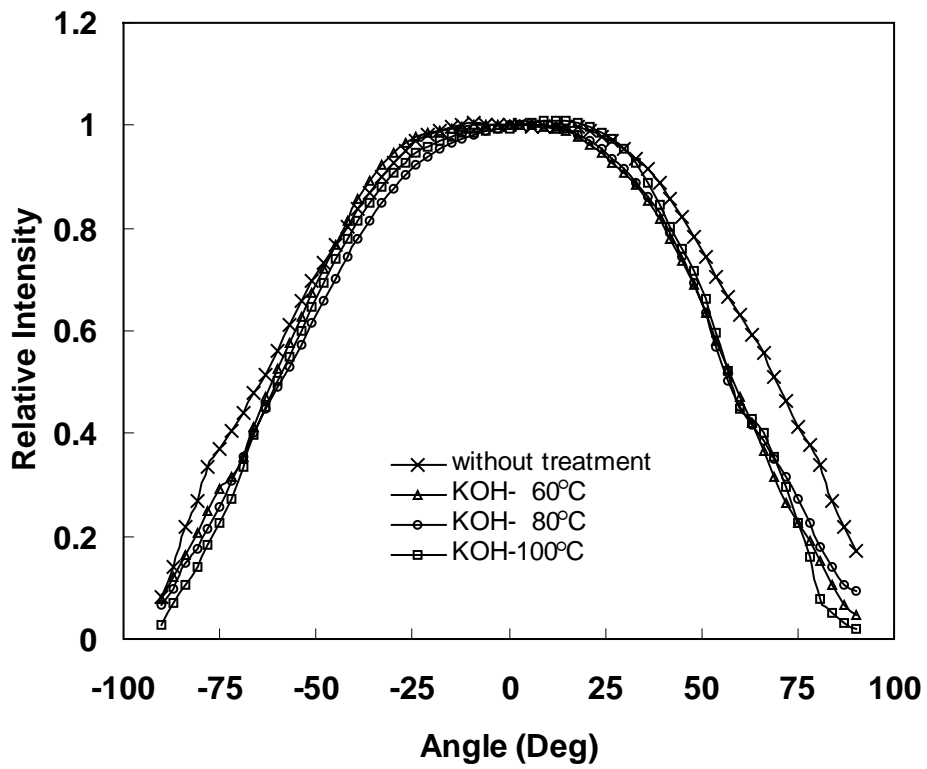


Fig. 4-14. The radiation patterns of DR-LED with various temperature treatments on u-GaN layer.

Chapter 5 Enhanced performance of an InGaN-GaN light-emitting diode by roughening the undoped-GaN surface and applying a mirror coating to the sapphire substrate

5-1 Introduction

Recently, epitaxial growth techniques have significantly improved the brightness and efficiency of light-emitting diode (LED). GaN-based LED are attractive devices for use in a variety of applications including traffic signals, full-color displays, back lighting in liquid-crystal displays, and mini projectors [1,2]. However, the light extraction efficiency of GaN-based LED is limited by the large difference in refractive index between the GaN film and the surrounding air. According to the Snell's law, light traveling from GaN to air travels only within a critical angle of 23° . The light reaching the surface beyond the critical angle will experience total internal reflection that will continue to be reflected within the LED until it is absorbed. One method of reducing the percentage of total internal light reflection is to create light scattering centers in the form of random texturing on the top of the p-GaN layer of the LED [3-6]. Another alternative is to utilize wafer-bonding and laser lift-off technologies to transfer the n-side-up textured surface of GaN-based LED onto Si substrates [7], or bond various mirror systems between the GaN LED structures and the substrate [8].

In this work, GaN LED with a roughened undoped-GaN surface and/or a silver (Ag) mirror on the sapphire substrate was successfully fabricated using wafer-bonding and laser

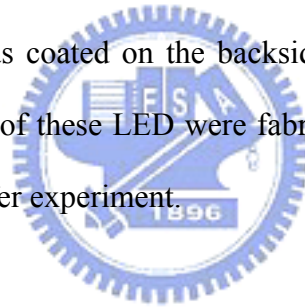
lift-off technologies. Their performances and light extraction efficiencies were also investigated.

5-2 Device Fabrication

Four kinds of LED were used in this study. As illustrated in **Fig. 5-1**, samples designated as "C-LED" were conventional LED without any surface-roughening treatment. Samples designated as "M-LED" and "R-LED" were LED with either a mirror system or roughened undoped-GaN surface between the GaN LED structure and sapphire substrate, respectively. The "RM-LED" were R-LED with an Ag mirror on the backside of sapphire substrate. The device processes of these LED were the same. The InGaN-GaN films were grown by low-pressure metal organic chemical vapor deposition (MOCVD) on a sapphire substrate. The LED structures consisted of a 0.4 μm -thick Mg-doped GaN, an InGaN-GaN multiple quantum well (MQW), a 2 μm -thick Si-doped GaN, a 2 μm -thick undoped-GaN (u-GaN) and a buffer layer on sapphire substrate. A device mesa with chip size of $250 \times 450 \mu\text{m}^2$ was defined by an inductively coupled plasma (ICP) which removed the Mg-doped GaN and MQW until the Si-doped GaN was exposed. Then, the indium tin oxide (ITO) layer was deposited onto the p-GaN layer to form a p-side contact layer and a current spreading layer. The Cr/Au was deposited onto the ITO layer as p-side and n-side electrode. The LED wafer was bonded to a host substrate with an adhesive layer. After bonding, the sapphire substrate was then removed by laser lift-off with a frequency-tripled Nd YAG laser at 355nm [9]. The Ga residues were subsequently removed by a wet chemical etch using diluted HCl: H₂O (1:1) solution for 60 sec. The u-GaN layer of the M-LED was polished to achieve a smooth surface and then coated with an Ag mirror. On the other hand, the u-GaN epilayer of the R-LED was treated with 45% KOH solution for 1 minute at 100°C to obtain a roughened u-GaN surface. **Fig. 5-2**

shows the side-view SEM micrograph of the undoped-GaN layer with the treatment of 45% KOH solution for 1 minute at 100°C. The SEM image was taken at an angle of 70 degrees from the perpendicular direction of the etched surface. The sample was measured using atomic force microscopy (AFM) to identify the degree of texturing. The root-mean-square (rms) roughness of the undoped-GaN layer was 146.7 nm. The heights and lengths of the GaN cone-like islands were 700 ~ 950 nm and 600 ~ 900 nm, respectively.

These wafers were then bonded to a sapphire substrate with an adhesive layer that consisted of a polycyclic aromatic hydrocarbon (C₈H₆) composed of a benzene ring fused to a cyclobutene ring. The optical transparency of the adhesive layer was exceeding than 90% across the visible spectrum. Wafers were annealed at 200°C for 60 min with a comprehensive load of 10 kg/cm². The host substrate and glue layer were subsequently removed. To fabricate the RM-LED, a Ag mirror was coated on the backside of R-LED's sapphire substrate. For comparison, the performances of these LED were fabricated from a single InGaN-GaN LED epitaxial wafer with a split wafer experiment.



5-3 Results and Discussion

Figure 5-4 shows the current-voltage (I - V) characteristics of the LED. It was found that the forward voltages of the M-LED, R-LED and RM-LED were in the range of 3.4~3.5 V at 20 mA, which were similar to the C-LED, indicating that transfer method did not degrade the performance.

Figure 5-5 depicts the effects of injection current on the luminous intensity of the LED. During the testing, LEDs were put onto a graphite plate with a collection angle of approximately 27°. The light intensities of M-LED, R-LED and RM-LED were greater than that of C-LED. The light intensity of M-LED was greater than the C-LED by 58 % at an

injection current of 20 mA. Similar results have been reported by Wu et al. [8] who fabricated GaN/mirror/Si LED using different mirror reflector materials such as Ag, Al, and Au. They found that the intensity strongly depended on the reflectivity of the mirror material. The LED with a Ag mirror achieved maximum luminance intensity as compared to other reflector materials. Therefore, in this study, Ag was chosen as a mirror material for the M-LED. The reflectivity of the Ag mirror was 96% at a wavelength of 470 nm as shown in **Fig. 5-3**.

The light intensity of R-LED was 242 mcd, which was 58 % larger than the C-LED at an injection current of 20 mA. These results are similar to the conclusions drawn by Hu, Lee, Kang and Park [4] during their studies of micro-roughening the p-GaN surface. They produced micro-roughened p-GaN top surfaces using metal clusters as a wet etching mask and measured the light-output power of unpackaged LED chips from both the front-side and the backside of the device. They found the light-output power was increased on both sides. In comparison with the conventional LED, the light-output power of the micro-roughened top surface LED improved by 52.4% for the front-side and by 30% for the backside. They believed that the micro-roughened surface structure improved the escape probability of photons due to the angular randomization of photons inside the LED structure, resulting in an increase of the light extraction efficiency of the LED.

In this study, we fabricated a roughened undoped-GaN surface within the GaN LED layer instead of a micro-roughened p-GaN top surface. We also found the light intensities of both sides were greatly enhanced. In contrast to the C-LED, the light intensity of the R-LED increased by 73 % for the front-side and by 53 % for the backside at an injection current of 20 mA. The optical transparency of the adhesive layer was very important. If the adhesive layer were opaque, it would degrade the light intensity by absorbing the downward-traveling light. Furthermore, by adding a mirror to the backside of the R-LED to create a RM-LED structure,

the light efficiency was enhanced by redirecting the downward-traveling light. As expected, the RM-LED provided the best performance with maximum light intensity of 312 mcd, which was 100 % greater than the C-LED and 29 % greater than the R-LED.

Figure 5-5 also indicates that the light intensity of RM-LED was greater than the M-LED, even though both LED had a Ag mirror. It is believed that the roughened surfaces of the RM-LED not only provided the photons multiple opportunities to escape the LED surface, but also redirected the photons that were originally emitted out of the escape cone, back into the escape cone (**Fig. 5-6(b)**). In contrast, as illustrated in **Fig. 5-6(a)**, the mirror of M-LED could only reflect the downward-traveling light to the p-GaN surface, but not necessarily redirect the photons back into the escape cone. Hence, the RM-LED provided the best light intensity of 312 mcd, which was 29 % larger than the M-LED.

The light output versus injection current curves for the LED was shown in **Fig. 5-5** LED were measured in an integrating sphere and were not encapsulated during the electrical and optical measurements. It was found that the RM-LED achieved a maximum output power of 11.8 mW (@ 20 mA), which was 49 % larger than the C-LED, and 16 % larger than the R-LED and the M-LED. The improvement of the light output was also due to the light scattering improvement and redirection of photons from the roughened undoped-GaN surface and the backside mirror on sapphire substrate.

5-4 Summary

In summary, a GaN RM-LED with a roughened undoped-GaN surface and a silver mirror on the sapphire substrate was successfully fabricated. The forward voltage was in the range of 3.4~3.5 V at 20 mA, which was similar to the C-LED. This indicated that the transfer method did not degrade the performance of LED. At an injection current of 20 mA, the

luminance intensity of the roughened LED was 312 mcd, which was 100 % larger than that of the C-LED. Furthermore, the output power was 11.8 mW, which was 49 % larger than the C-LED. The roughened undoped-GaN of the RM-LED redirected the photons into the escape cone of the LED surface to improve the extraction efficiency of the LED. The backside mirror on sapphire substrate also played a critical role in reflecting the downward-traveling light back to the surface of the LED.



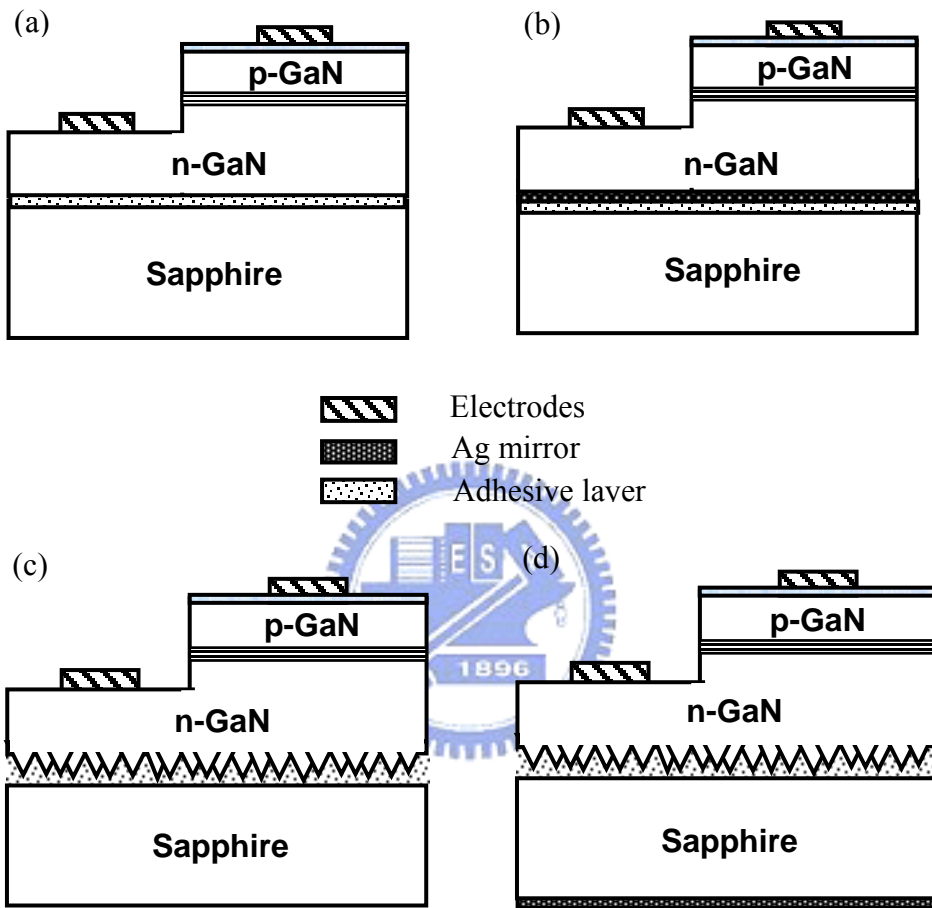


Fig. 5-1. Schematic diagrams of the (a) C-LED, (b) M-LED, (c) R-LED and (d) RM-LED.

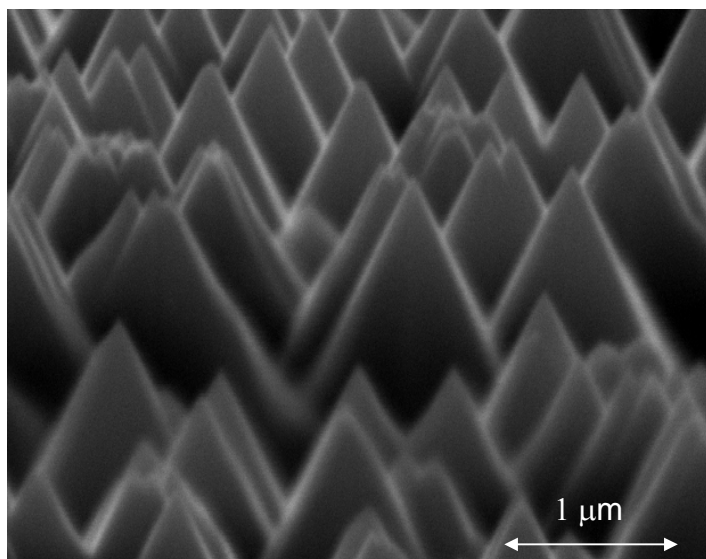


Fig. 5-2. Scanning electron micrograph of roughened undoped-GaN surface treated with 45 % KOH solution for 1 minute at 100°C.

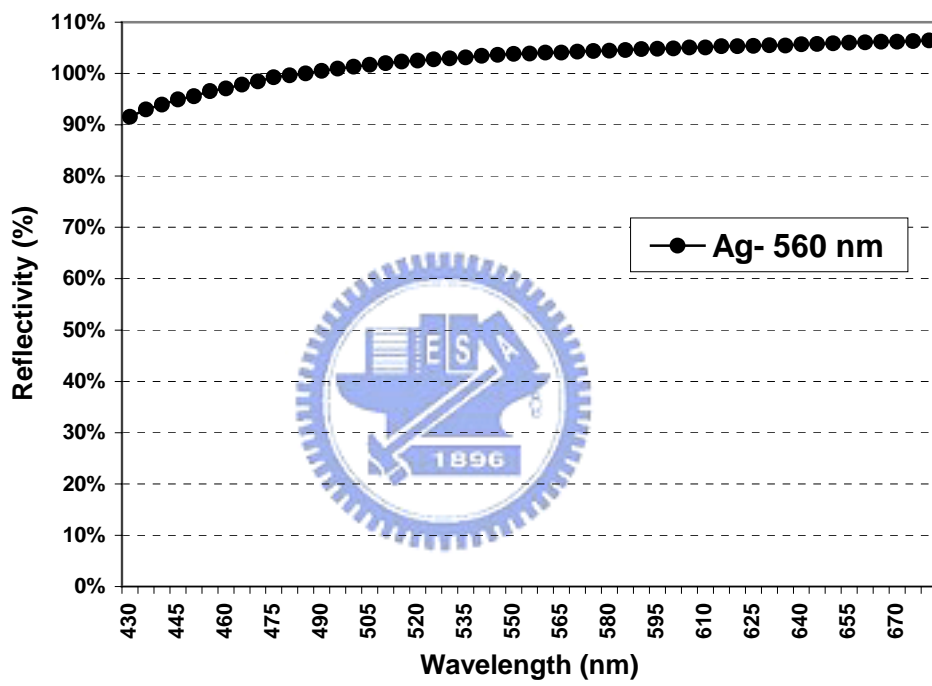


Fig. 5-3. The reflectivity of Ag mirror.

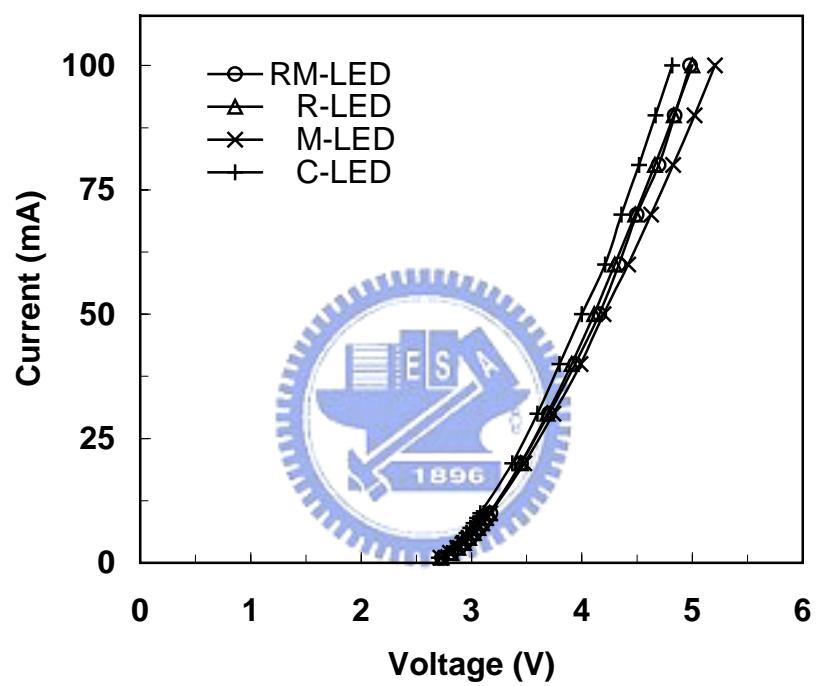


Fig. 5-4. The $I-V$ characteristic of the LEDs.

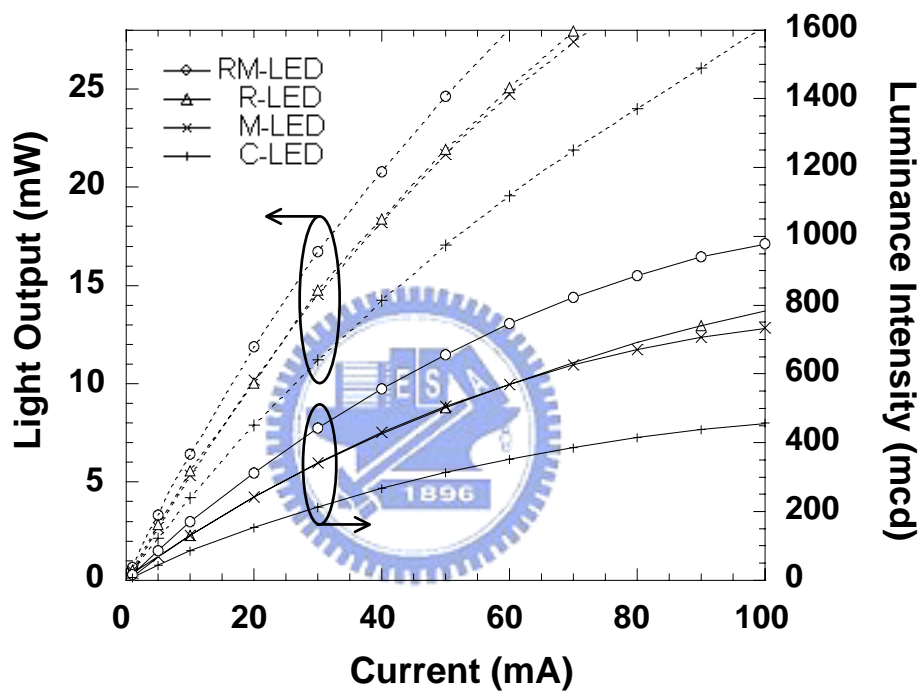


Fig. 5-5. The effects of injection current on the luminous intensity and the light output of the LEDs.

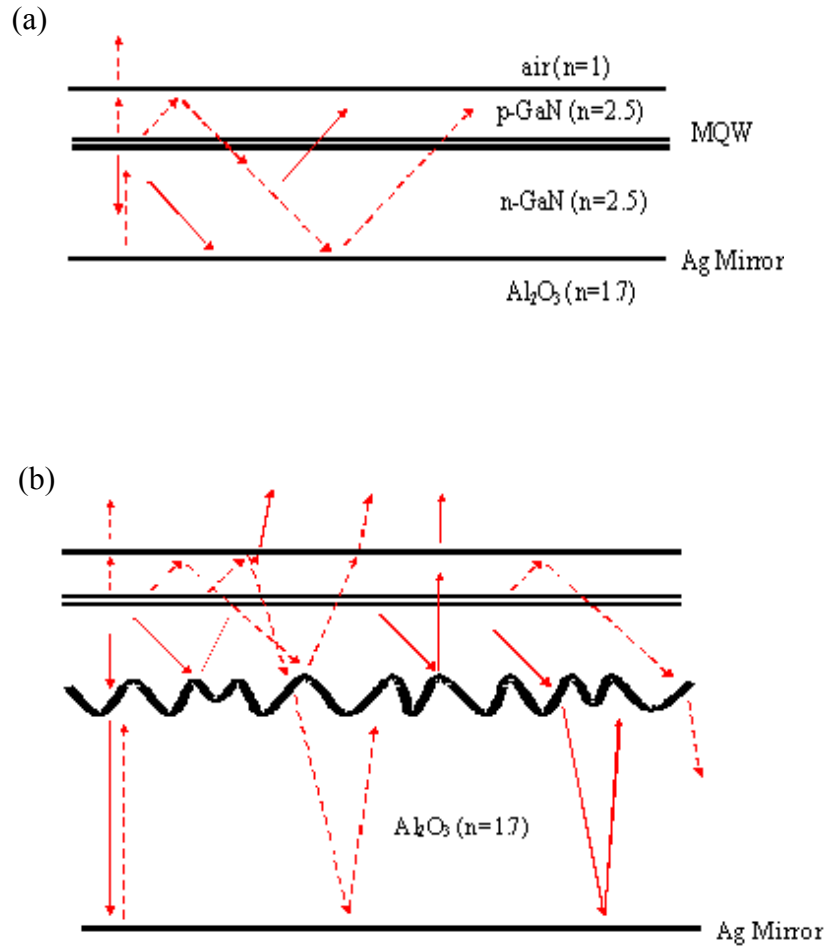


Fig. 5-6. Possible photon paths of the (a) M-LED and (b) RM-LED.

Chapter 6 Conclusion and Future work

6-1 Conclusion

High-power light-emitting diodes (LED) fabricated on Cu and SiC substrates were investigated in this study. The AlGaInP LED structure was bonded to a Cu substrate by using indium-tin-oxide (ITO) as the diffusion barrier layer. It was found that Cu-substrate-bonded LED devices could be operated in a much higher injection forward current, 800 mA, which was eight times higher than that used in traditional GaAs-substrate LED. The luminous intensity of the Cu-substrate LED could reach as high as 1230 mcd, which was three times higher than that of the GaAs-substrate LED. For the SiC-substrate-bonded LED, the luminous intensity of SiC-substrate LED was 3.2 times higher than that of conventional LED at the injection current of 20 mA. The saturation current could reach at 650 mA, which was better than GaAs-substrate LED.

For the GaN-based LED, vertical InGaN-GaN LED epitaxial films were successfully fabricated on a 50mm Si substrate using glue bonding and laser lift-off technology. A high-temperature stable organic film, rather than a solder metal, was used as the bonding agent. It was found that the light output of the vertical InGaN LED chip exceeded that of the conventional sapphire-substrate LED by about 20% at an injection current of 20 mA. The vertical InGaN LED operated at a much higher injection forward current (280mA) than were sapphire substrate LED (180mA). The radiation pattern of the vertical InGaN LED is more symmetrical than that of the sapphire substrate LED. Furthermore, the vertical InGaN LED remain highly reliable after 1000 h of testing.

Another structure of an InGaN-GaN LED with double roughened (p-GaN and

undoped-GaN) surfaces was fabricated by surface-roughening, wafer-bonding and laser lift-off technologies. It was found that the frontside luminance intensity of double roughened LED was 2.77 times higher than that of the conventional LED at an injection current of 20 mA. The backside luminance intensity was 2.37 times higher than that of the conventional LED. This is because the double roughened surfaces can provide photons multiple chances to escape from the LED surface, and redirect photons, which were originally emitted out of the escape cone, back into the escape cone. Furthermore, the effect of the roughness of the undoped-GaN layer on the performance of double roughened LED was also investigated. It was found as the root mean square (rms) roughness of undoped-GaN layer increased from 18.6 to 146.7 nm, the output power increased from 7.2 to 10.2 mW, and the view angle decreased from 133.6 to 116°, respectively. Finally, an InGaN-GaN light emitting diode (LED) with a roughened undoped-GaN surface and a silver mirror on the sapphire substrate was fabricated through a double transfer method. It was found that, at an injection current of 20 mA, its luminance intensity was 100 % larger than conventional LED's. Its output power was 49% larger than conventional LED's.

6-2 Future work

The following work is recommended as a follow-up to this study:

1. Fabrication and life testing of AlGaInP LED/mirror/SiC substrate with roughened top surface.
2. Further analysis of the GaN epitaxy film after laser lift-off (LLO) process by Nd-YAG laser or excimer laser, particularly a microstructure study using TEM and further study the effect of leakage current by varying the laser source.

References

Chapter 1 Introduction

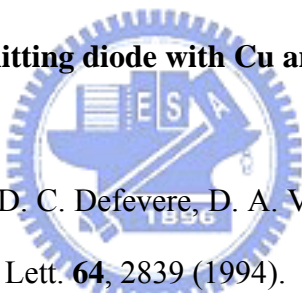
- [1] J. I. Pankove, E. A. Miller, J. E. Berkeyheiser, *J. Luminescence* **5**, 84 (1992).
- [2] H. Amano, N. Sawaki, I. Akasaki, and Y. Toyoda, *Appl. Phys. Lett.* **48**, 353 (1986).
- [3] H. Amano, N. Sawaki, I. Akasaki, and Y. Toyoda, *Jpn. J. Appl. Phys.* **28**, L2112 (1989).
- [4] S. Nakamura, T. Mukai, M. Senoh, and N. Jwasa, *Jpn. J. Appl. Phys.* **31**, 1258 (1992).
- [5] C. H. Chen, S. A. Stockman, M.J. Peanasky, and C.P. Kuo, in *High-Brightness Light-Emitting Diodes, Vol 48, Semiconductors and Semimetals*. G. B. Stringfellow and M.G. Craford, Eds. New York: Academic (1997)
- [6] E. Fred Schubert, *Light-emitting diodes*, Cambridge University Press (2003).
- [7] L. Raleigh, *Proc. Phys. Soc. A* **156**, 326 (1936).
- [8] M. Shimbo, K. Furukawa, K. Fukuda, K. Tanzawa, *J. Appl. Phys.* **60**, 2987(1986).
- [9] J.B. Lasky, *Appl. Phys. Lett.* **48**, 78 (1986).
- [10] S. Blackstone, *Microelectronic Engineering*, **48**, 313 (1999).
- [11] Q.-Y. Tong and U. Gösele, *Semiconductor Wafer Bonding: Science and Technology* (Wiley, New York, 1999).
- [12] U. Gosele, Q.-Y. Tong , A. Schumacher, G. Krauter, M. Reiche, A. Ploßl, P. Kopperschmidt, T.-H. Lee , W.-J. Kim, *Sensors and Actuators*, **74**, 161 (1999)
- [13] K. T. Turner, S. M. Spearing, *J. Appl. Phys.* **92**, 7658 (2002)
- [14] M. Alexe and U. Gösele, *Wafer Bonding Applications and Technology* (Springer –Verlag , Berlin, 2004).
- [15] M. A. Schmidt, *Proc. IEEE* **86**, 1575 (1998).
- [16] Shimbo M, Furukawa K, Fukuda K and Tanzawa K, *J. Appl. Phys.* **60**, 2987 (1986).

- [17] Pomerantz D I 1968 Anodic bonding US Patent 3,397,278.
- [18] Y. T. Cheng, L. Lin, and K. Najafi, *J. Microelectromech. Syst.* **9**, 3 (2000).
- [19] D. Sparks, G. Queen, R. Weston, G. Woodward, M. Putty, L. Jordan, S. Zarabadi, and K. Jayakar, *J. Micromech. Microeng.* **11**, 630 (2001).
- [20] Niklaus F, Enoksson P, Kalvesten E and Stemme G, *J. Micromech. Microeng.* **11**, 100 (2001).
- [21] F. Niklaus, G. Stemme, J. -Q. Lu and R. J. Gutmann, *J. Appl. Phys.* **99**, 031101 (2006)
- [22] F. A. Kish et al., *Appl. Phys. Lett.* **64**, 2839 (1994).
- [23] J. J. Dudley, D. I. Babic', R. Mirin, L. Yang, B. I. Miller, R. J. Ram, T. Reynolds, E. L. Hu, and J. E. Bowers, *Appl. Phys. Lett.* **64**, 1263 (1994).
- [24] Y. Okuno, K. Uomi, M. Aoki, T. Taniwatari, M. Suzuki, and M. Kondow, *Appl. Phys. Lett.* **66**, 451 (1995)
- [25] Y. H. Lo, R. Bhat, D. M. Hwang, M. A. Koza, and T. P. Lee, *Appl. Phys. Lett.* **58**, 1962 (1991).
- [26] G. Cha, R. Gafiteanu, Q. -Y. Tong, and U. Gosele, *Electrochem. Soc. Proc.* **9329**, 257 (1993).
- [27] Wei Chih Peng and Y. S. Wu, *Appl. Phys. Lett.*, **84**, 1841 (2004).
- [28] Tan I-H, Vanderwater DA, Huang J-W, Hofler GE, Kish FA, Chen EI, Ostentowski TD, *Journal of Electronic Materials*, **29**, no.2, 188 (2000).
- [29] R. H. Horng, D. S. Wu, S. C. Wei, C. Y. Tseng, M. F. Huang, K. H. Chang, P. H. Liu and K. C. Lin, *Appl. Phys. Lett.*, **75**, 3054 (1999).
- [30] R. H. Horng, D. S. Wu, S. C. Wei, C. Y. Tseng, M. F. Huang, K. H. Chang, P. H. Liu and K. C. Lin, *Appl. Phys. Lett.*, **75**, 3054 (1999).
- [31] R. H. Horng, Y. C. Lien, W. C. Peng, D. S. Wu, C. Y. Tseng, C. H. Seieh, M. F. Huang, S. J. Tsai and J. S. Liu, *Jpn. J. Appl. Phys.* **40**, 2747 (2001).

- [32] Daniel A. Steigerwald, Jerome C. Bhat, Dave Collins, Robert M. Fletcher, Mari Ochiai Holcomb, Michael J. Ludowise, Paul S. Martin, and Serge L. Rudaz, *IEEE Journal of Selected Topics in Quantum Electronics*, **8**, 310 (2002)
- [33] W. S. Wong, T. Sands, N. W. Cheung, M. Kneissl, D. P. Bour, P. Mei, L. T. Romano, and N. M. Johnson, *Appl. Phys. Lett.*, vol. 77, pp. 2822-2824, 2000.
- [34] T. Fujii, Y. Gao, R. Sharma, E. L. Hu, S. P. DenBaars, and S. Nakamura, *Appl. Phys. Lett.*, vol. 84, pp. 855-857, 2004.
- [35] Y. K. Song, M. Diagne, H. Zhou, A. V. Nurmikko, C. Carter-Coman, R. S. Kern, F. A. Kish, and M. R. Krames, *Appl. Phys. Lett.*, vol 74, pp. 3720-3722, 1999.

Chapter 2

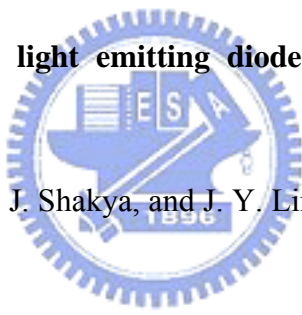
High power AlGaInP light emitting diode with Cu and SiC substrate fabricated by wafer bonding

- 
- [1] F. A. Kish, F. M. Steranka, D. C. Defever, D. A. Vanderwater, K. G. Park, C. P. Kuo, and G. Craford, *Appl. Phys. Lett.* **64**, 2839 (1994).
- [2] G. E. Hofer, D. A. Vanderwater, D. C. DeFever, F. A. Kish, M. D. Camras, F. M. Steranka, and I. -H. Tan, *Appl. Phys. Lett.* **69**, 803, (1996).
- [3] F. A. Kish, D. A. Vanderwater, D. C. Defever, D. A. Steigerwald, G. E. Hofler, K. G. Park and F. M. Steranka, *Electron. Lett.* **32**, 132, (1996).
- [4] I. H. Tan, D. A. Vanderwater, J. -W. Huang, G. E. Hofler, F. A. Kish, E. I. Chen and T. D. Ostentowski, *J. Electron. Mater.* **29**, 188, (2000).
- [5] R. H. Horng, D. S. Wu, S. C. Wei, C. Y. Tseng, M. F. Huang, K. H. Chang, P. H. Liu and K. C. Lin, *Appl. Phys. Lett.* **75**, 3054, (1999).
- [6] R. H. Horng, D. S. Wu, C. H. Seih, W. C. Peng, M. F. Huang, S. J. Tsai and J. S. Liu, *J. Electron. Mater.* **30**, 907, (2001).

- [7] R. H. Horng, Y. C. Lien, W. C. Peng, D. S. Wu, C. Y. Tseng, C. H. Seieh, M. F. Huang, S. J. Tsai and J. S. Liu, *Jpn. J. Appl. Phys.* **40**, 2747, (2001).
- [8] Y. S. Wu, R. S. Feigelson, P. K. Route, D. Zheng, L. A. Gordon, M. M. Fejer and R. L. Byer, *J. Electrochem. Soc.* **145**, No.1, 366, (1998).
- [9] R. H. Horng, D. S. Wu, S. C. Wei, C. Y. Tseng, M. F. Huang, K. H. Chang, P. H. Liu and K. C. Lin, *Jpn. J. Appl. Phys.* **40**, 2747, (2001).
- [10] G. B. Stringfellow and M. George Craford, *High Brightness Light Emitting Diodes*, (Academic Press, Boston, 1997), p 216.
- [11] W. Schairer, *J. Electron. Mater.* **13**, No.3, 559, (1984).

Chapter 3

Performance of InGaN-GaN light emitting diode fabricated using glue bonding on 50mm Si substrate

- 
- [1] H. X. Jiang, S. X. Jin, J. Li, J. Shakya, and J. Y. Lin, *Appl. Phys. Lett.*, **78**, pp.1303-1305, 2001.
- [2] H. Kim, S.-J. Park, and H. Hwang, *IEEE Trans. Electron Devices*, **48**, pp. 1065-1069, 2001.
- [3] J. S. Kwak, J. Cho, S. Chae, O. H. Nam, C. Sone, and Y. Park, *Jpn. J. Appl. Phys., Part 1*, **40**, pp. 6221–6225, 2001
- [4] J. K. Sheu, Y. K. Su, G. C. Chi, M. J. Jou, C. C. Liu, and C. M. Chang, *Solid-State Electron*, **43**, pp.2081-2084, 1999.
- [5] W. S. Wong, T. Sands, N. W. Cheung, M. Kneissl, D. P. Bour, P. Mei, L. T. Romano, and N. M. Johnson, *Appl. Phys. Lett.*, **77**, pp. 2822-2824, 2000.
- [6] T. Fujii, Y. Gao, R. Sharma, E. L. Hu, S. P. DenBaars, and S. Nakamura, *Appl. Phys. Lett.*, **84**, pp. 855-857, 2004.

- [7] Y. K. Song, M. Diagne, H. Zhou, A. V. Nurmikko, C. Carter-Coman, R. S. Kern, F. A. Kish, and M. R. Krames, *Appl. Phys. Lett.*, **74**, pp. 3720-3722, 1999.
- [8] M. K. Kelly, O. Ambacher, R. Dimitrov, R. Handschuh, and M. Stutzmann, *Phys. Status Solid, A* 159, R3, 1997.
- [9] S. Chhajed, Y. Xi, Y.-L. Li, Th. Gessmann and E. F. Schubert, *J. Appl. Phys.*, **97**, pp.054506-1-054506-8, 2004.
- [10] D. S. Wu, S. C. Hsu, S. H. Huang, C. C. Wu, C. E. Lee and R. H. Horng, *Jpn. J. Appl. Phys.*, **43**, No. 8A, pp.5239-5242, 2004.

Chapter 4

Enhanced performance of InGaN-GaN light emitting diode by roughening both the p-GaN surface and the undoped-GaN surface

- [1] S. Nakamura, S. Senoh, N. Iwasa, and S. Nagahama, *Jpn. J. Appl. Phys.*, **34**, L797 (1995).
- [2] I. Kidoguchi, A. Ishibashi, G. Sugahara, Y. Ban, *Appl. Phys. Lett.*, **76**, 3768 (2000).
- [3] T. Mukai, K. Takekawa, S. Nakamura, *Jpn. J. Appl. Phys.*, **37**, L839 (1998).
- [4] K. Tadatomo, H. Okagawa, T. Tsunekawa, T. Jyouichi, Y. Imada, M. Kato, H. Kudo, T. Taguchi, *Phys. Stat. Sol. (a)* **188**, 121 (2001).
- [5] S.J. Chang, Y.C. Lin, Y.K. Su, C.S. Chang, T.C. Wen, S.C. Shei, J.C. Ke, C.W. Kuo, S.C. Chen, C.H. Liu, *Solid State Electron.* **47**, 1539 (2003).
- [6] R.C. Tu, C. C. Chuo, S. M. Pan, Y. M. Fan, C. E. Tsai, T. C. Wang, C. J. Tun, G. C. Chi, B. C. Lee, C. P. Lee, *Appl. Phys. Lett.*, **83**, 3608 (2003).
- [7] H. X. Jiang, S. X. Jin, J. Li, J. Shakya, and J. Y. Lin, *Appl. Phys. Lett.*, **78**, 1303 (2001).
- [8] S. Nakamura, M. Senoh, S. Nagahama, N. Iwasa, T. Yamada, T. Mukai, Y. Sugimoto, and H. Kiyoku, *Appl. Phys. Lett.*, **69**, 4056 (1996).
- [9] E. Woelk, G. Strauch, D. Schmitz, M. Deschler, and H. Jurgensen, *Mater. Sci. Eng.*, **1**, **B**

- 44**, 419, (1997).
- [10] I. Schnitzer, E. Yablonovitch, C. Caneau, T. J. Gmitter, and A. Scherer, *Appl. Phys. Lett.*, **63**, 2174 (1993).
- [11] Windisch R, Dutta B, Kuijk M, Knobloch A, Meinschmidt S, Schoberth S, Kiesel P, Borghs G, Dohler GH, Heremans P, *IEEE Trans. Electron Dev.*, **47**, 1492 (2000).
- [12] Chul Huh, Kug-Seung Lee, Eun-Jeong Kang, and Seong-Ju Park, *J. Appl. Phys.*, **93**, no. 11, 9383 (2003).
- [13] Y. P. Hsu, S. J. Chang, Y. K. Su, S. C. Chen, J. M. Tsai, W. C. Lai, C. H. Kuo, and C. S. Chang, *IEEE Photon. Technol. Lett.*, **17**, no. 8, 1620 (2005).
- [14] C. M. Tsai, J. K. Sheu, W. C. Lai, Y. P. Hsu, P. T. Wang, C. T. Kuo, C. W. Kuo, S. J. Chang, Y. K. Su, *IEEE Electron Dev. Lett.*, **26**, 464 (2005).
- [15] C.H. Liu, R.W. Chuang, S.J. Chang, Y.K. Su, L.W. Wu, C.C. Lin, *Mater. Sci. Eng.*, **B 112**,10 (2004).
- [16] C.F. Lin, Z. H. Yang, J. H. Zheng, J. H. Dai, *IEEE Photon. Technol. Lett.*, **17**, 2038 (2005).
- [17] T. Fujii, Y. Gao, R. Sharma, E. L. Hu, S. P. DenBaars, and S. Nakamura. *Appl. Phys. Lett.* **84**, 855 (2004).
- [18] M. K. Kelly, O. Ambacher, R. Dimitrov, R. Handschuh, and M. Stutzmann, *Phys. Status Solidi A* **159**, R3 (1997).
- [19] S. J. Chang, S. C. Chen, Y. K. Su, R. W. Chung, W. C. Lai, C. H. Kuo, Y. P. Hsu, Y. C. Lin, S. C. Shei, H. M. Lo, J.C. Ke, and J. K. Sheu, *IEEE Photon. Technol. Lett.*, **16**, no. 4, 1002, (2004).
- [20] R. H. Horng, C. C. Yang, J. Y. Wu, S. H. Huang, C. E. Lee, and D. S. Wu. *Appl. Phys. Lett.* **86**, 221101 (2005)
- [21] J. H. Cheng, W. C. Peng, Y. S. Wu, submitted to *Appl. Phys. Lett.*

[22] W. C. Peng, Y. S. Wu, Appl. Phys. Lett., **88**, 181117, (2006).

Chapter 5

Enhanced performance of an InGaN-GaN light -emitting diode by roughening the undoped -GaN surface and applying a mirror coating to the sapphire substrate

- [1] S. Nakamura, S. Senoh, N. Iwasa, and S. Nagahama, Jpn. J. Appl. Phys., **34**, L797 (1995).
- [2] H. X. Jiang, S. X. Jin, J. Li, J. Shaky, and J. Y. Lin, Appl. Phys. Lett., **78**, 1303 (2001).
- [3] I. Schnitzer, E. Yablonovitch, C. Caneau, T. J. Gmitter, and A. Scherer, Appl. Phys. Lett. **63**, 2174 (1993).
- [4] Chul Huh, Kug-Seung Lee, Eun-Jeong Kang, and Seong-Ju Park, J. Appl. Phys., **93**, no. 11, 9383 (2003).
- [5] Y. P. Hsu, S. J. Chang, Y. K. Su, S. C. Chen, J. M. Tsai, W. C. Lai, C. H. Kuo, and C. S. Chang, IEEE Photon. Technol. Lett., **17**, no. 8, 1620 (2005).
- [6] C.H. Liu, R.W. Chuang, S.J. Chang, Y.K. Su, L.W. Wu, C.C. Lin, Mater. Sci. Eng B **112**, 10 (2004).
- [7] T. Fujii, Y. Gao, R. Sharma, E. L. Hu, S. P. DenBaars, and S. Nakamura. Appl. Phys. Lett. **84**, 855 (2004).
- [8] D. S. Wu, S. C. Hsu, S. H. Huang, C. C. Wu, C. E. Lee and R. H. Horng. JJAP **43**, No. 8A, 5239 (2004)
- [9] M. K. Kelly, O. Ambacher, R. Dimitrov, R. Handschuh, and M. Stutzmann, Phys. Status Solid A **159**, R3 (1997).

簡 歷

姓名：彭韋智

性別：男

出生日期：1976 年 11 月 25 號

出生地：臺灣省新竹縣

永久住址：304 新竹縣新豐鄉松林村明新街 234 巷 3 號

學歷：

1995 ~ 1999 私立大葉大學電機工程學系學士

1999 ~ 2001 私立大葉大學電機工程(光電組)研究所碩士

2001 ~ 2006 國立交通大學材料科學與工程研究所博士



研究題目：

碩士-

(中文) 以晶片黏貼技術研製面射型發光元件

(英文) Fabrication of Surface Emitting Devices Using Wafer Bonding Technology

博士-

(中文) 發光二極體功率與亮度的提升

(英文) Enhancement the power and the brightness of light emitting diodes

Publication List

Journal Paper

1. Wei Chih Peng and Y. S. Wu, " Enhanced light output in double roughened GaN light-emitting diodes via various texturing of undoped-GaN layer" submit to *Jpn. J. Appl. Phys.* (accepted-2006/06/25). (1st author)
2. Wei Chih Peng and Y. S. Wu, "Improved luminance intensity of InGaN-GaN light-emitting diode by roughening both the p-GaN surface and the undoped-GaN surface," *Appl. Phys. Lett.*, (accepted-2006/06/24) (1st author)
3. Wei Chih Peng and Y. S. Wu, "Enhanced performance of an InGaN-GaN light-emitting diode by roughening the undoped-GaN surface and applying a mirror coating to the sapphire substrate," *Appl. Phys. Lett.*, 88, 181117 (2006). (1st author)
4. Wei Chih Peng and Y. S. Wu, "Performance of InGaN-GaN LEDs fabricated using glue bonding on 50-mm Si substrate," *IEEE Photon. Technol. Lett.*, 18, 613 (2006). (1st author)
5. Wei Chih Peng and Y. S. Wu, "High-power AlGaInP light-emitting diodes with metal substrates fabricated by wafer bonding," *Appl. Phys. Lett.*, 84, 1841 (2004). (1st author)
6. R. H. Horng, W. C. Peng, D. S. Wu, W. J. Ho, Y. S. Huang, "Surface treatment and electrical properties of directly wafer-bonded InP epilayer on GaAs substrate", *Solid State Electron.*, 46, pp.1103-1108, 2002. (2nd author)
7. R. H. Horng, D. S. Wu, C. H. Seieh, W. C. Peng, M. F. Huang, S. J. Tsai, and J. S. Liu, "Wafer bonding of 50-mm-diameter mirror substrates to AlGaInP light-emitting diode wafers", *J. of Electronic Materials*, 30, pp. 907-910, 2001 (4th author)
8. R. H. Horng, Y. C. Lien, W. C. Peng, D. S. Wu, C. Y. Tseng, C. H. Seieh, M. F. Huang, S. J. Tsai, and J. S. Liu, "High-brightness wafer-bonded ITO/LED/ Mirror/Si", *Jpn. J. Appl. Phys.* 40, pp.2747-2751, 2001. (3rd author)

Conference Paper

1. Wei Chih Peng and Y. S. Wu “Performance and Reliability of InGaN-GaN Light-Emitting Diodes with Mirror Wafer Bonding Technology” *The Symposium "State-of-the-Art Program on Compound Semiconductors XLII", of the 207th Meeting of The Electrochemical Society, Quebec, Canada, May 2005.*
2. Wei Chih Peng and Y. S. Wu “Improvement of InGaN-GaN Light-Emitting Diodes with Vertical Omni-directional Mirror Adhesion Technology” *IEDMS, Hsin-Chu, Taiwan, December 2004.*
3. Wei Chih Peng, Ting Cheng Lin and Y. S. Wu “High-Performance Poly-Si and Single Crystal Silicon Thin Film Transistors on Plastic Substrates by Using Transfer Methods” *MRS Spring Meeting Symposium, San Francisco, USA, April 2004.*
4. Wei Chih Peng and Y. S. Wu “AlGaInP Light-Emitting Diodes with Metal Substrates Fabricated by Wafer Bonding” *The 7th International Symposium on Semiconductor Wafer Bonding Science Technology and Application, Paris, France, April 2003.*
5. R. H. Horng, W. C. Peng, and D. S. Wu, “Wafer-bonded 850-nm VCSEL on Si substrate with metal mirror”, International Photonics Conference, Kaohsiung, Taiwan, Dec. 13-14, 2001.
6. R. H. Horng, D. S. Wu, W. C. Peng, W. J. Ho, Y. S. Huang, “Optoelectronic Device Bonded to Metal-Mirror Substrate”, 10th Canadian Semiconductor Technology Conference, Ottawa, Canada, Aug. 13-17, 2001.
7. R. H. Horng, W. C. Peng, D. S. Wu, T. T. Shih, W. J. Ho, and Y. S. Huang ‘Surface treatment and electrical properties of directly bonded InP on GaAs’, *IEDMS, Chung-Li, Taiwan, Dec. 20-21, 2000, pp. 122-125.*

8. W. C. Peng, R. H. Horng, D. S. Wu, T. T. Shih, W. J. Ho, and Y. S. Huang, '1.3/1.55-um VCSELs bonded to metal-mirror substrates', International Photonics Conf., HsinChu, Taiwan, Dec. 12-15, 2000, pp. 316-318.
9. R. H. Horng, Y. C. Lien, W. C. Peng, and D. S. Wu, 'High-brightness wafer-bonded ITO/AlGaInP/Mirror/Si light emitting diodes', SSDM 2000, Sendai, Japan, Aug. 29-31, 2000 (C-2-5).
10. R. H. Horng, D. S. Wu, W. C. Peng, M. F. Huang, P. H. Liu, C. H. Seieh, and K. C. Lin, 'Performance and reliability of wafer-bonded AlGaInP/mirror/Si light-emitting diodes', *Proc. SPIE* Vol. 4078, Photonics Taiwan, July. 26-28, 2000 (507-513).
11. W. C. Peng, R. H. Horng, D. S. Wu, M. F. Huang, K. H. Chang, P. H. Liu, K. C. Lin, and C. Y. Tseng, "High-performance wafer-bonded AlGaInP/mirror/Si light-emitting diodes", *Optics & Photonics Taiwan'99*, pp. 383-386.

